

Biomedical Polymers (Biomaterials)

Ask Precise Questions



What made da Vinci truly brilliant wasn't just creativity - it was the questions he asked. He didn't settle for general curiosity. He drilled down into "precise, actionable questions" that led straight to real answers.

Want to level up your thinking?
Start by refining a vague goal into "three specific, evidence-based questions."
Try it today and watch your clarity skyrocket.

Stephen Petro (Thinkitthrough411)

Biomaterials Science. An Introduction to Materials in Medicine

Table of contents

Part I: Materials Science and Engineering

Section 1.1: Overview of Biomaterials

- 1.1.1 - Introduction to Biomaterials Science: An Evolving, Multidisciplinary Endeavor
- 1.1.2 - A History of Biomaterials

Section 1.2: Properties of Biomaterials

- 1.2.1 - Introduction: Properties of Materials—the Palette of the Biomaterials Engineer
- 1.2.2 - The Nature of Matter and Materials
- 1.2.3 - Bulk Properties of Materials
- 1.2.4 - Surface Properties and Surface Characterization of Biomaterials
- 1.2.5 - Role of Water in Biomaterials

Section 1.3: Classes of Materials Used in Medicine

- 1.3.1 - The Materials Side of the Biomaterials Relationship
- 1.3.2 - Polymers: Basic Principles
 - 1.3.2A - Polyurethanes
 - 1.3.2B - Silicones
 - 1.3.2C - Fluorinated Biomaterials
 - 1.3.2D - The Organic Matrix of Restorative Composites and Adhesives
 - 1.3.2E - Hydrogels
 - 1.3.2F - Degradable and Resorbable Polymers
 - 1.3.2G - Applications of “Smart Polymers” as Biomaterials
- 1.3.3 - Metals: Basic Principles
 - 1.3.3A - Titanium Alloys, Including Nitinol
 - 1.3.3B - Stainless Steels
 - 1.3.3C - CoCr Alloys
 - 1.3.3D - Biodegradable Metals
- 1.3.4 - Ceramics, Glasses, and Glass-Ceramics: Basic Principles
 - 1.3.4A - Natural and Synthetic Hydroxyapatites
 - 1.3.4B - Structural Ceramic Oxides
- 1.3.5 - Carbon Biomaterials
- 1.3.6 - Natural Materials
 - 1.3.6A - Processed Tissues
 - 1.3.6B - Use of Extracellular Matrix Proteins and Natural Materials in Bioengineering
- 1.3.7 - Composites
- 1.3.8A - Microparticles
- 1.3.8B - Nanoparticles

Section 1.4: Materials Processing

- 1.4.1 - Introduction to Materials Processing for Biomaterials
- 1.4.2 - Physicochemical Surface Modification of Materials Used in Medicine
 - 1.4.3A - Nonfouling Surfaces
 - 1.4.3B - Nonthrombogenic Treatments and Strategies
- 1.4.4 - Surface-Immobilized Biomolecules
- 1.4.5 - Surface Patterning
- 1.4.6 - Medical Fibers and Biotextiles
- 1.4.7 - Textured and Porous Biomaterials
- 1.4.8 - Biomedical Applications of Additive Manufacturing

Part II: Biology and Medicine

Section 2.1: Some Background Concepts

- 2.1.1 - Introduction to Biology and Medicine—Key Concepts in the Use of Biomaterials in Surgery
- 2.1.2 - Adsorbed Proteins on Biomaterials
- 2.1.3 - Cells and Surfaces in Vitro
- 2.1.4 - Functional Tissue Architecture, Homeostasis, and Responses to Injury
- 2.1.5 - The Extracellular Matrix and Cell–Biomaterial Interactions
- 2.1.6 - Effects of Mechanical Forces on Cells and Tissues

Section 2.2: Host Reaction to Biomaterials and Their Evaluation

- 2.2.1 - Introduction to Biological Responses to Materials
- 2.2.2 - Inflammation, Wound Healing, the Foreign-Body Response, and Alternative Tissue Responses
- 2.2.3 - Innate and Adaptive Immunity: The Immune Response to Foreign Materials
- 2.2.4 - The Complement System
- 2.2.5 - Systemic and Immune Toxicity of Implanted Materials
- 2.2.6 - Blood Coagulation and Blood–Material Interactions
- 2.2.7 - Tumorigenesis and Biomaterials
- 2.2.8 - Biofilms, Biomaterials, and Device-Related Infections

Section 2.3: Characterization of Biomaterials

- 2.3.1 - How Well Will It Work? Introduction to Testing Biomaterials
- 2.3.2 - The Concept and Assessment of Biocompatibility
- 2.3.3 - In Vitro Assessment of Cell and Tissue Compatibility
- 2.3.4 - In Vivo Assessment of Tissue Compatibility
- 2.3.5 - Evaluation of Blood–Materials Interactions
- 2.3.6 - Animal Surgery and Care of Animals

Section 2.4: Degradation of Materials in the Biological Environment

- 2.4.1 - Introduction: The Body Fights Back—Degradation of Materials in the Biological Environment
- 2.4.2 - Chemical and Biochemical Degradation of Polymers Intended to Be Biostable
- 2.4.3 - Metallic Degradation and the Biological Environment
- 2.4.4 - Degradative Effects of the Biological Environment on Ceramic Biomaterials
- 2.4.5 - Pathological Calcification of Biomaterials

Section 2.5: Application of Biomaterials

- 2.5.1 - Introduction to Applications of Biomaterials
 - 2.5.2a - Cardiovascular Medical Devices: Heart Valves, Pacemakers and Defibrillators, Mechanical Circulatory Support, and Other Intracardiac Devices
 - 2.5.2B - Cardiovascular Medical Devices: Stents, Grafts, Stent-Grafts and Other Endovascular Devices
- 2.5.3 - Extracorporeal Artificial Organs and Therapeutic Devices
- 2.5.4 - Orthopedic Applications
- 2.5.5 - Dental Applications
- 2.5.6 - Ophthalmologic Applications: Introduction
- 2.5.7 - Bioelectronic Neural Implants
- 2.5.8 - Burn Dressings and Skin Substitutes
- 2.5.9 - Description and Definition of Adhesives, and Related Terminology
- 2.5.10 - Biomaterials for Immunoengineering
- 2.5.11 - Biomaterials-Based Model Systems to Study Tumor–Microenvironment Interactions
- 2.5.12 - Drug Delivery Systems
- 2.5.13 - Responsive Polymers in the Fabrication of Enzyme-Based Biosensors

Section 2.6: Applications of Biomaterials in Functional Tissue Engineering

- 2.6.1 - Rebuilding Humans Using Biology and Biomaterials
- 2.6.2 - Overview of Tissue Engineering Concepts and Applications
- 2.6.3 - Tissue Engineering Scaffolds
- 2.6.4 - Micromechanical Design Criteria for Tissue-Engineering Biomaterials
- 2.6.5 - Tendon Tissue-Engineering Scaffolds
- 2.6.6 - Bone Tissue Engineering
- 2.6.7 - Biomaterials for Cardiovascular Tissue Engineering
- 2.6.8 - Soft Tissue Engineering

Part III: The Medical Product Life Cycle

- 3.1.1 - Introduction: Biomaterials in Medical Devices
- 3.1.2 - Total Product Lifecycle for Biomaterial-Based Medical Devices
- 3.1.3 - Safety and Risk Considerations in Medical Device Development
- 3.1.4 - Sterilization and Disinfection of Biomaterials for Medical Devices
- 3.1.5 - Verification and Validation: From Bench to Human Studies
- 3.1.6 - Commercial Considerations in Medical Device Development
- 3.1.7 - Regulatory Constraints for Medical Products Using Biomaterials
- 3.1.8 - Role of Standards for Testing and Performance Requirements of Biomaterials
- 3.1.9 - Medical Device Failure—Implant Retrieval, Evaluation, and Failure Analysis
- 3.1.10 - Legal Concepts for Biomaterials Engineers
- 3.1.11 - Moral and Ethical Issues in the Development of Biomaterials and Medical Products

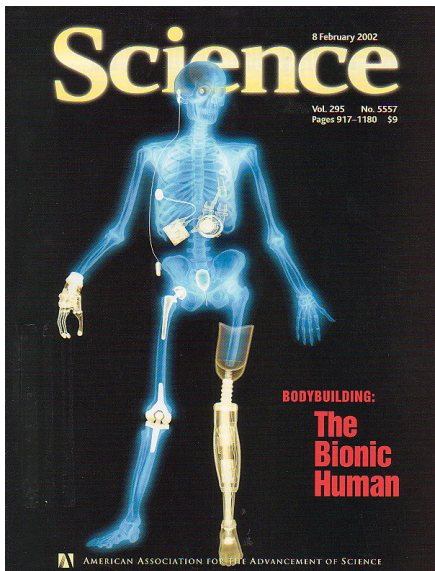
Wagner 2020, Biomaterials Science.
An Introduction to Materials in Medicine

Biomaterials

Biomaterials are any (natural or synthetic) materials which are in contact with the body or body components to **protect, support, restore, augment, or replace** damaged tissue or a biological function.

<https://www.nibib.nih.gov/science-education/science-topics/biomaterials>

2002



2011



Blood-contacting biomaterials

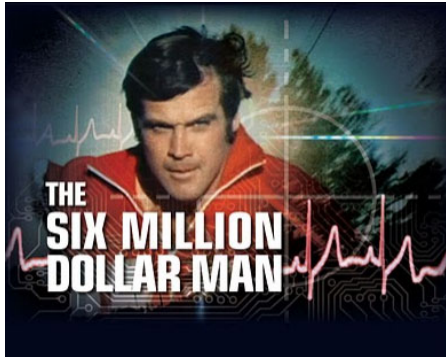
Non-blood-contacting biomaterials

Biomaterials in Current Medical Practice

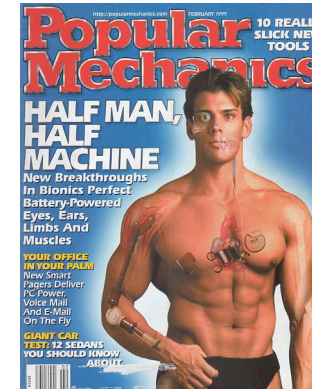
- **Medical implants**, including heart valves, stents, and grafts; artificial joints, ligaments, and tendons; hearing loss implants; dental implants; and devices that stimulate nerves.
- **Methods to promote healing of human tissues**, including sutures, clips, and staples for wound closure, and dissolvable dressings.
- **Regenerated human tissues**, using a combination of biomaterial supports or scaffolds, cells, and bioactive molecules. Examples include a bone regenerating hydrogel and a lab-grown human bladder.
- **Molecular probes and nanoparticles** that break through biological barriers and aid in cancer imaging and therapy at the molecular level.
- **Biosensors** to detect the presence and amount of specific substances and to transmit that data. Examples are blood glucose monitoring devices and brain activity sensors.
- **Drug-delivery systems** that carry and/or apply drugs to a disease target. Examples include drug-coated vascular stents and implantable chemotherapy wafers for cancer patients.

The Bionic Man

1973-1978



1999 - 2002



2024 Neuralink



Six Million Dollar Man
The Bionic Woman

<https://www.youtube.com/watch?v=0CPJ-AbCsT8>
https://www.youtube.com/watch?v=Pz_DT54sfAo



More Advanced than Neuralink: Professor Krishna Jayant

Professor Jayant's research is focused on **inventing revolutionary electrical and optical neurotechnologies that can map circuit dynamics in the awake mammalian brain with unparalleled precision**. These technologies have made groundbreaking discoveries in brain function, unravel novel algorithms underlying neural computation, and **pinpoint potential therapeutic targets** for even the most intractable diseases. Furthermore, he has invented cutting-edge complementary metal-oxide-semiconductor (CMOS) circuits that enable seamless interfacing with cells and biomolecules, thus making previously infeasible measurements in the life sciences a reality.



To date, his work has delivered several firsts; some examples include (select papers on the next slide)

First direct electrical recordings from dendritic spines using nanopipette electrophysiology

First targeted intracellular recordings from deep-layer neurons in awake locomoting animals

First chip-scale multi-clamp amplifier

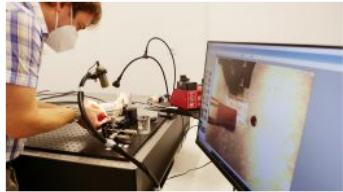
First Neuromorphic CMOS transistor biosensor

First multisite 3D stimulation of spines

First 3D electrophysiology probe compatible with two-photon imaging

His works have been cited by some of the foremost leaders in the field, and given his recent chapters in the AXON handbook and Handbook of Electrophysiology. In Neurosciences, one metric of widespread impact is how many folks adopt one's methods and experimental approach to make new discoveries.

Biomedical Engineering: 2020



TECHNOLOGY OCTOBER 23, 2020

Early Detection of SARS-CoV-2 (COVID-19 Virus) With New Photonic Sensor System

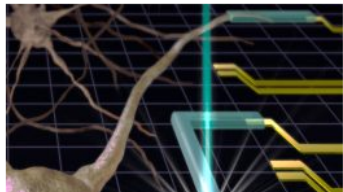
Scientists are working on the development of a new equipment, more functional and cheaper, that could be deployed in primary healthcare centers. Detecting SARS-CoV-2 virus...



TECHNOLOGY OCTOBER 16, 2020

Engineers Print Wearable, High-Performance Biometric Sensors Directly on Skin

An international team of researchers developed a novel technique to produce precise, high-performing biometric sensors. Wearable sensors are evolving from watches and electrodes to bendable...



TECHNOLOGY OCTOBER 3, 2020

New Method of 3D-Printing Soft Materials Could Jump-Start Creation of Tiny Medical Devices for the Body

Researchers at the National Institute of Standards and Technology (NIST) have developed a new method of 3D-printing gels and other soft materials. Published in a...



HEALTH JULY 22, 2020

Bioengineered Membrane to Capture Airborne COVID-19 Droplets – Inspired by Plant That Traps Insects

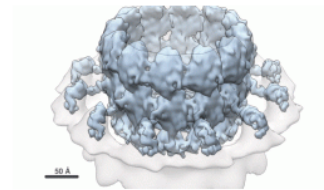
Team's inspiration comes from nature — the pitcher plant, with its liquid membrane that traps insects. Detection and analysis of airborne coronavirus droplets using a...



TECHNOLOGY AUGUST 17, 2020

New “Cyborg” Technology Could Enable Merger of Humans and AI

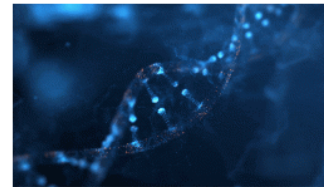
Although true “cyborgs” — part human, part robotic beings — are science fiction, researchers are taking steps toward integrating electronics with the body. Such devices...



BIOLOGY AUGUST 2, 2020

Advanced Cryo-EM Reveals Viral RNA Replication Complex Structure in “Game-Changing” Detail

For the first time, scientists at the Morgridge Institute for Research have generated near atomic resolution images of a major viral protein complex responsible for...



BIOLOGY AUGUST 1, 2020

Solving a DNA Mystery: “The Bizarre Thing About the Bubbling DNA”

Exposure to enzymes causes peculiar response in liquid droplets formed by DNA; new study explains mechanisms behind it. “A watched pot never boils,” as the...



HEALTH JULY 27, 2020

Seaweed Extract Outperforms Remdesivir in Blocking COVID-19 Virus in Cell Studies

Heparin, a common antiticoagulant, could also form basis of a viral trap for SARS-CoV-2. In a test of antiviral effectiveness against the virus that causes...

<https://scitechdaily.com/tag/biomedical-engineering/>

Biomedical Engineering: 2023



TECHNOLOGY JANUARY 8, 2024

Not Science Fiction: Brain Implant May Enable Communication From Thoughts Alone

A prosthetic device deciphers signals from the brain's speech center to predict what sound a person is trying to say. A team of neuroscientists, neurosurgeons,...



HEALTH DECEMBER 31, 2023

A New Wireless, Handheld, Non-Invasive Device Successfully Detects Alzheimer's and Parkinson's Biomarkers

The next steps involve testing saliva and urine samples with the biosensor. An international team of scientists has created a handheld.

HEALTH DECEMBER 21, 2023

The \$1 Cure: How Programmable Bacteria Are Reshaping Cancer Therapy

Texas A&M University researchers are co-leading a \$20 million project to develop a \$1 cancer treatment. What if a single one-dollar dose could cure cancer?...

TECHNOLOGY DECEMBER 15, 2023

Echoes of Innovation: Caltech's 3D Leap in Laser Photoacoustic Imaging

Caltech's improved photoacoustic imaging technology, PACTER, simplifies procedures, enables 3D imaging, and reduces operational complexity, marking a significant advancement in medical imaging.

HEALTH DECEMBER 14, 2023

Revolutionizing Amputee Care: Spinal Cord Stimulation Alleviates Pain and Enhances Balance

Spinal cord stimulation by University of Pittsburgh researchers effectively reduces phantom limb pain and restores sensation in amputees, marking a significant advance in prosthetic technology...



TECHNOLOGY NOVEMBER 11, 2023

Revolutionizing CRISPR: Quantum Biology and AI Merge to Enhance Genome Editing

Oak Ridge National Laboratory's research in quantum biology and AI has significantly improved the efficiency of CRISPR Cas9 genome editing in microbes, aiding in renewable...



BIOLOGY NOVEMBER 9, 2023

Breathing Life Into Medicine: "Living Pharmacy" Implant Gets Oxygenating Boost

New device could improve the outcomes of cell-based therapies. Cell-based therapies show promise for drug delivery, replacing damaged tissues, harnessing the body's own healing mechanisms,...

HEALTH NOVEMBER 6, 2023

Nanowired Cardiac Organoids - New Technology Could Revolutionize Recovery After Heart Attack

Preclinical research indicates that nanowired cardiac organoids could one day repair hearts instead of just preventing further damage. Heart disease is a leading cause of...



TECHNOLOGY OCTOBER 14, 2023

Revolutionizing Prosthetics - Scientists Develop Bionic Hand That Merges With User's Nervous and Skeletal Systems

A Swedish woman who lost her right hand due to a farming accident was implanted with a novel human-machine interface into her residual bone, nerves,...



TECHNOLOGY OCTOBER 7, 2023

Rapid Disease Diagnosis: Bioengineering Breakthrough Boosts DNA Detection Sensitivity by 100x

Scientists discover that letting small amounts of DNA 'dance' can speed disease detection. UMass Amherst researchers have pushed forward the boundaries of biomedical engineering one...



<https://scitechdaily.com/tag/biomedical-engineering/>

Biomedical Engineering: 2025



12 Years in the Making: Groundbreaking Human "Molecular Map" Reveals Secrets of the Body

SEPTEMBER 15, 2024



The Mystery of Human Wrinkles: Scientists Unveil Secret Mechanisms

SEPTEMBER 21, 2024

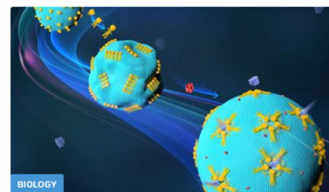
A POSTECH research team has recreated biological wrinkles in vitro, revealing that ECM dehydration and...



Not Science Fiction: Paralyzed Man Controls Robotic Arm Using Only His Thoughts

MARCH 11, 2025

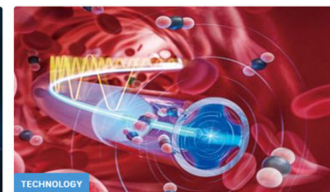
newly developed artificial intelligence can adapt to brain changes during learning, allowing individuals with paralysis...



DNA Nanorobots Unlock New Frontiers in Targeted Drug Delivery

JANUARY 16, 2025

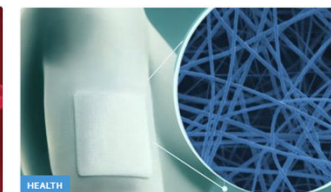
Scientists develop DNA nanorobots capable of modifying artificial cells. Scientists at the University of Stuttgart...



Miniaturized Spectroscopy Delivers Real-Time Monitoring in Narrow Spaces

DECEMBER 24, 2024

The all-in-one optical fiber spectrometer offers a compact microscale design with performance on par with...



Revolutionary Smart Drug-Delivering Bandage Developed by Polish Scientists

JUNE 14, 2025

Polish scientists developed electrospun polymer mats containing metronidazole for targeted, controlled drug delivery to wounds...



Beyond Cochlear Implants: A Flexible Brainstem Device Restores Hearing Without Side Effects

APRIL 18, 2025

A new soft auditory brainstem implant (ABI) developed by researchers at EPFL may revolutionize hearing...



Smaller Than a Grain of Rice: Engineers Develop World's Smallest Pacemaker

APRIL 17, 2025

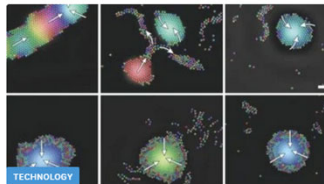
A tiny device can be inserted using a syringe and then safely dissolves once it...



Hidden Danger: Brain Implants Could Allow Bacteria To Invade the Brain

MARCH 23, 2025

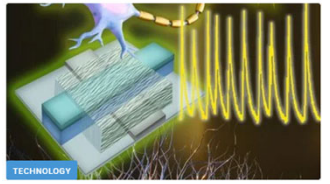
New research has the potential to transform the design of brain implants for neurological disorders...



These Tiny Robots Can Swarm, Adapt, and Heal Themselves

OCTOBER 16, 2025

Scientists designed microrobots that use sound to swarm, adapt, and heal themselves — working together...



Scientists Create Artificial Neuron That "Speaks" the Language of the Brain

OCTOBER 4, 2025

Built from low-powered protein nanowires made by bacteria, these neurons could enable vastly more efficient...



New Breath Test Detects Diabetes in Minutes

SEPTEMBER 13, 2025

A Penn State team created a breath sensor that identifies diabetes by detecting acetone. The...



Scientists Develop "Lung-on-a-Chip" That Could Help Stop the Next Pandemic

JULY 27, 2025

Using iPSCs on microfluidic chips to unravel respiratory illnesses. Respiratory illnesses like COVID-19 have triggered...



A 100-Year-Old Problem Solved? Scientists Discover How To Freeze Organs Without Cracking Them

NOVEMBER 25, 2025

The breakthrough approach could lead to successful, long-term organ transplants, bringing science fiction closer to...



New Paper-Thin Brain Implant Could Transform How Humans Connect With AI

DECEMBER 8, 2025

A radically miniaturized brain implant called BISC is redefining what's possible in human-computer interaction, offering...



Scientists Develop Spray-On Powder That Instantly Seals Life-Threatening Wounds

JANUARY 13, 2026

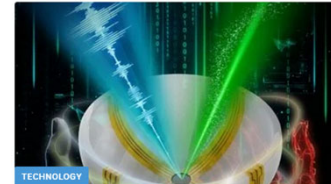
KAIST scientists have created a fast-acting, stable powder hemostat that stops bleeding in one second...



Nanoparticles That Destroy Disease Proteins Could Unlock New Treatments for Dementia and Cancer

JANUARY 22, 2026

Scientists have developed a new nanoparticle-based strategy that could dramatically expand the range of disease-causing...



Scientists Develop a New Way To See Inside the Human Body Using 3D Color Imaging

JANUARY 26, 2026

A newly developed imaging method blends ultrasound and photoacoustics to capture both tissue structure and...

<https://scitechdaily.com/tag/biomedical-engineering/>

Evolutionary Timeline of Implantable Biomaterials

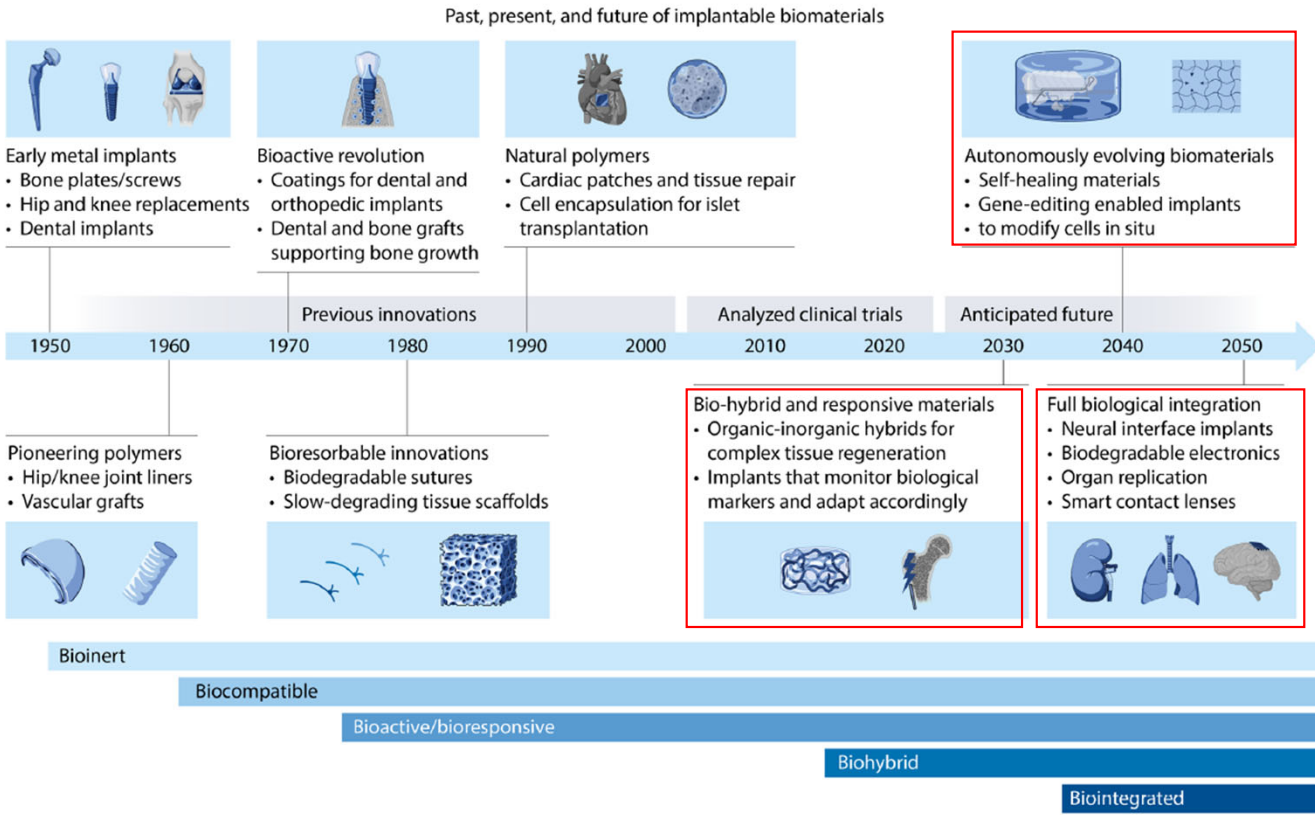
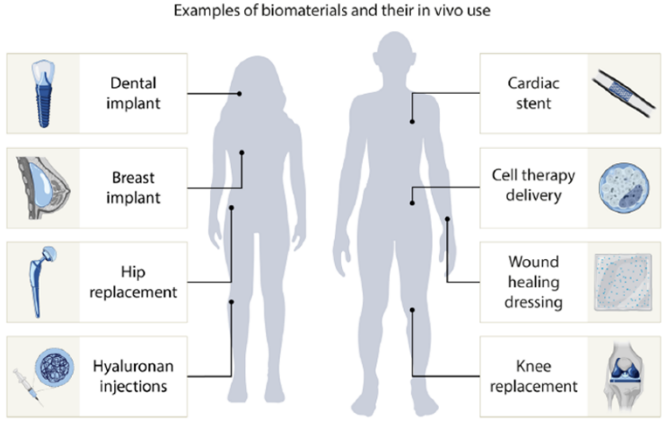
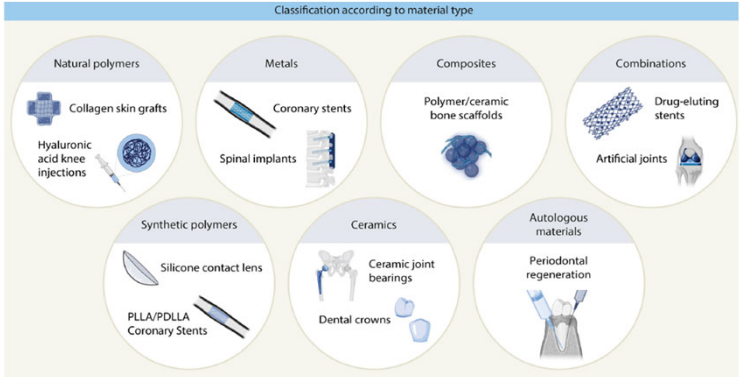


Fig. 1. Evolutionary timeline of implantable biomaterials. This timeline depicts the advancement of biomaterials from the 1950s bioinert metal implants to the envisioned 2050 biointegrated organ replicas. Notable milestones such as biocompatible polymers, bioactive coatings, and future smart implants, predicting a shift toward self-healing materials and organ replication, are marked in the timeline. Figure was created using icons from BioRender.com and modified and finalized in Adobe Illustrator.



Lele 2024, Global trends in clinical trials involving engineered biomaterials

Polymer-based Medical Implants

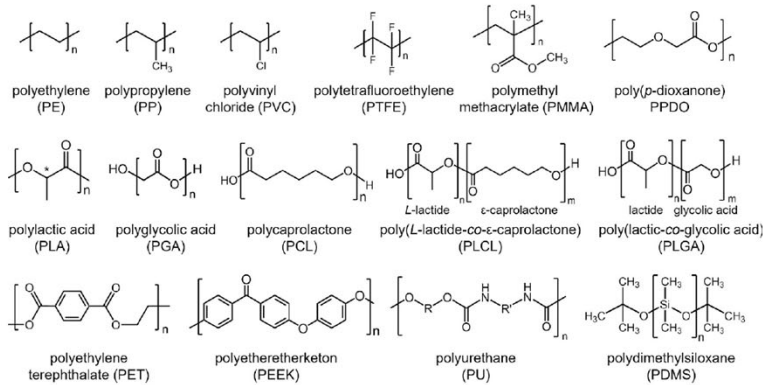


Fig. 2. Chemical structures of typical polymers for medical implants.

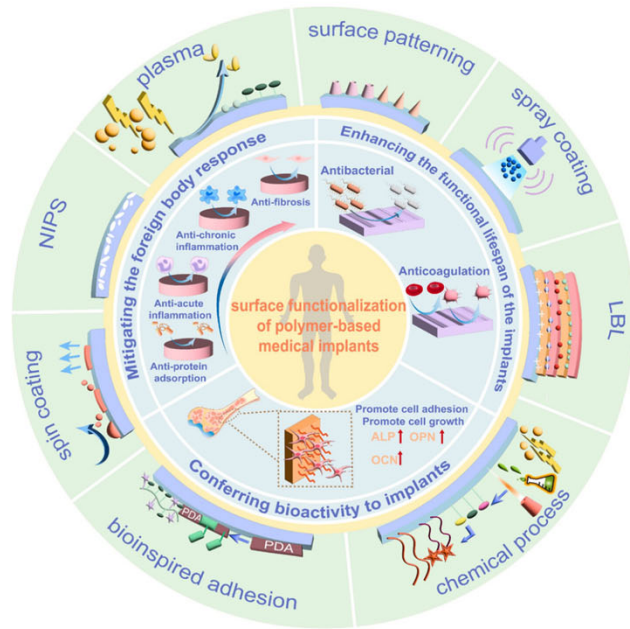


Table 1

Typical polymers in the fabrication of medical implants for clinical applications.

Types of medical polymers	Advantages	Disadvantages	Application
PDMS	Excellent mechanical flexibility and chemical stability	Surface hydrophobicity leading to biofouling, fibrous encapsulation	Breast prosthesis, artificial joint spacer, catheter
Ultra-High Molecular Weight Polyethylene	Biocompatibility, low coefficient of friction, high impact resistance and toughness	Wear particles trigger osteolysis, poor thermal stability	Artificial joint liners, spinal implants
PMMA	Excellent biocompatibility, injectability and mechanical strength	Biological inertness, exothermic reaction burns surrounding tissues	Bone cement, dental fillings, artificial lenses
PTFE	Excellent biocompatibility, chemical stability, and flexibility	Biological inertness	Artificial blood vessels, heart patches
PEEK	Excellent mechanical and physicochemical tolerance	Biological inertness, poor osteoinduction	Spinal fusion devices, dental implants, cranial prosthetic plates
PU	Excellent elasticity and flexibility, controllable degradation properties	Surface easily calcified, potential toxicity of long-term degradation products	Artificial heart valves, artificial blood vessels
PET	Excellent biocompatibility, mechanical properties	Biological inertness	Artificial blood vessels, artificial ligament
Polypropylene	Excellent biocompatibility, mechanical properties, ease of processing, low cost	Surface inertness	Hernia repair mesh, non-absorbable sutures
PVC	Adjustable flexibility	Plasticizer migration problems, lack of biocompatibility, limited mechanical properties	Catheter
PLA	Biodegradability and biocompatibility	Rapid decay of mechanical properties	Absorbable bone nails/plates
Polyglycolic acid (PGA)	Rapid degradation and absorption, biocompatibility	Excessive degradation rate, acidic degradation products induce localized inflammatory responses	Absorbable Suture
Polycaprolactone (PCL)	Superior flexibility and toughness, excellent biocompatibility, ideal material for drug slow-release carriers	Acidic degradation products induce localized inflammatory responses	Sutures, soft tissue repair implants
PLCL	Excellent mechanical properties and biocompatibility, controlled degradation rate, high machinability	Lack of bioactivity	Absorbable sutures, biodegradable stents
poly(lactic-co-glycolic acid) (PLGA)	Controlled degradation rate, excellent biocompatibility and safety, high machinability	Low mechanical strength, degradation rate influenced by the environment	Absorbable sutures, biodegradable stents
Poly(p-dioxanone)	Excellent biodegradability, biocompatibility, bioabsorbability	Easily hydrolyzed, poor thermal stability	Absorbable Suture
Hyaluronic acid hydrogel	Excellent biocompatibility, degradability, and functional modifiability	Limited mechanical properties, uncontrolled degradation, and insufficient long-term stability	Facial fillers, artificial vitreous substitutes
Polyvinyl alcohol hydrogel	Excellent biocompatibility, tunable mechanical properties, and 3D printing suitability	Limited mechanical properties, insufficient long-term stability	Cartilage implant

Design of Future Polymeric Biomaterials

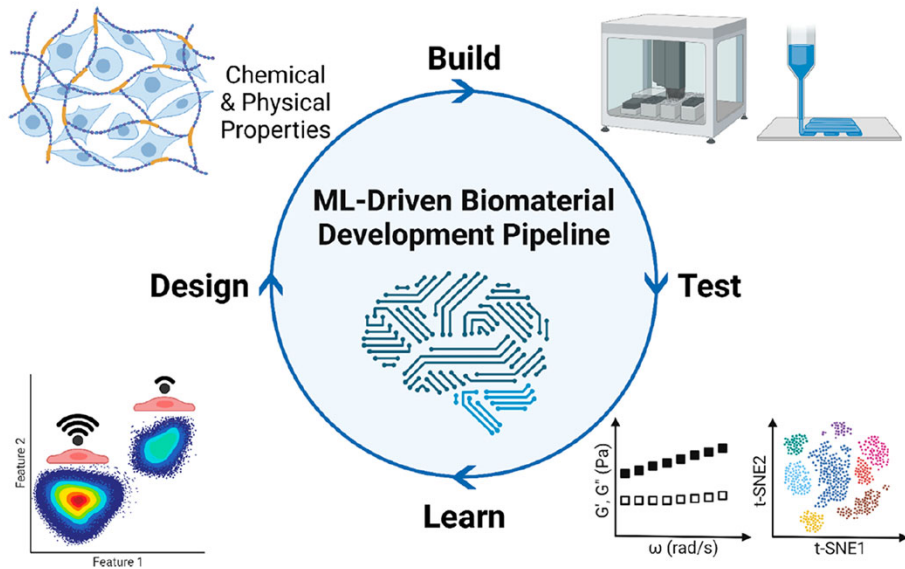


Figure 1. Schematic of an example Design-Build-Test-Learn paradigm for biomaterials development. Materials are initially designed with certain chemical and physical properties based on either rational design or a comprehensive survey of material features. Materials are then built and tested for desirable characteristics, ideally through high-throughput laboratory automation. This data, alongside design parameters, are then fed into a machine learning (ML) pipeline, where key patterns are extracted to create predictive models. These models can then be used to help design new material generations with targeted functionality. This figure was created with BioRender.

Meyer 2022, A user's guide to machine learning for polymeric biomaterials

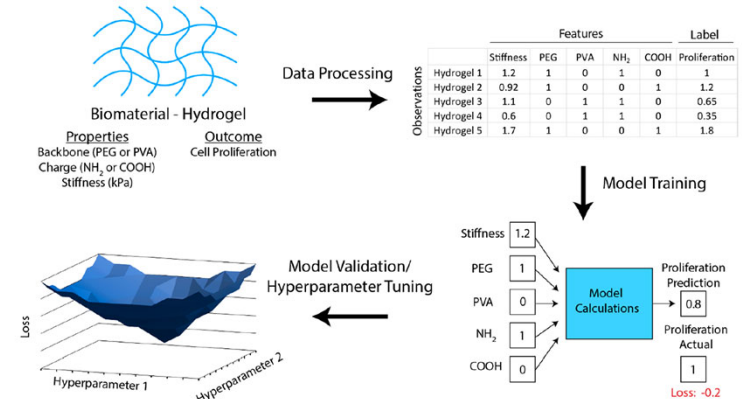


Figure 3. General machine learning (ML) pipeline. The first step involves the conversion of material features and labels into tabular data where categorical data has been encoded and numerical data has been scaled and normalized. In the second step, the model is trained such that the features are fed into the model and a predicted label is compared to the actual label to generate a loss term. Training iterations focus on modifying model parameters to minimize loss across the training data set. Finally, the model is validated against a test data set and model hyperparameters can be systematically tuned to minimize test set loss and find the optimal model design.

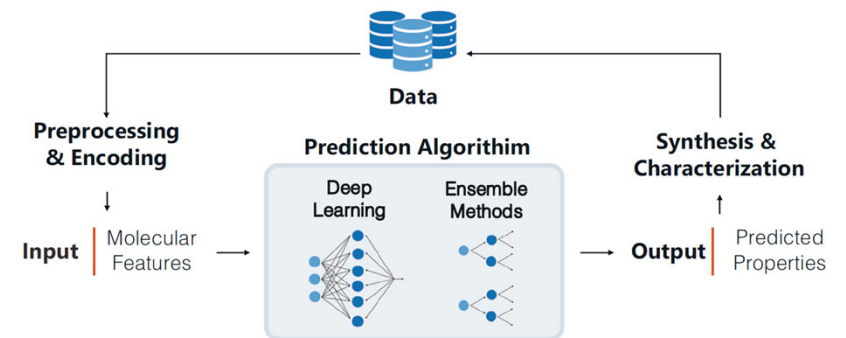


Fig. 2. General ML workflow for property prediction tasks.

McDonald 2023, Applied machine learning as a driver for polymeric biomaterials design

AI in Polymer Science

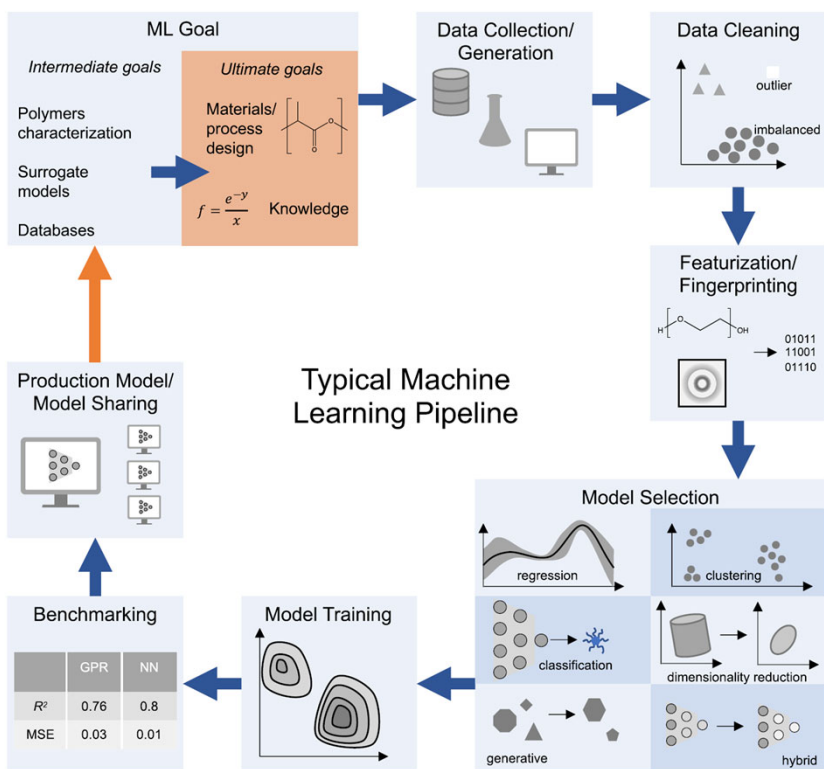


Figure 1. Typical pipeline for polymer ML. We emphasize that due to the rapidly growing field of ML, this pipeline does not cover all potential use cases. Acronyms include Gaussian process regression (GPR), neural network (NN), mean squared error (MSE).

Martin 2023, Emerging trends in machine learning: A polymer perspective

Table 1. Challenges Facing the Polymer Machine Learning Community.

category	challenge
polymer nature	polymer structure is stochastic and hierarchical
polymer nature	morphology is <u>process history dependent</u>
polymer nature, community	data is <u>not produced in standardized formats</u>
community	(meta)data is not complete, accessible, or shared
community	code is not accessible or open
community	<u>available data is small and disperse</u>
community	analyses are not reproducible
community	<u>models do not provide uncertainty quantification</u>
community	models are not explainable
community	models do not extrapolate
hardware	custom hardware is hard to use and adapt outside of initial study
hardware	commercial hardware has poorly documented or closed interfaces
all	large combination of skills needed to carry out studies

Polymers-focused researchers are using machine learning (ML) to accelerate the discovery of new materials and new knowledge, as well as working to overcome barriers such as **data scarcity**. For example, ML has enabled the generation of potential new polymer chemistries, new materials for gas separation membranes, prediction of properties for sequence-defined polymers, bioplastic design, guidance for improving 3D printing, improved contrast agents for magnetic resonance imaging (MRI) measurements, and methods for improved predictions of very small data sets.

Despite this progress, the field is still plagued by a variety of challenges that arise from both the unique and nonunique problems associated with polymer science. Unlike many kinds of materials, **the structure of polymers is inherently stochastic (that may be analyzed statistically) rather than a single structure**. This makes the representation of polymers in ML models a challenge. Furthermore, **“big data” ML (i.e., data set sizes close to a billion)** is currently out of reach for the polymer community as there are no publicly available databases that provide enough well-tagged polymer data to support such an endeavor. Many of the key measurements leveraged in the polymer community rely on instruments made by manufacturers that do not provide open interfaces and data models for their devices, impeding the creation of databases and making the integration of these devices into high-throughput and automation platforms nearly impossible. Table 1 expands upon the current list of challenges facing the polymers community and categorizes them into broad areas.

The Future

eLegs Exoskeleton: The Best Inventions of 2010

(https://content.time.com/time/specials/packages/article/0,28804,2029497_2030618_2029794,00.html)



Sarcos Robotics Guardian XO Full-Body Powered Exoskeleton. The Best Inventions of 2020

(<https://time.com/collection/best-inventions-2020/5911405/sarcos-robotics-guardian-xo/>)

Decades after RoboCop filled moviegoers' heads with cyborg-suit fantasies, science has finally delivered: next year, the Salt Lake City firm Sarcos Robotics will release the Guardian XO—one of the first commercially available full-body powered exoskeletons (\$8,500 monthly lease). The exoskeleton—an earlier iteration of which was recognized in TIME's 2010 list of Best Inventions—is effectively a wearable robot shell that enables wearers to lift as much as 200 lb. It's designed to prevent on-the-job injuries by reducing the strain of manual labor, and boasts as much as six hours of battery life. —J.R. Sullivan



5:1 Reduction of Weight

Hypershell X Ultra. Innovation for All Winner 2025

(<https://hypershell.tech/en-us/products/hypershell-x-ultra?variant=46795829477612>)



IFA Innovation Award Winner 2025



Edge of Tomorrow (Tom Cruise, Emily Blunt)

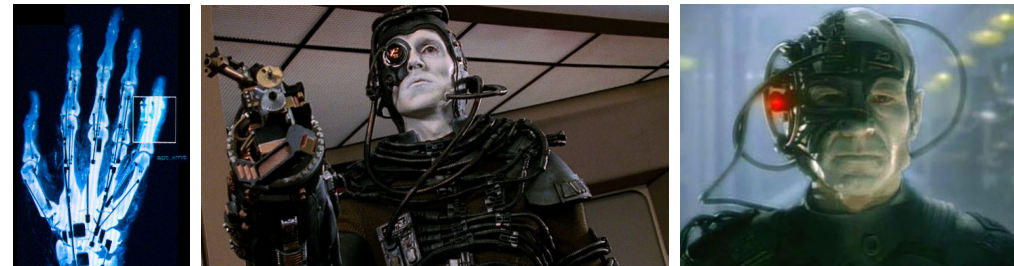
The film (2014) takes place in the year 2020 where Earth is invaded by an alien race called the Mimics, which hit Earth in 2015 via meteorite.

https://allyouneediskill.fandom.com/wiki/Edge_of_Tomorrow



Elysium (Matt Damon). In the year 2154, the very wealthy live on a man-made space station while the rest of the population resides on a ruined Earth.

<https://www.imdb.com/title/tt1535108/>



Star Date 2265

The Borg: Half Machine, Half Human

The Borg are cyborgs, having outward appearances showing both mechanical and biological body parts. Individual Borg are referred to as **drones**. Borg commonly have one eye replaced with a sophisticated ocular implant. Borg usually have one arm replaced with a prosthesis, bearing one of a variety of multipurpose tools in place of a humanoid hand. Since different drones have different roles, the arm may be specialized for myriad purposes such as medical devices, scanners, and weapons. Borg have flat, white skin, giving them an almost zombie-like appearance.

<https://en.wikipedia.org/wiki/Borg>

<https://www.denofgeek.com/tv/star-trek-and-the-taming-of-the-borg/>

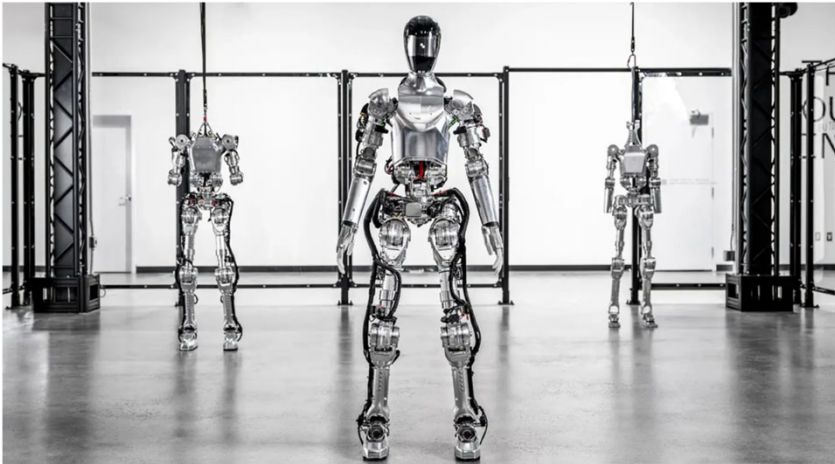
Avatar: The Year 2154 on Pandora



From 2024 to 2154

BMW plans to put humanoid robots in a South Carolina factory to do... something. In a race with Tesla, the automaker is 'exploring the latest technology' but remains vague on its automation goals.

By Mack DeGeurin | Published Jan 23, 2024



https://www.popsci.com/technology/bmw-humanoid-robot/?utm_term=pscene012424&utm_campaign=PopSci_Actives_Newsletter&utm_source=Social&utm_medium=email

Hyundai to deploy AI-powered humanoid robots at Georgia auto factory

Korean auto giant plans to use humanoid robots at its Georgia factory starting in 2028.

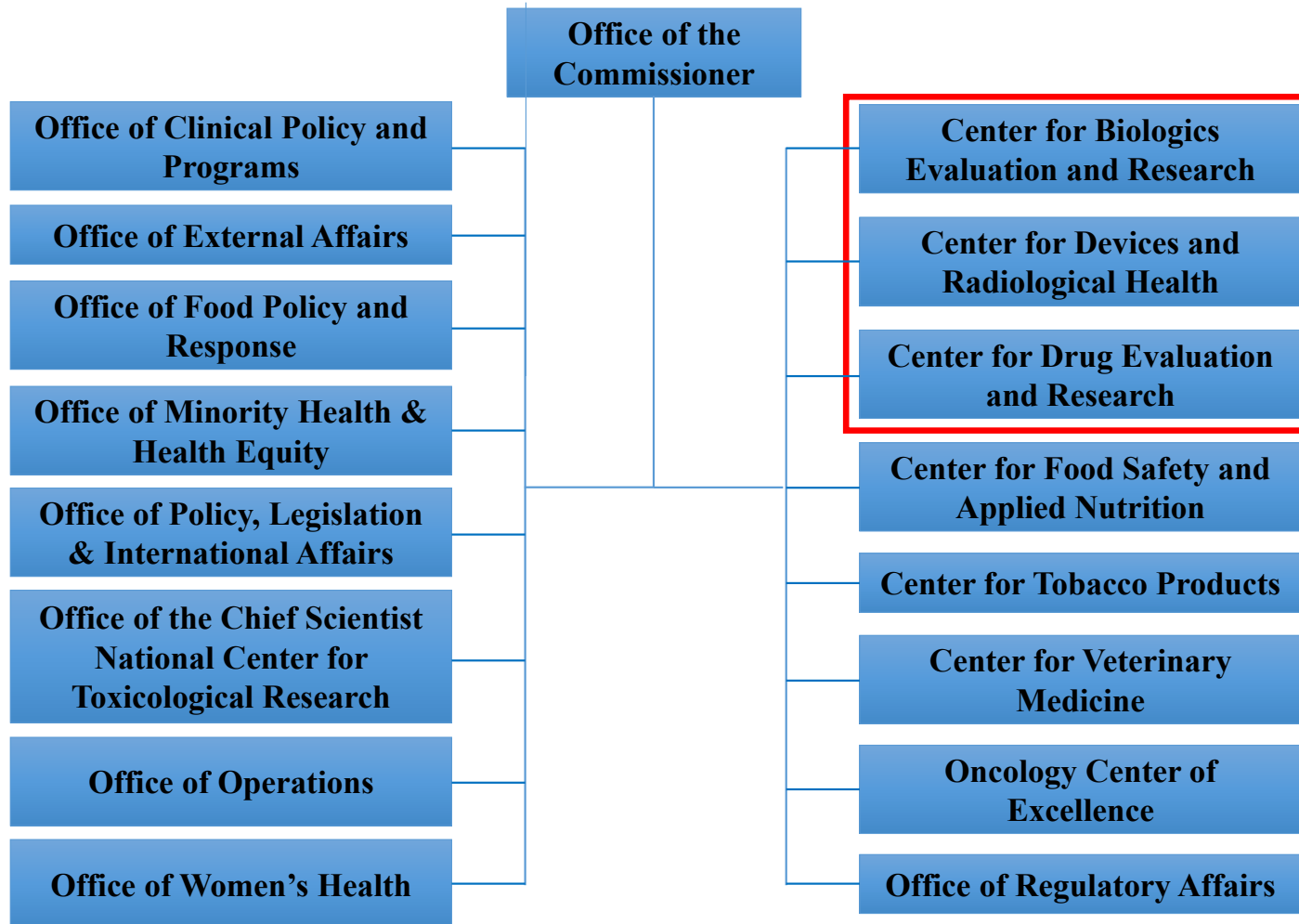


Hyundai Motor Group and its subsidiary, Boston Dynamics, unveil humanoid robots on Monday, Jan. 5, 2026, that will be deployed at the company's auto factories, including in Georgia. (Courtesy of Hyundai Motor Group)

<https://www.ajc.com/business/2026/01/hyundai-to-deploy-ai-powered-humanoid-robots-at-georgia-auto-factory/>

From Bench to Clinic

FDA Organization



Slide by **Kyung Sung, Ph.D.**
FDA Branch Chief
Cellular and Tissue Therapies Branch (CTTB)
Office of Cellular Therapy and Human Tissue (OCTHT)
Center for Biologics Evaluation and Research (CBER)
<https://www.fda.gov/vaccines-blood-biologics/biologics-research-projects/investigating-effects-cell-materials-interactions-safety-and-effectiveness-cell-based-products>

Diversity of Products Regulated by OTP (Office of Therapeutic Products)

CBER has established the new Office of Therapeutic Products (OTP) in 2023

- **Gene therapies (GT)**
 - Ex vivo genetically modified cells
 - Non-viral vectors (e.g., plasmids)
 - Replication-deficient viral vectors (e.g., adenovirus, adeno-associated virus, lentivirus)
 - Replication-competent viral vectors (e.g., measles, adenovirus, vaccinia)
 - Microbial vectors (e.g., Listeria, Salmonella)
- **Stem cells/stem cell-derived**
 - Adult (e.g., hematopoietic, neural, cardiac, adipose, mesenchymal)
 - Perinatal (e.g., placental, umbilical cord blood)
 - Fetal (e.g., neural)
 - Embryonic
 - Induced pluripotent stem cells (iPSCs)
- **Products for xenotransplantation**
- **Functionally mature/differentiated cells**
(e.g., retinal pigment epithelial cells, pancreatic islets, chondrocytes, keratinocytes)
- **Therapeutic vaccines and other antigen-specific active immunotherapies**
- **Blood- and Plasma-derived products**
 - Coagulation factors
 - Fibrin sealants
 - Fibrinogen
 - Thrombin
 - Plasminogen
 - Immune globulins
 - Anti-toxins
 - Snake venom antisera
- **Combination products**
 - Engineered tissues/organs
- **Devices**
- **Tissues**

Type of Devices Regulated by OTP



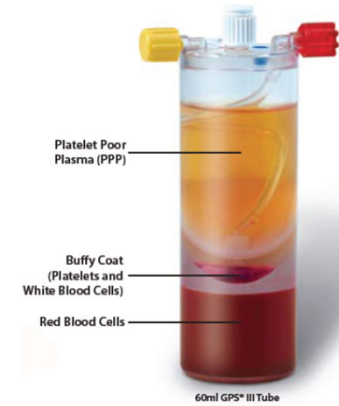
Cell Separators



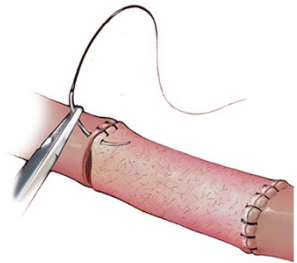
Fibrin Sealant Applicator



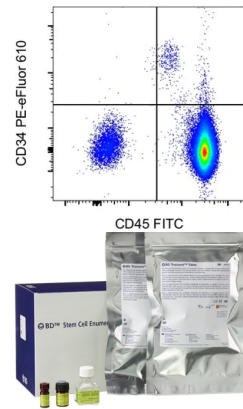
Autologous Skin Processor for Cell Suspension



PRP Devices and Kits



Tissue Engineered Vascular Graft



Stem Cell Enumeration IVD



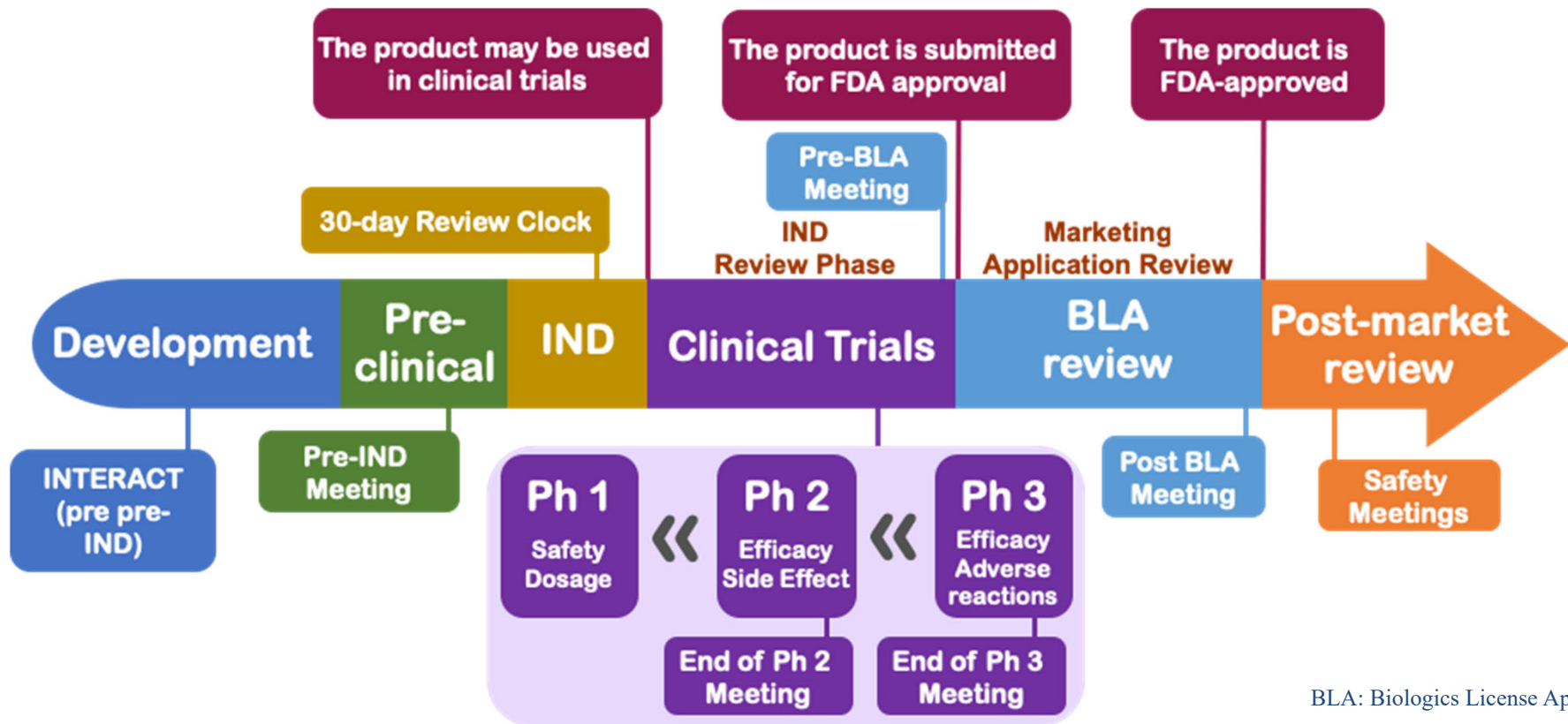
Extracorporeal Systems



Fat Processing Systems

Interactions with FDA Throughout the Product Lifecycle

Product development is an iterative process, with frequent FDA and sponsor interaction.

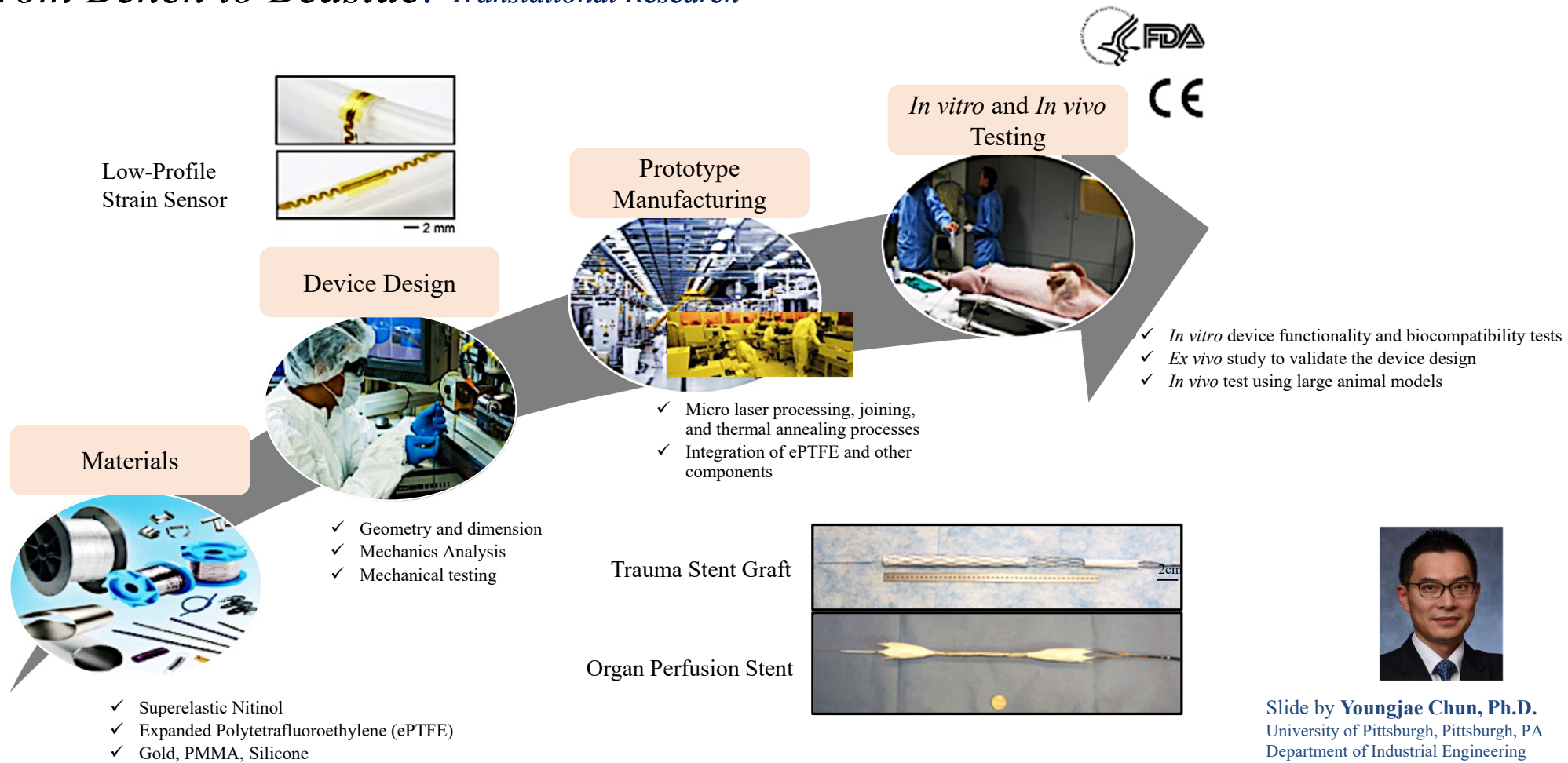


Sung et al., 2019, *Principles of Tissue Engineering*

Slide by Kyung Sung, Ph.D., FDA

Medical Device Development Process

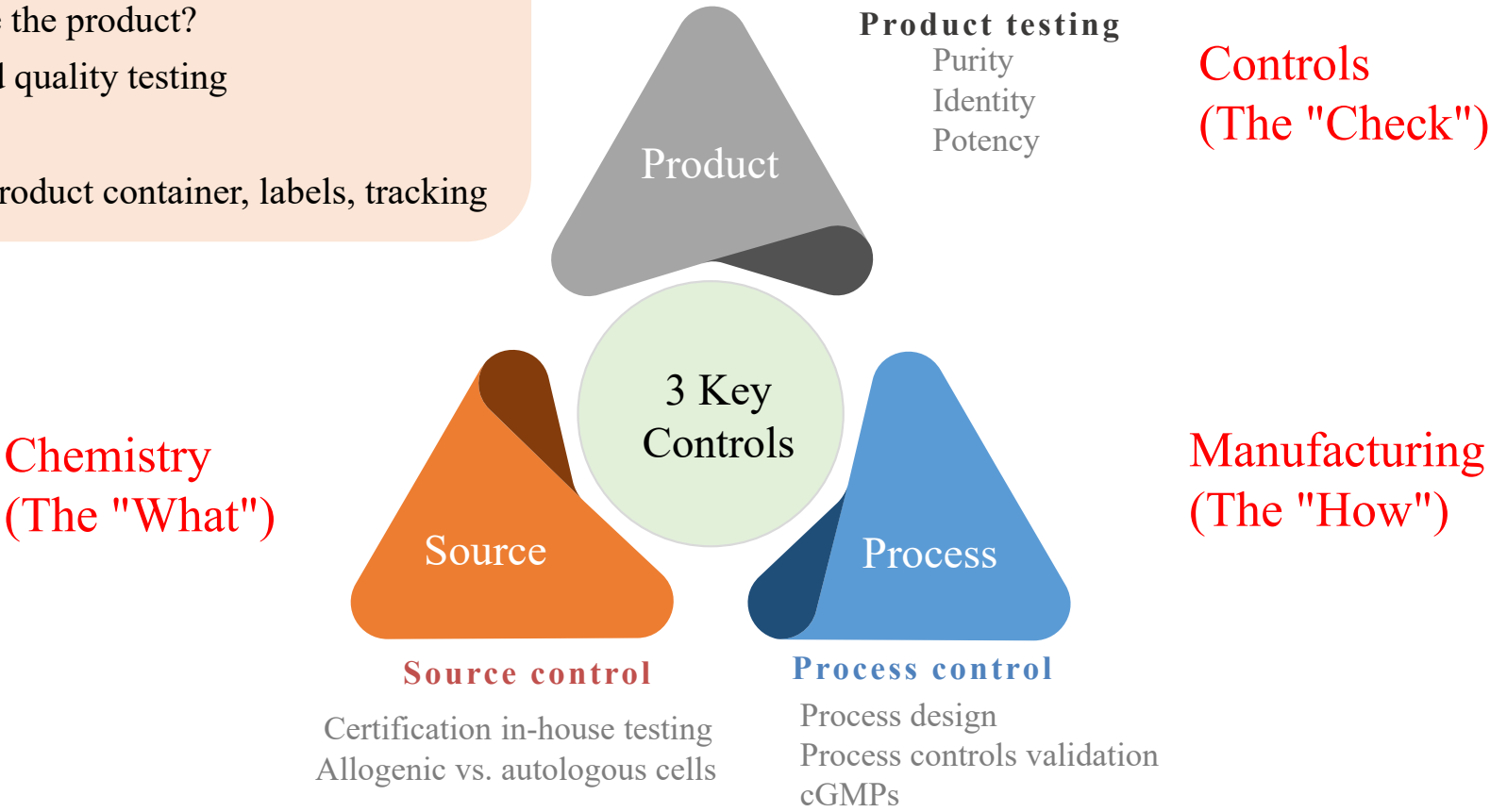
From Bench to Bedside: Translational Research



Slide by **Youngjae Chun, Ph.D.**
University of Pittsburgh, Pittsburgh, PA
Department of Industrial Engineering
Department of Bioengineering
<https://www.engineering.pitt.edu/people/faculty/young-jae-chun/>

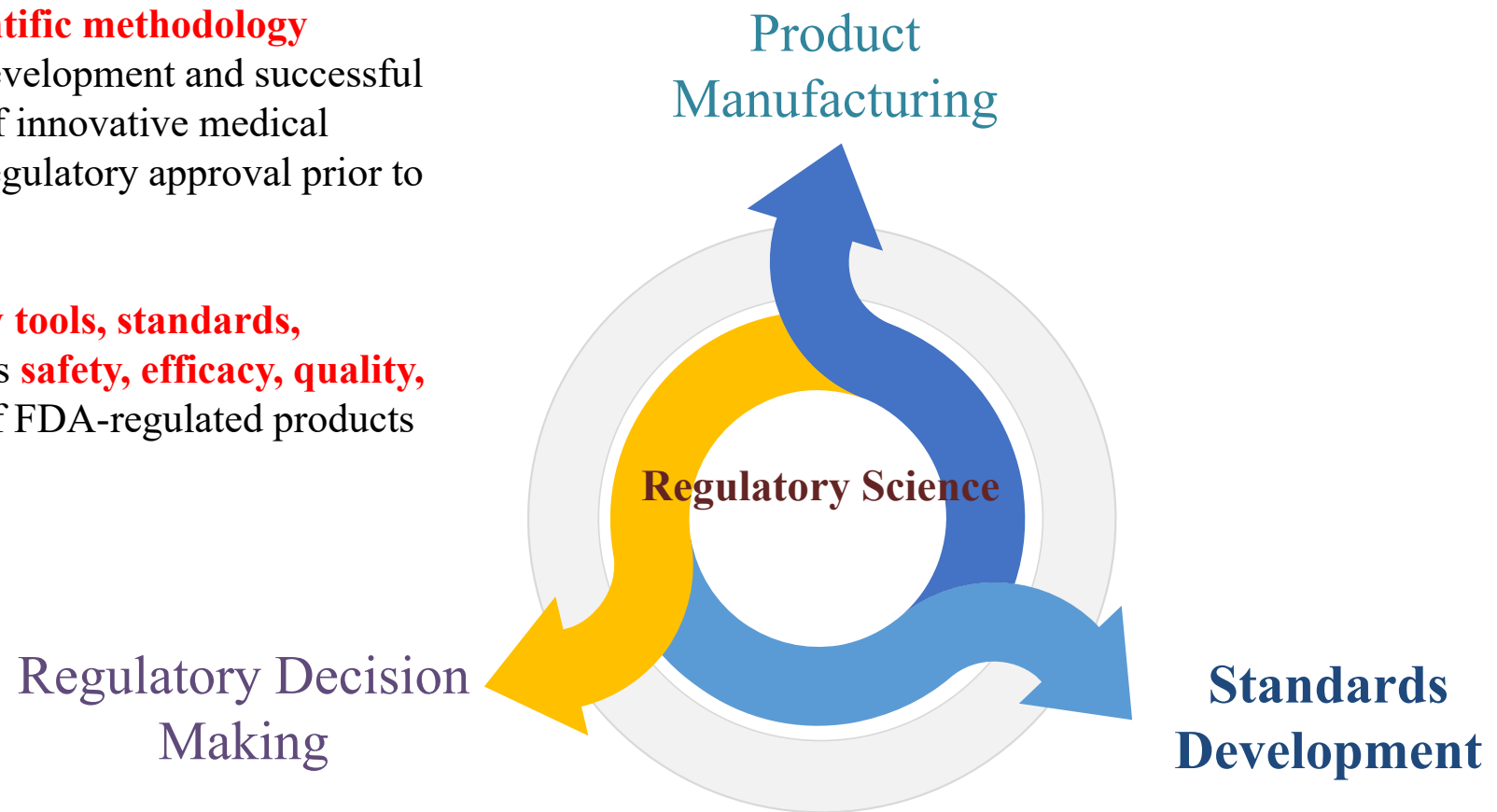
Chemistry, Manufacturing, and Controls (CMC)

- **CMC** = Product manufacturing and testing
- What do you use to make the product?
- How do you make the product?
- Product safety and quality testing
- Product stability
- Other controls – product container, labels, tracking

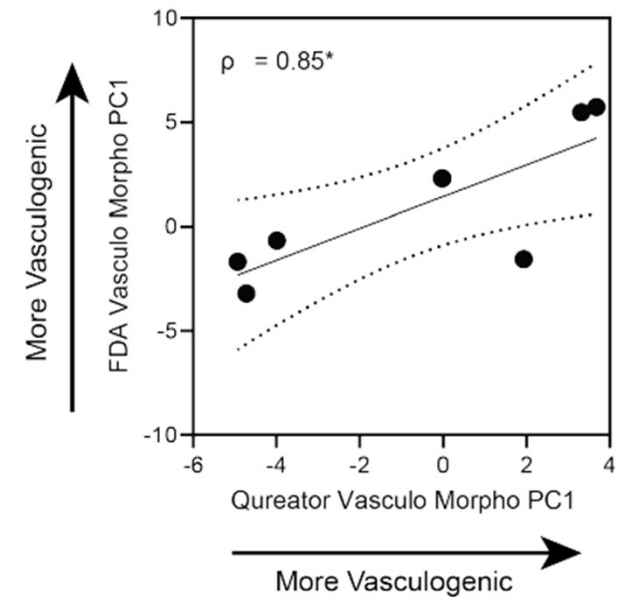


The Role of Regulatory Science

- **Application of scientific methodology** toward improving development and successful clinical translation of innovative medical products requiring regulatory approval prior to marketing
- Development of **new tools, standards, approaches** to assess **safety, efficacy, quality, and performance** of FDA-regulated products



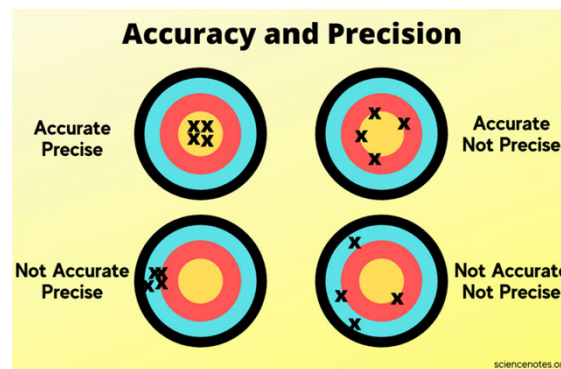
Interlaboratory Precision and Assay Reproducibility



Accuracy vs. Precision

Accuracy is how close a measurement is to the true value, while precision is how close measurements are to each other.

<https://sciencenotes.org/what-is-the-difference-between-accuracy-and-precision/>



Lam et al., 2022, Biomaterials

Slide by Kyung Sung, Ph.D., FDA

Contact Information

- **Kyung Sung, Ph.D.**
FDA Branch Chief
Cellular and Tissue Therapies Branch (CTTB)
Office of Cellular Therapy and Human Tissue (OCTHT)
Center for Biologics Evaluation and Research (CBER)
Kyung.sung@fda.hhs.gov
- **Regulatory Questions:**
OTP Main Line – (240) 402-8190
Email: OTPRPMS@fda.hhs.gov
- **Interactions with Office of Tissues and Advanced Therapies website:**
[Interactions with Office of Tissues and Advanced Therapies | FDA](#)
- **OTP Learn Webinar Series:**
<http://www.fda.gov/BiologicsBloodVaccines/NewsEvents/ucm232821.htm>
- **CBER website:** www.fda.gov/BiologicsBloodVaccines/default.htm
- **Phone:** 1-800-835-4709 or 240-402-8010
- **Consumer Affairs Branch:** ocod@fda.hhs.gov
- **Manufacturers Assistance and Technical Training Branch:**
industry.biologics@fda.hhs.gov
- **Follow us on Twitter:** <https://www.twitter.com/fdacber>

www.fda.gov



FDA Headquarters



Slide by Kyung Sung, Ph.D., FDA

Biocompatibility

Biocompatibility

The appropriate biological performance, either local or systemic, of a given implant in a specific application.

The desirable host response depends on the type of material implanted and its intended use. It may be complete inactivity and no interaction with the tissues surrounding the implanted materials, or a positive interaction that results in active participation by the cells surrounding the materials.

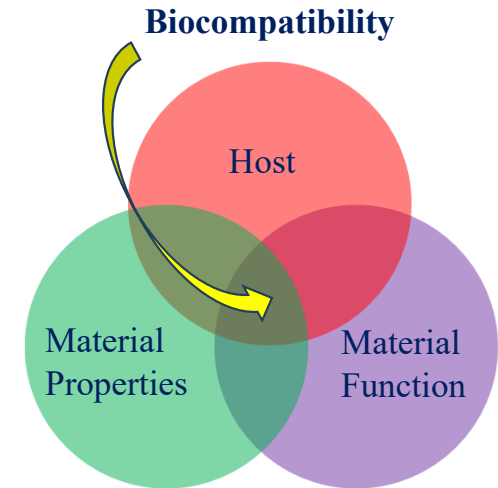
Biocompatibility is a dynamic, two-way process involving the time-dependent effects of the host on the material and of the material on the host.

The performance of a biomaterial should not be affected by the host, and the host should not be negatively affected by the implanted biomaterials.

No clear, absolute definition of biocompatibility exists yet, mainly because biomaterials are diverse and the field is still evolving.

Potential side effect:

Toxic, carcinogenic, immunogenic, and inflammatory responses.



Failure of Biomaterials and Biomedical Devices

1. Tissue Biocompatibility (Inflammation and Wound Healing)
2. Thrombosis (Blood Clotting)
3. Infections

Biomaterials-Tissue Local Interactions (at biomaterial-tissue interface)

Effect of material on host tissues

- Blood material interactions
- Modification of healing
- Inflammation
- Infection
- Tumorigenesis

Effect of environment on materials Physical-mechanical effects

- Wear
- Fatigue
- Corrosion
- Stress-corrosion cracking

Biological Effects

- Adsorption of tissue constituents by implant
- Enzymatic degradation
- Calcification

Systemic Interactions

- Embolization
- Hypersensitivity (itchy/redness)
- Elevation of implant elements in blood
- Particle transport to distal tissues

Device Associated Complications

- Thrombosis/thromboembolism
- Infection
- Exuberant or poor healing
- Biomaterial failure
- Adverse local tissue reaction
- Adverse systemic effect

ISO 10993

The ISO 10993 standard and the FDA guidance document present a structured program for **biocompatibility evaluation** in which matrices are presented that indicate required tests according to specific types of tissue contact and contact duration.

ISO 10993-18:2020. Biological evaluation of medical devices
Part 18: Chemical characterization of medical device materials within a risk management process

Components of ISO 10993 relevant to medical device manufacturers and available from MET include:

- ISO 10993-1:** Part 1: Evaluation and testing.
- ISO 10993-3:** Part 3: Tests for genotoxicity, carcinogenicity and reproductive toxicity.
- ISO 10993-4:** Part 4: Selection of tests for interactions with blood.
- ISO 10993-5:** Part 5: Tests for in vitro cytotoxicity.
- ISO 10993-6:** Part 6: Tests for local effects after implantation.
- ISO 10993-9:** Part 9: Framework for identification and quantification of potential degradation products.
- ISO 10993-10:** Part 10: Tests for skin sensitisation
- ISO 10993-11:** Part 11: Tests for systemic toxicity.
- ISO 10993-13:** Part 13: Identification and quantification of degradation products from polymeric medical devices.
- ISO 10993-14:** Part 14: Identification and quantification of degradation products from ceramics.
- ISO 10993-15:** Part 15: Identification and quantification of degradation products from metals and alloys.
- ISO 10993-16:** Part 16: Toxicokinetic study design for degradation products and leachables.
- ISO 10993-17:** Part 17: Establishment of allowable limits for leachable substances.
- ISO 10993-18:** Part 18: Chemical characterization of materials.
- ISO/TS 10993-19:** Part 19: Physico-chemical, morphological and topographical characterization of materials.
- ISO/TS 10993-20:** Part 20: Principles and methods for immunotoxicology testing of medical devices.
- ISO 10993-23:** Part 23: Tests for irritation.

Body Contact		Contact Duration Days	Testing Required													
			Chemical Characterisation	Cytotoxicity	Sensitisation	Irritation	Pyrogenicity	Acute Toxicity	Subacute Toxicity	Sub-Chronic Toxicity	Genotoxicity	Implantation	Haemocompatibility	Chronic Toxicity	Carcinogenicity	
Surface Devices	Skin	<=1	x	x	x	x										
		1-30	x	x	x	x										
		>30	x	x	x	x										
	Mucosal Membrane	<=1	x	x	x	x										
		1-30	x	x	x	x		x	x			x				
		>30	x	x	x	x		x	x	x	x	x		x		
Breached or compromised surfaces	<=1	x	x	x	x	x	x									
	1-30	x	x	x	x	x	x	x			x					
	>30	x	x	x	x	x	x	x	x	x	x		x	x		
Externally Communicating Devices	Blood path indirect	<=1	x	x	x	x	x	x					x			
		1-30	x	x	x	x	x	x	x				x			
		>30	x	x	x	x	x	x	x	x	x	x	x	x	x	x
	Tissue, Bone, Dentin	<=1	x	x	x	x	x	x								
		1-30	x	x	x	x	x	x	x		x	x				
		>30	x	x	x	x	x	x	x	x	x	x		x	x	
	Circulation blood	<=1	x	x	x	x	x	x				x		x		
		1-30	x	x	x	x	x	x	x		x	x	x			
		>30	x	x	x	x	x	x	x	x	x	x	x	x	x	x
Implant Devices	Tissue, Bone	<=1	x	x	x	x	x	x								
		1-30	x	x	x	x	x	x	x		x	x	x			
		>30	x	x	x	x	x	x	x	x	x	x		x	x	
	Blood	<=1	x	x	x	x	x	x				x	x	x		
		1-30	x	x	x	x	x	x	x		x	x	x			
		>30	x	x	x	x	x	x	x	x	x	x	x	x	x	x

Blood-Contacting Biomaterials

Blood-contacting Soft Tissue Replacements Biomaterials

1960

A GLANCE AT THE PAST



MEDICINE

First successful artificial heart valve

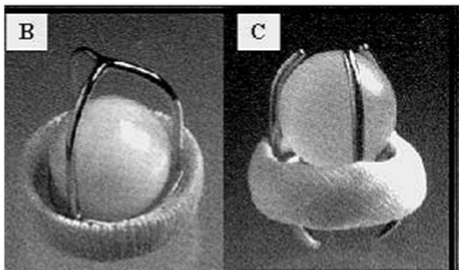
Surgeons in Oregon have saved a man's life and restored him to health by implanting a plastic and metal valve in his heart. The man has survived for three months since the operation—the longest anyone has ever lived with an artificial heart valve. A team of 23 surgeons and assistants, led by Dr. Albert Starr of the University of Oregon Medical School, implanted the new valve. Dr. Starr also designed the new valve, in collaboration with engineer Lowell Edwards.



▲ The valve consists of a silicone ball that moves freely within a metal cage.

Heart surgery developments

During World War II, surgeons began operating to remove fragments of bullets lodged inside combatants' hearts. To do so, they cut a small hole in the still-beating heart muscle, inserted a finger, and removed the foreign object. By around 1950, surgeons had extended this technique to widening narrowed heart valves. But more complex procedures were not possible until the invention of the heart-lung machine.



Calcification

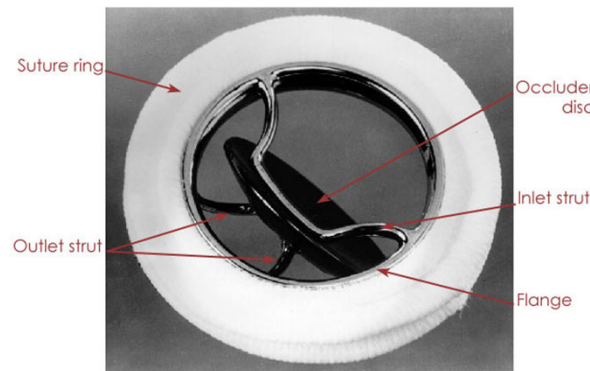
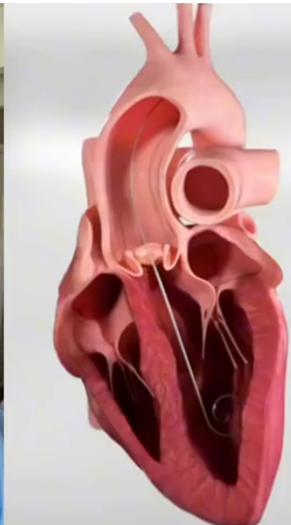
Heart valve prostheses

Mechanical heart valves:

Caged ball or caged disc type: polished CoCr alloy cage and silicone rubber ball, valve sewing ring made of knitted composite of PTFE and polypropylene cloth.

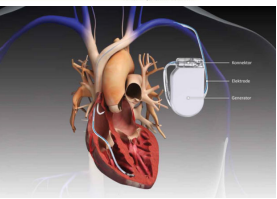
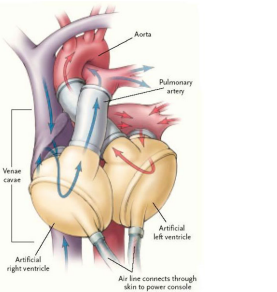
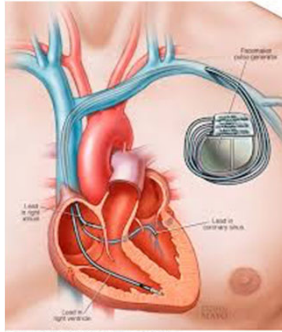
Tilting disc type: Pyrolytic carbon disc, guiding struts made of titanium or CoCr.

Bileaflet type: Pyrolytic carbon valves



Blood-contacting Soft Tissue Replacements Biomaterials

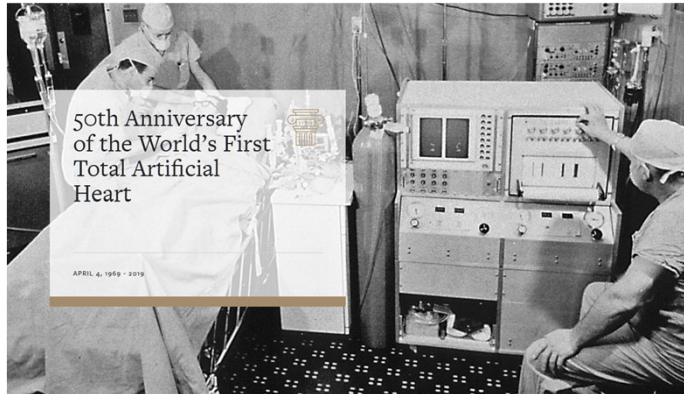
- Heart valve prostheses
- Vascular prostheses: Dacron, PTFE, Silicone rubber
- Cardiac pacemakers
- Blood oxygenator
- Extracorporeal dialysis
- Blood circulation tubing
- Intravascular catheter
- Cardiovascular stent



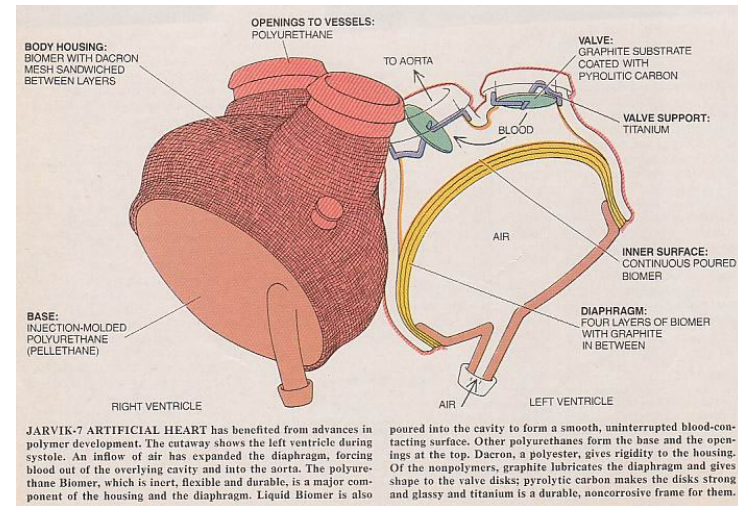
Silicone rubber

https://www.tiktok.com/@hashem.alghaili/video/7490277116450196758?_r=1&_t=ZP-8veSn1Y9qxC

Total Artificial Heart



<https://www.texasheart.org/50th-anniversary-of-the-worlds-first-total-artificial-heart/>

JARVIK-7 ARTIFICIAL HEART has benefited from advances in polymer development. The cutaway shows the left ventricle during systole. An inflow of air has expanded the diaphragm, forcing blood out of the overlying cavity and into the aorta. The polyurethane Biomer, which is inert, flexible and durable, is a major component of the housing and the diaphragm. Liquid Biomer is also poured into the cavity to form a smooth, uninterrupted blood-contacting surface. Other polyurethanes form the base and the openings at the top. Dacron, a polyester, gives rigidity to the housing. Of the nonpolymers, graphite lubricates the diaphragm and gives shape to the valve disks; pyrolytic carbon makes the disks strong and glassy and titanium is a durable, noncorrosive frame for them.

Polyurethane-coating

Scientific American

Left Ventricular Assist Device

LEFT VENTRICULAR ASSIST DEVICES

Restoring Flow

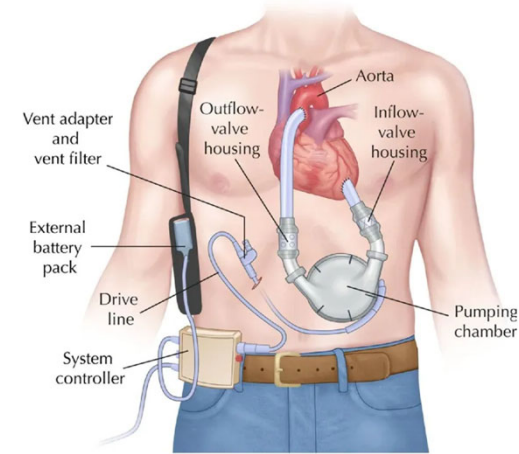
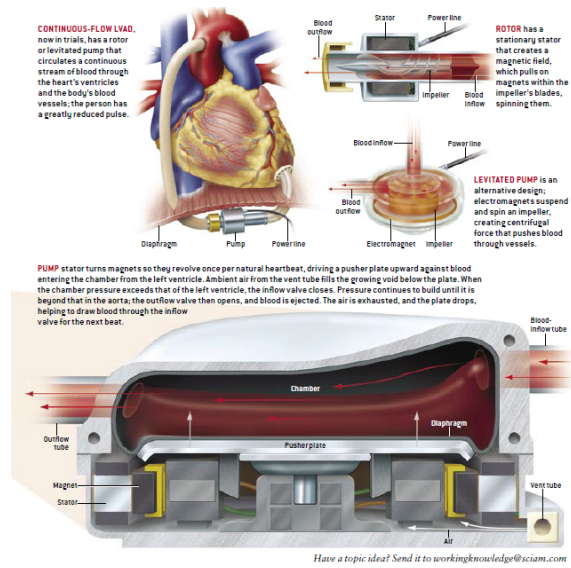
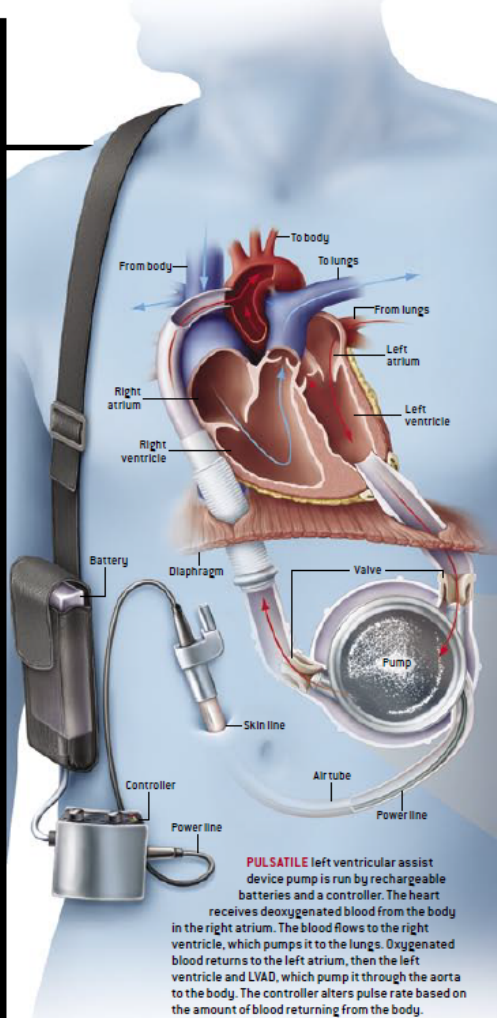
Although artificial hearts are stymied by complications, left ventricular assist devices (LVADs) are extending lives. Doctors began implanting them two decades ago to keep heart failure patients alive while they waited for weeks or months for an available transplant organ. Today improved designs are being installed as final fixes. Indeed, the distinction between an LVAD used as a bridge to transplant and as a permanent aid "is disappearing," says Kiyotaka Fukamachi, head of the Cleveland Clinic's Cardiovascular Dynamics Laboratory. "Some patients who received an LVAD as a bridge have been living with it for two or three years."

A healthy left ventricle pumps freshly oxygenated blood through the aorta to the body. LVADs help the ventricle or take over its operations if the chamber is weak or has stopped functioning. First-generation designs, which still prevail, are pulsatile: an implanted pump pushes blood in pulses like a natural heart. Second-generation LVADs are smaller, relying on a rotor that continuously streams blood. Engineers are evaluating experimental, third-generation devices that use magnetically levitated rotors, reducing moving parts.

Yet "no one approach is necessarily better than the others," Fukamachi says. "The choice depends on a patient's circumstances." The pulsatile machines, including Thoratec Corporation's HeartMate I and World Heart Corporation's Novacor, may still provide the best option if a patient needs a full takeover. Continuous-flow models such as MicroMed Cardiovascular's DeBakey can be smaller and simpler because they do not require valves or a vent tube. Levitated machines may show less wear over time. (In the U.S., HeartMate I is approved for bridge and permanent therapy; Novacor is approved for bridge. Other models are in trials.)

Complications are involved, of course. A wire must protrude from the body to a controller and batteries, leading to infection in up to 15 percent of patients. Blood clots can form inside pumps, so patients must live on anticoagulants, which increase the chance for problematic bleeding. Device failure occurs, too. But doctors are likely to implant more LVADs because heart donors remain scarce. Only 2,100 transplants are performed in the U.S. every year, whereas 3,500 to 4,000 people are perennially on the waiting list.

—Mark Fischetti



<https://coreem.net/core/ventricular-assist-devices/>

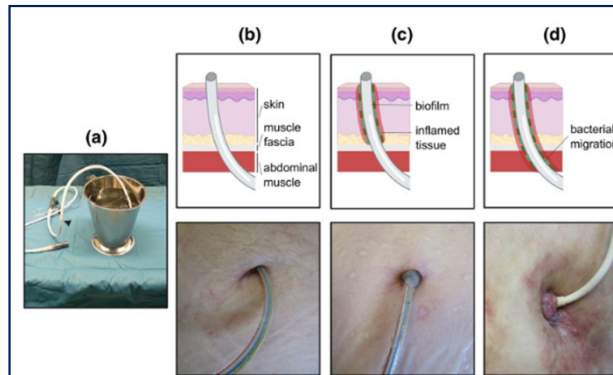


Fig. 2 Percutaneous LVAD drivelines may be subject to **infections**. (a) Pre-implanted LVAD driveline with the velour section immersed in the container. (b) An implanted LVAD driveline through the human skin. The lower image depicts an infection-free exit of the percutaneous LVAD driveline. © Biofilm formation at the upper layers of the human skin may lead to superficial infection, sparing the muscle fascia. The lower image depicts a patient with a **superficial infection**. (d) Bacterial migration into the lower layers of the skin may lead to deep infection involving the muscle fascia. The lower picture depicts a patient with **deep driveline infection**. (Kourouklis 2021, Systems of conductive skin for power transfer in clinical applications)

Biohybrid Robotic Ventricular Platform

Robotic: the use of programmable actuators that mimic the mechanical function of biological muscle.

The increasing recognition of the right ventricle (RV) necessitates the development of RV-focused interventions, devices and testbeds. In this study, we developed a soft robotic model of the right heart that accurately mimics RV biomechanics and hemodynamics, including free wall, septal and valve motion. This model uses a biohybrid approach, combining a chemically treated endocardial scaffold with a soft robotic synthetic myocardium. When connected to a circulatory flow loop, the robotic right ventricle (RRV) replicates real-time hemodynamic changes in healthy and pathological conditions, including volume overload, RV systolic failure and pressure overload. The RRV also mimics clinical markers of RV dysfunction and is validated using an in vivo porcine model. Additionally, the RRV recreates chordae tension, simulating papillary muscle motion, and shows the potential for tricuspid valve repair and replacement in vitro. This work aims to provide a platform for developing tools for research and treatment for RV pathophysiology.

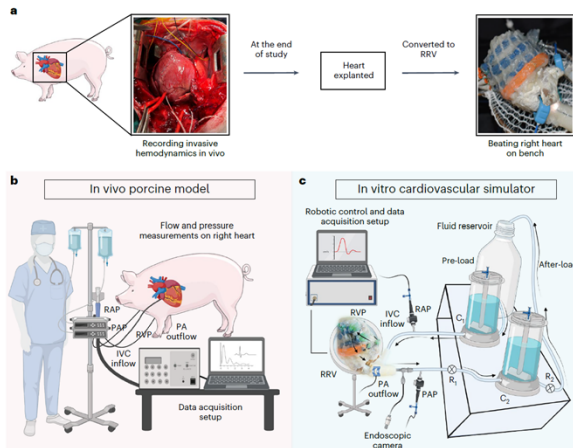


Fig. 3 | Comparison of in vivo and in vitro RRV hemodynamics. **a**, The RRV was constructed using a freshly explanted porcine heart. Hemodynamic data were collected from juvenile pigs in vivo and used to validate the accuracy of the in vitro model. **b**, The surgical and data acquisition setup to record invasive hemodynamic measurements in pig models. **c**, A mock circulatory flow loop incorporating hydraulic and mechanical components to simulate the pulmonary and systemic circulation on a laboratory bench. The RRV serves as the primary pump, driving flow through the loop. **d**, Right-sided pressure waveforms

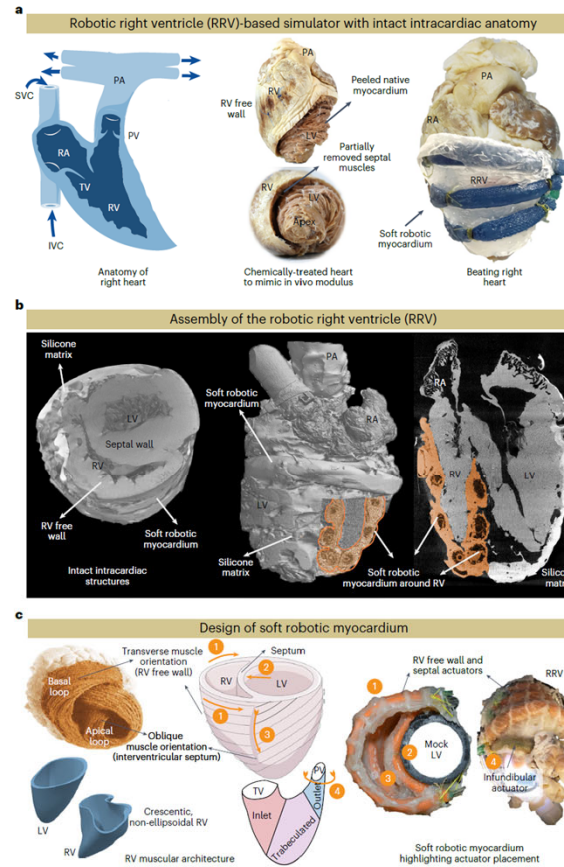


Fig. 4 | An overview of the RRV and its architecture. **a**, Overview of the bioinspired and biomimetic approach used to create a biohybrid beating right heart. Initially, a freshly explanted porcine heart underwent chemical treatment, after which the native myocardium was hand-dissected and replaced with a robotic counterpart while preserving the endocardial scaffold. **b**, The assembly of the RRV was imaged with micro-CT, revealing the preserved intracardiac structures. **c**, Schematic of the RV's complex shape, fiber orientation and wall motion (left). The image of the heart showing fiber orientation in the basal and

apical loops is reprinted from Buckberg et al., with permission from Elsevier. The physical model of the soft robotic myocardium shows the placement of individual actuators in the synthetic myocardium (right). The outflow tract of the RV contains infundibular muscles that also contribute to RV ejection through contraction. The contraction of the outflow region can be achieved by placing a circumferential actuator across the infundibulum. The numbers denote the respective actuator placement corresponding to the RV motion shown in the schematics on the left. SVC, superior vena cava.

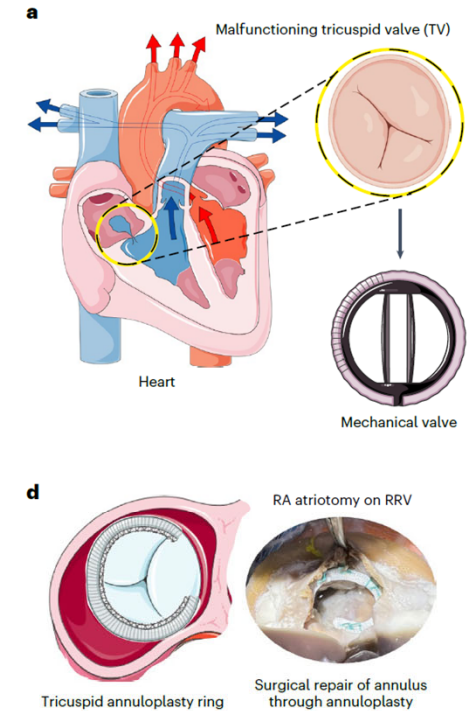


Fig. 5 | A platform for testing right heart interventions. **a**, As an example, the benchtop RRV model is used to test devices for TR. In this scenario, a mechanical valve is substituted for the damaged valve. **b**, To replace the native valve, a surgical right atrial atriotomy is performed. **c**, TR before and after intervention, shown by flow measurements for three cycles and a regurgitant fraction calculated over 10 cycles, demonstrating that the ability to study both healthy and pathological tricuspid flow in the same model allows for more accurate and comprehensive comparisons of the impact of different interventions on the cardiovascular system. Data show average \pm s.d. for 10 cycles ($*P < 0.0001$ (exact value: 1.18631×10^{-7}), calculated using one-way ANOVA (Tukey test with a significance level of 0.05)). **d**, Surgical implantation of prosthetic annuloplasty rings (32 mm and 24 mm) at the tricuspid annulus through right atrial atriotomy.

Singh 2023, Robotic right ventricle is a biohybrid platform that simulates right ventricular function

Biohybrid Robotic Ventricular Platform

In the context of the **Robotic Right Ventricle (RRV)** system—a biohybrid model often used in cardiovascular research—the term "**robotic**" refers to **the use of soft, programmable actuators that mimic the mechanical function of biological muscle**.

Instead of a traditional metal robot, this "robotic" system uses advanced materials to replicate the complex pumping action of the heart's right ventricle. Here is what "robotic" specifically implies in this system:

1. Soft Actuation (Artificial Muscles)

The "robotic" component consists of **soft robotic actuators** (often made of silicone or specialized polymers) that wrap around a biological heart or a synthetic inner chamber. When pressurized with air or fluid, these actuators contract and expand, mimicking how real myocardial fibers shorten to pump blood.

2. Programmable Motion

Unlike a passive pump, a robotic system allows researchers to precisely control:

- **Timing:** Synchronizing the "beat" to match specific heart rates.
- **Contraction Patterns:** Adjusting which part of the ventricle squeezes first (e.g., mimicking a bundle branch block or a healthy rhythm).
- **Force:** Increasing or decreasing the pressure to simulate high or low blood pressure scenarios.

3. Biohybrid Integration

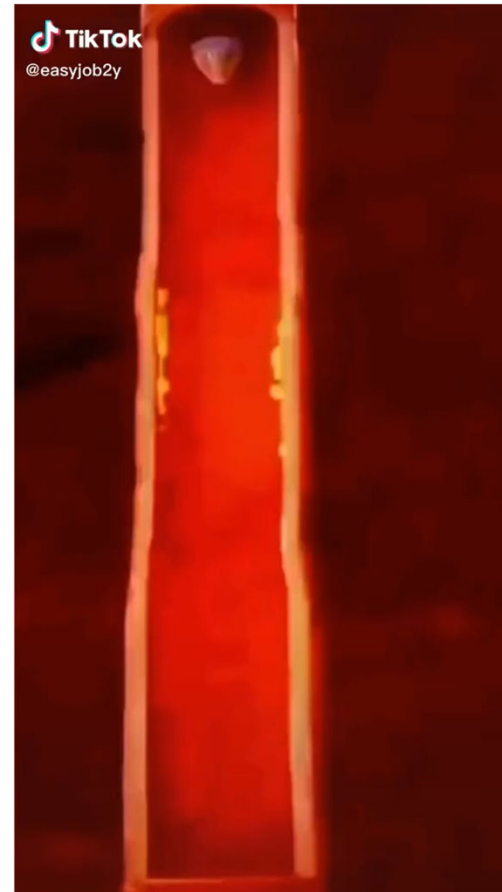
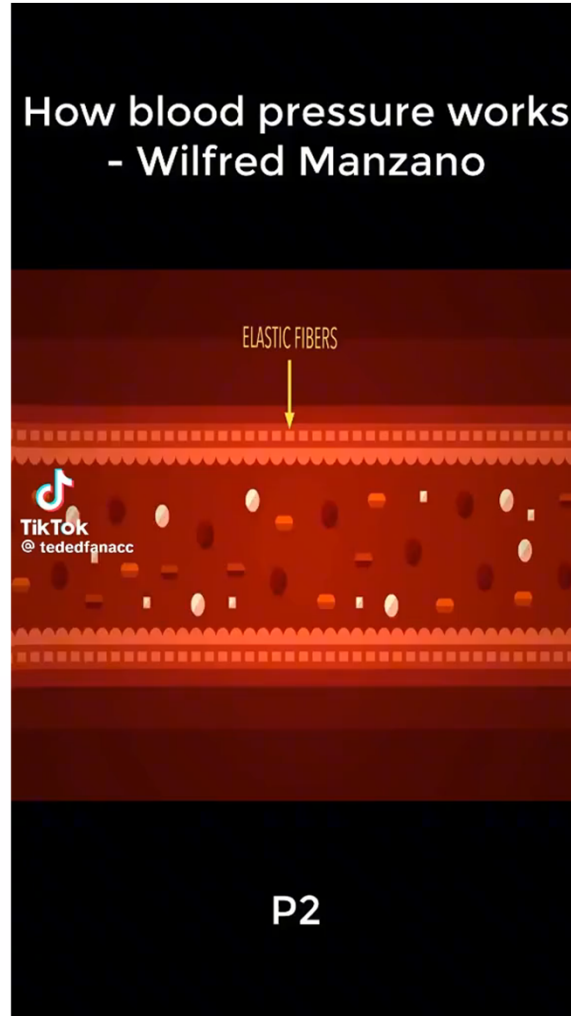
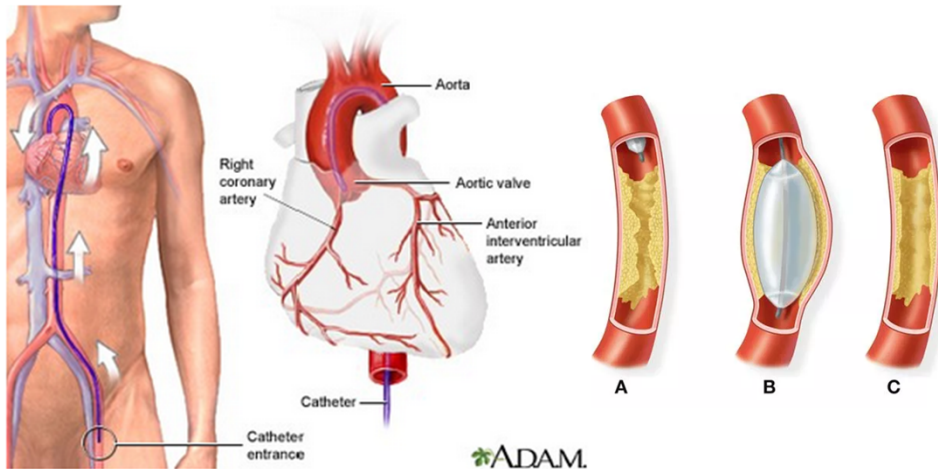
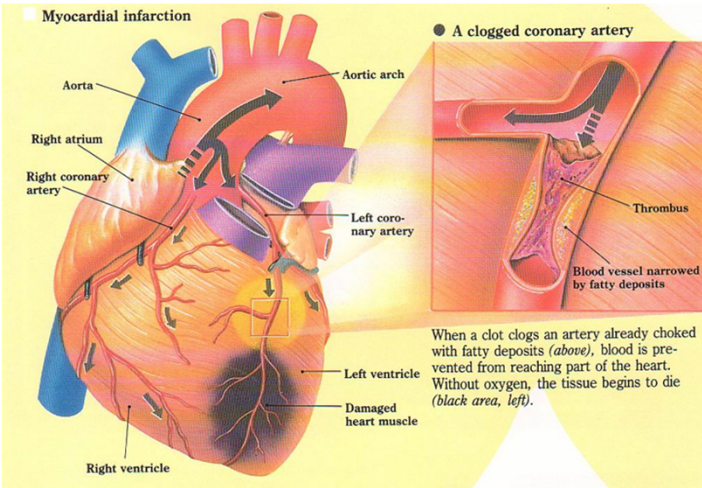
The term "robotic" is used because it creates a **biohybrid interface**. It combines:

- **Biological Tissue:** Often a chemically "fixed" or decellularized natural heart (the scaffold).
- **Synthetic Robotics:** The external "sleeve" or internal "matrix" that provides the mechanical energy to make that tissue move again.

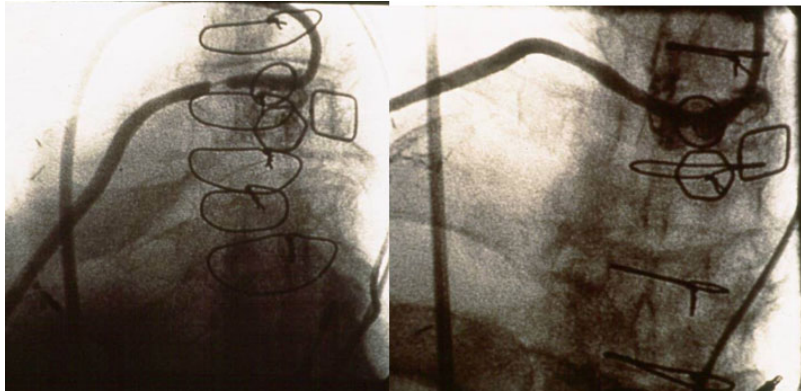
In the RRV, **the polymer isn't just a casing; it is the engine of the heart**.

Interventional Cardiology and Removing Plaque

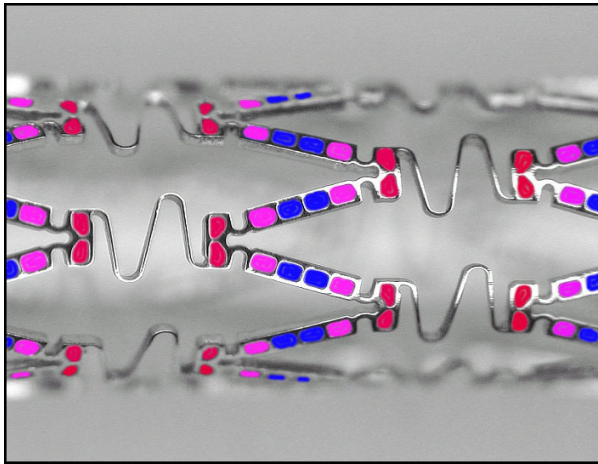
Heart Attack



Cardiovascular Stents & Drug-Eluting Stents



Drug-Eluting Stents



**Drug-Device
Combination Product**

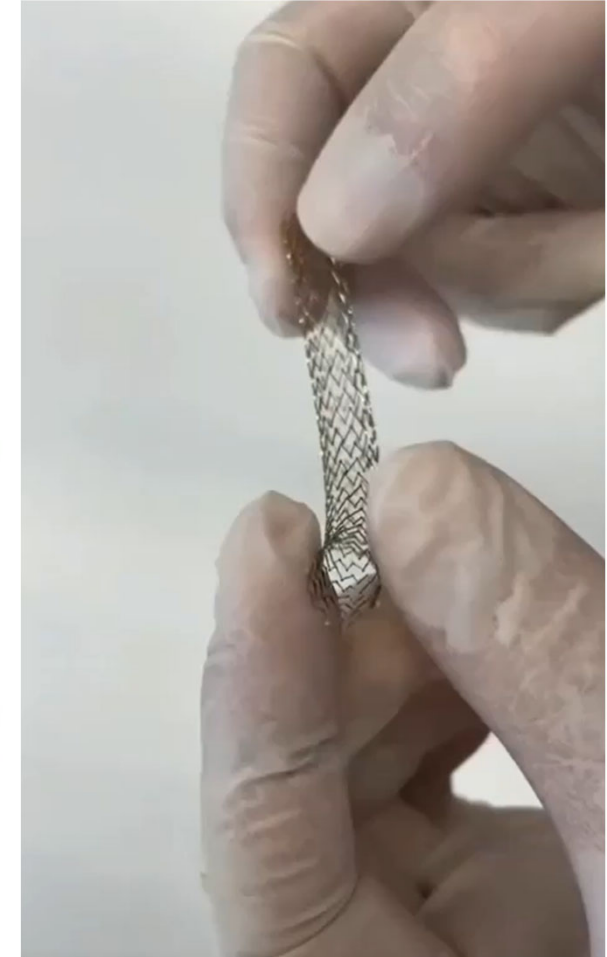
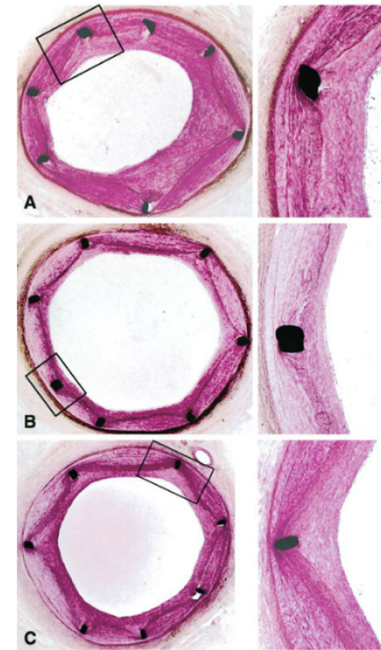
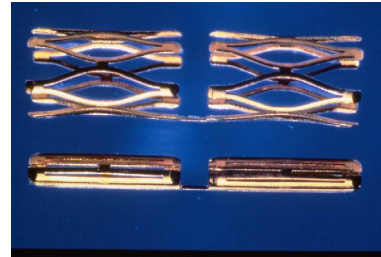
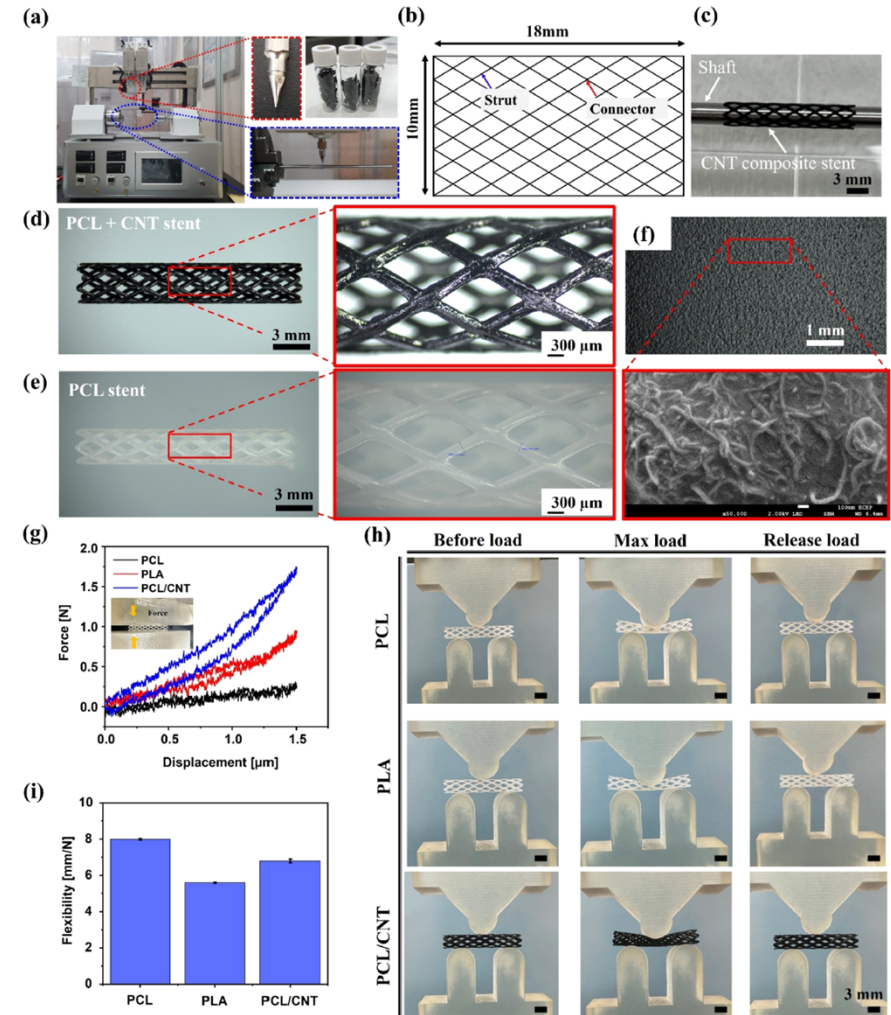
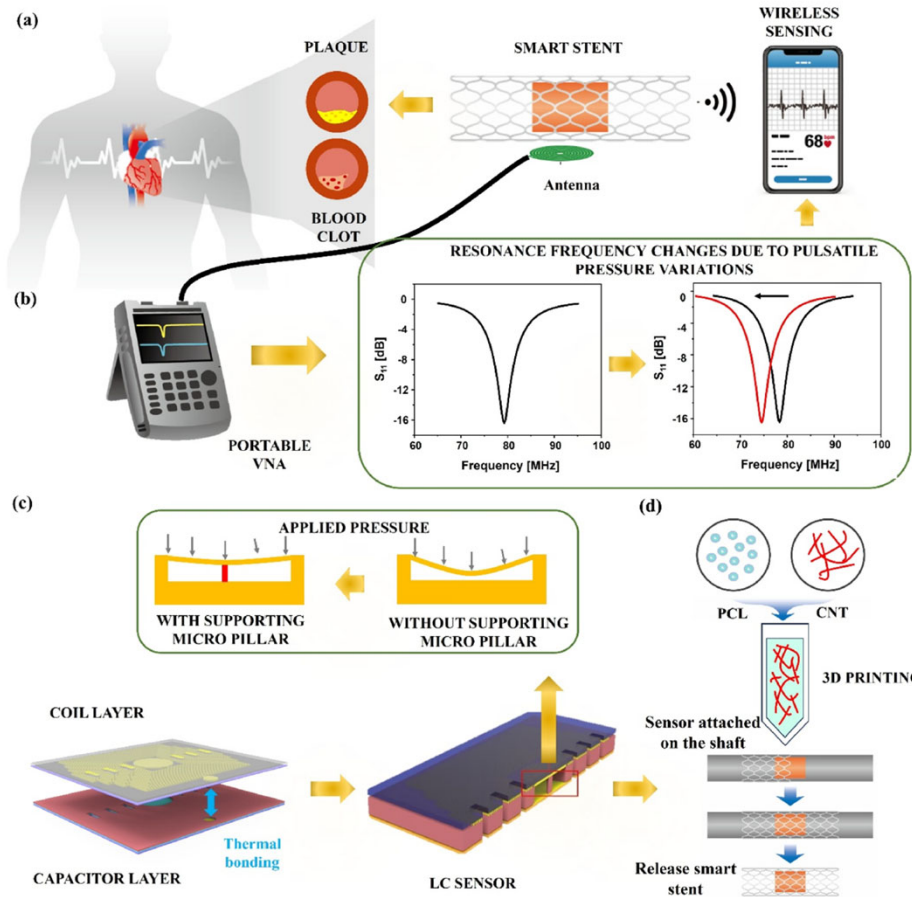


Figure 5. Representative sections of arteries at site of stent bridges (Paragon stain at 20 and 80 magnification). A, Bridge from bare metal control. Healing is complete with bridge (B) covered by the fibromuscular neointima. B, Bridge from paclitaxel stent. C, Control with polymer but no drug in any part of the stent. (Finkelstein 2003, Local drug delivery via a coronary stent with programmable release pharmacokinetics. Circulation DOI: 10.1161/01.CIR.0000050367.65079.71)

Cardiovascular Stents

3D-Printed carbon nanotube (CNT)-Reinforced **Bioresorbable** Vascular Scaffold (polycaprolactone (PCL)-based scaffolds)



Oyunbaatar 2025, 3D-printed CNT-reinforced bioresorbable vascular scaffold with enhanced mechanical stability and integrated wireless pressure

Surface Modification

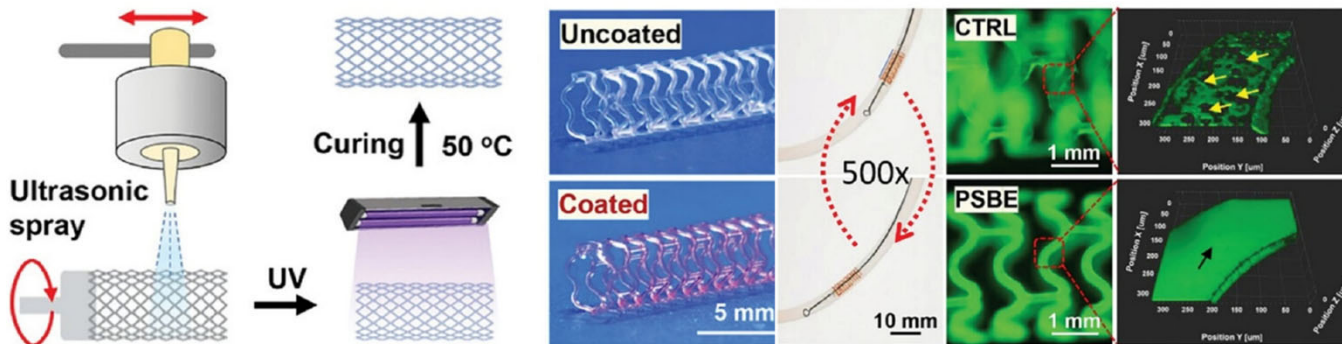


Fig. 8. Surface functionalization based on the atomized spraying method. (C) Hydrogel coating on PLLA scaffolds.

Drug-Device Combination Product

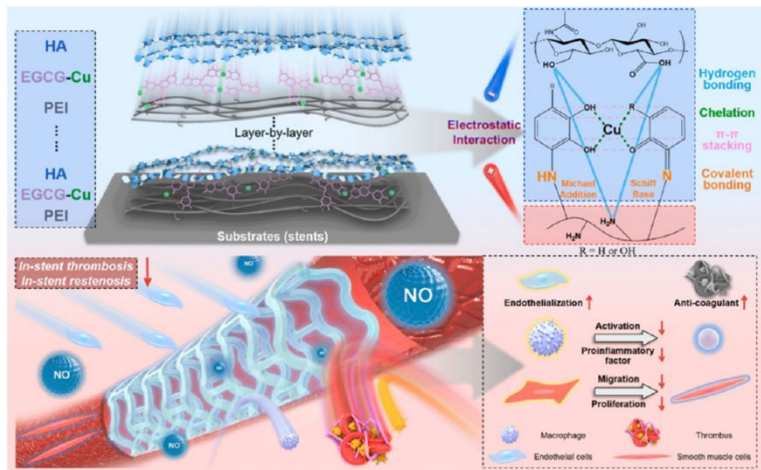
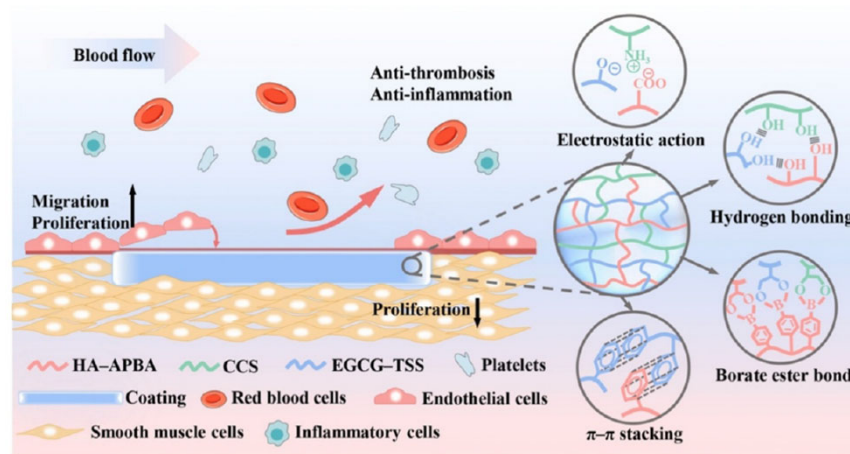


Fig. 9. Surface functionalization based on the layer-by-layer assembly method. (C) Metal-phenolic network-assisted construction of multilayer analog endothelial coatings for vascular scaffolds.



Fig. 5. Surface functionalization of implants based on the plasma treatment method. (A) Schematic of the process flow for constructing stable anti-adhesion and lubrication coatings on the TPU surfaces.



Luo 2026, Engineering surfaces of polymer-based medical implants for tissue repair and regeneration

(Drug-Device) Combination Product

Combination products are therapeutic and diagnostic products that combine drugs, devices, and/or biological products. FDA expects to receive large numbers of combination products for review as technological advances continue to merge product types and blur the historical lines of separation between FDA’s medical product centers, which are made up of the Center for Biologics Evaluation and Research (CBER), the Center for Drug Evaluation and Research (CDER), and the Center for Devices and Radiological Health (CDRH). **Because combination products involve components that would normally be regulated under different types of regulatory authorities**, and frequently by different FDA Centers, they raise challenging regulatory, policy, and review management challenges. **Differences in regulatory pathways for each component can impact the regulatory processes for all aspects of product development and management**, including preclinical testing, clinical investigation, marketing applications, manufacturing and quality control, adverse event reporting, promotion and advertising, and post-approval modifications.

<https://www.fda.gov/combination-products/about-combination-products>

Combination products are defined in 21 CFR 3.2(e). (Code of Federal Regulations)

The term combination product includes:

1. **A product comprised of two or more regulated components**, i.e., drug/device, biologic/device, drug/biologic, or drug/device/biologic, that are physically, chemically, or otherwise combined or mixed and produced as a single entity;
2. Two or more separate products packaged together in a single package or as a unit and comprised of drug and device products, device and biological products, or biological and drug products;
3. A drug, device, or biological product packaged separately that according to its investigational plan or proposed labeling is intended for use only with an approved individually specified drug, device, or biological product where both are required to achieve the intended use, indication, or effect and where upon approval of the proposed product the labeling of the approved product would need to be changed, e.g., to reflect a change in intended use, dosage form, strength, route of administration, or significant change in dose; or
4. Any investigational drug, device, or biological product packaged separately that according to its proposed labeling is for use only with another individually specified investigational drug, device, or biological product where both are required to achieve the intended use, indication, or effect.

<https://www.fda.gov/combination-products/about-combination-products/combination-product-definition-combination-product-types>

Type	Description	Common Example(s)
1	Convenience Kit or Co-Package <i>Drug and device are provided as individual constituent parts within the same package</i>	Drug or biological product vials packaged with device(s) or accessory kits (empty syringes, auto-injectors, transfer sets), first aid or surgical kits containing devices and drugs
2	Prefilled Drug Delivery Device/System <i>Drug is filled into or otherwise combined with the device AND the sole purpose of the device is to deliver drug</i>	Prefilled drug syringe, auto-injectors, metered-dose inhalers, dry powder inhalers, nasal-spray, pumps, transdermal systems, prefilled iontophoresis system or microneedle “patch”
3	Prefilled Biologic Delivery Device/ System <i>Biological product is filled into or otherwise combined with the device AND the sole purpose of the device is to deliver biological product</i>	Vaccine or other biological product in a prefilled syringe, autoinjector, nasal spray, transdermal systems or microneedle patch pre-loaded with biological product
4	Device Coated/ Impregnated/ Otherwise Combined with Drug <i>Device has an additional function in addition to delivering the drug</i>	Drug pills embedded with sensors, contact lens coated with a drug, drug-eluting stents, drug-eluting leads, condoms with spermicide, dental floss with fluoride, antimicrobial coated catheters/sutures, bone cements with antibiotics
5	Device Coated or Otherwise Combined with Biologic <i>Device has an additional function in addition to delivering the drug</i>	Live cells seeded on or in a device scaffold, extracorporeal column with column-bound protein
6	Drug/Biologic Combination	Antibody-drug conjugates, progenitor cells combined with a drug to promote homing
7	Separate Products Requiring Cross Labeling	Light-activated drugs or biological products not co-packaged but labeled for use with a specific light source device
8	Possible Combination Based on Cross Labeling of Separate Products	Drug/biological product under development utilizes a device, but unclear whether the final product will require that the two be cross-labeled
9	Other Type of Part 3 Combination Product (e.g., Drug/Device/ Biological Product) <i>Combination product not otherwise described</i>	All 3 articles are combined in a single product (e.g., a prefilled syringe containing an antibody-drug conjugate), device to manufacture a biologic also includes a drug or biologic in the kit, or the product contains two different combination product types (e.g., Type 1 and Type 2 are provided together)

Fluoropolymers in Medical Applications

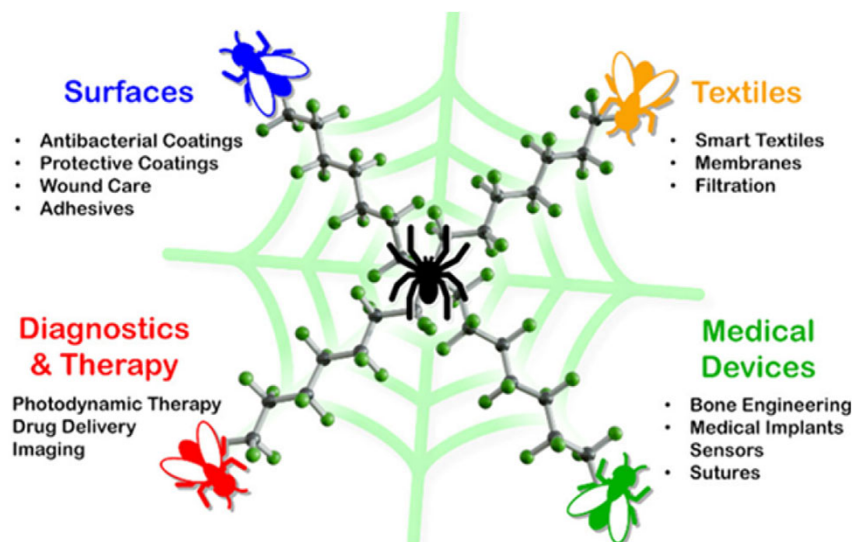


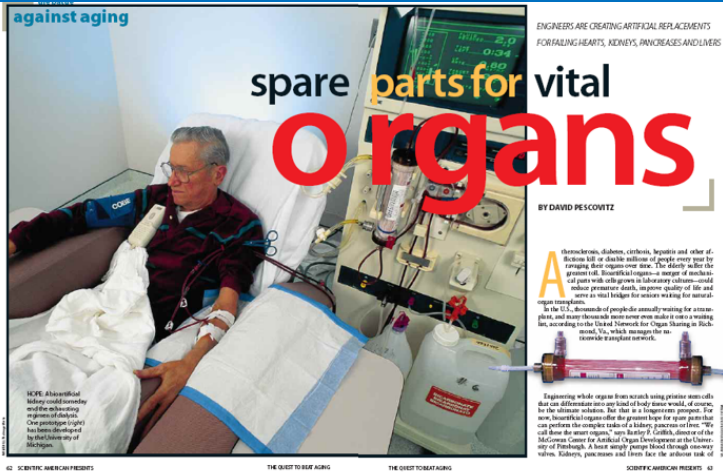
Figure 2. Commonly used preparation methods for cardiac patches.

Table 1. Fluoropolymers Used in Medical Applications

	Chemical Structure	Medical applications
Polytetrafluoroethylene (PTFE)	$\left(\begin{array}{c} F_2 \\ \\ -C-C- \\ \\ F_2 \end{array} \right)_n$	<ul style="list-style-type: none"> • Artificial blood vessels • Sutures • Stents
Polyvinylidene fluoride (PVDF)	$\left(\begin{array}{c} H_2 \\ \\ -C-C- \\ \\ F_2 \end{array} \right)_n$	<ul style="list-style-type: none"> • Water treatment membrane • Piezoelectric biomaterial sensors • Hemodialyzer
Tetrafluoroethylene-hexafluoropropylene copolymer (FEP)	$\left[\begin{array}{c} F_2 \\ \\ -C- \\ \\ F_2 \end{array} \right]_m \left[\begin{array}{c} F_2 \\ \\ -C- \\ \\ F \\ \\ CF_3 \end{array} \right]_n$	Transcutaneous implants
Polyvinyl fluoride (PVF)	$\left(\begin{array}{c} H_2 \\ \\ -C- \\ \\ F \end{array} \right)_n$	Substrate of protein-repelling
Poly(ethylene-co-tetrafluoroethylene) (ETFE)	$\left[\begin{array}{c} F_2 \\ \\ -C- \\ \\ F_2 \end{array} \right]_m \left[\begin{array}{c} H_2 \\ \\ -C- \\ \\ H_2 \end{array} \right]_n$	Patch mesh for augmenting myocardial tissue
<i>Fluoroelastomer:</i> Tetrafluoroethylen-propylene (FEPM)	$\left[\begin{array}{c} F_2 \\ \\ -C- \\ \\ F_2 \end{array} \right]_m \left[\begin{array}{c} H_2 \\ \\ -C- \\ \\ CH_3 \end{array} \right]_n$	<ul style="list-style-type: none"> • Soft denture liners • Organs-on-Chips
<i>Amorphous fluoropolymer:</i> Perfluoro(3-butenyl vinyl ether) cyclopolymer	$\left(\begin{array}{c} F_2 \\ \\ -C-CF_2-CF_2- \\ \\ F_2 \end{array} \right)_n$	Film for cell observation
<i>Fluoroalkyl homo or copolymer:</i> Fluoroalkyl polymer	$\left(\begin{array}{c} F_2 \\ \\ -C- \\ \\ F_2 \end{array} \right)_m \left(\begin{array}{c} F_2 \\ \\ -C- \\ \\ CF_3 \end{array} \right)_n$	Protein-repelling coating
<i>Ion exchange fluoropolymer:</i> Tetrafluoroethylene-co-perfluoro-3,6-dioxa-4-methyl-7-octensulfonic acid (Nafion®)	$\left[\begin{array}{c} F \\ \\ -C- \\ \\ F \end{array} \right]_m \left[\begin{array}{c} F \\ \\ -C- \\ \\ F \end{array} \right]_n \left[\begin{array}{c} F \\ \\ -C- \\ \\ F \end{array} \right]_p \left[\begin{array}{c} F_3C \\ \\ -C- \\ \\ CF_2 \\ \\ O \\ \\ O=S=O \\ \\ OH \end{array} \right]_x$	Antimicrobial coating

Hemodialysis

The Filter that Fights Ebola



Hemopurifier Developed by Aethlon Medical



What makes the Ebola virus so frightening is its speed. In a matter of days, it can pump out enough copies of itself to overtake the immune system. But the Hemopurifier, a specially designed cartridge that attaches to a dialysis machine, can tip the balance back in the body's favor: its lectin filter attracts Ebola viruses and sucks them from the blood as it flows through. It's been used only once, on a patient in Germany, but it did the trick—effectively curing his Ebola infection. In the future, doctors hope similar tech could be used on viruses like hepatitis.

<http://time.com/3594971/the-25-best-inventions-of-2014/?xid=newsletter-brief>



DIALYSIS

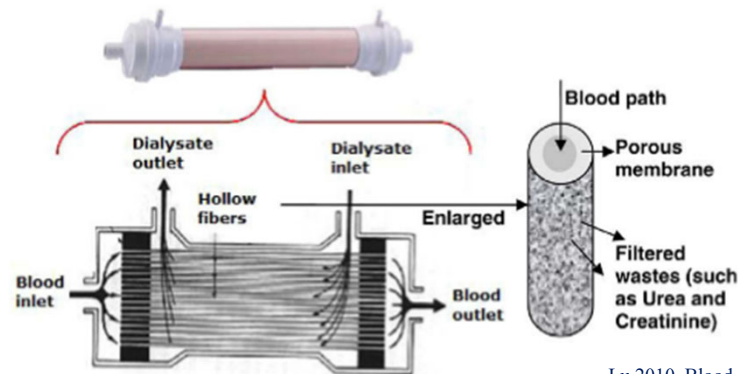
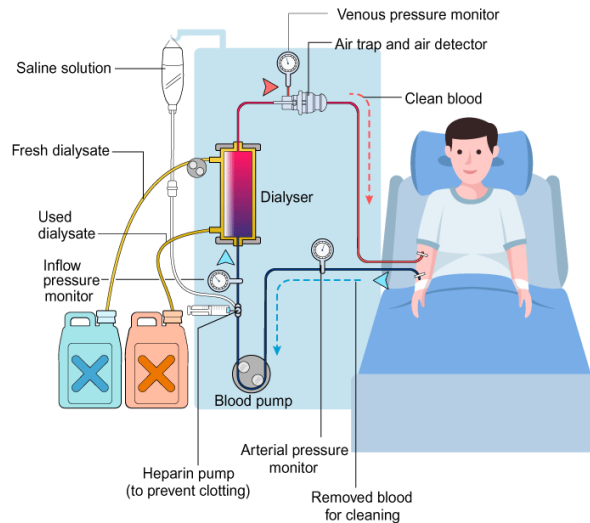
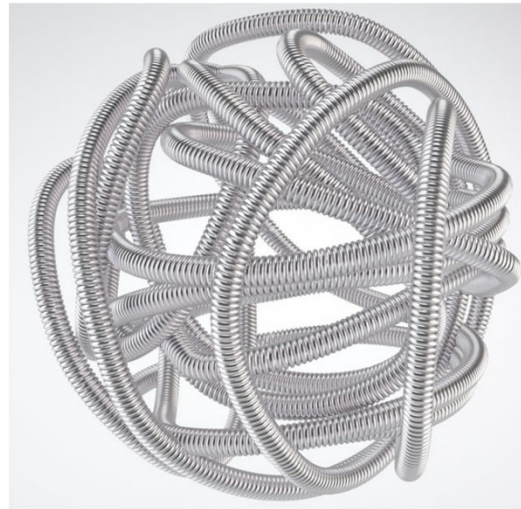
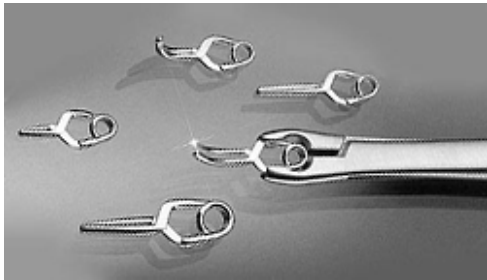
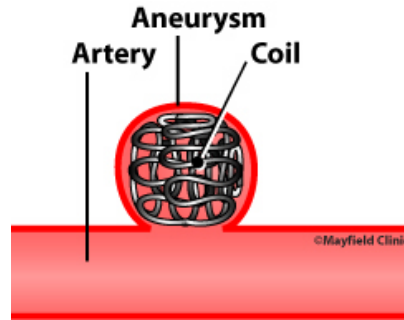
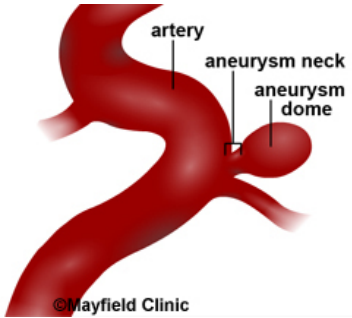


Fig. 1. Hollow fiber dialyzer.

Lu 2010, Blood flow velocity and ultra-filtration velocity measured by CT imaging system inside a densely bundled hollow fiber dialyzer. International Journal of Heat and Mass Transfer 53 (2010) 1844–1850

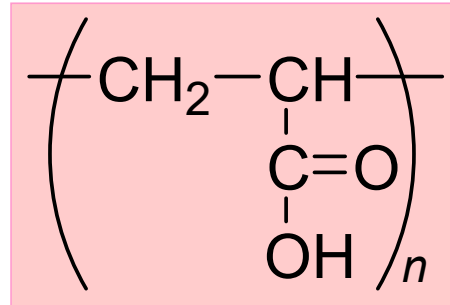
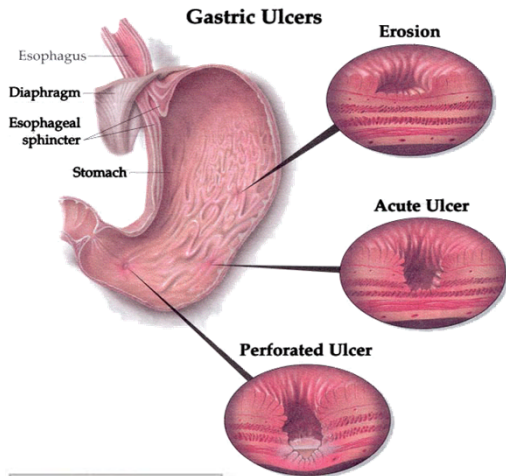
Fast Swelling Hydrogels for Aneurysm Treatment



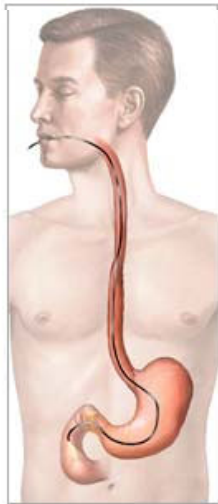
Hydrogel core expands to provide a uniform scaffold for neointimal growth and additional volumetric filling of the aneurysm
<https://www.microvention.com/product/hydroframe>

<https://www.microvention.com/news/microvention-and-terumo-corporation-announce-data-multicenter-great-study>

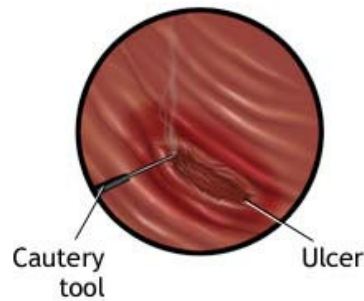
Adhesive Hydrogels as Gastric Bandage



Mucoadhesive hydrogel films to cover the ulcer area.
Delivery of blood clotting agents.



View of a duodenal ulcer through the endoscope



ADAM.

The procedure called gastroscopy involves the placing of an endoscope (a small flexible tube with a camera and light) into the stomach and duodenum to search for abnormalities. Tissue samples may be obtained to check for *H. pylori* bacteria, a cause of many peptic ulcers. An actively bleeding ulcer may also be cauterized (blood vessels are sealed with a burning tool) during a gastroscopy procedure

Thrombosis & Blood Compatibility

Failure of Blood-Contacting Biomaterials and Biomedical Devices

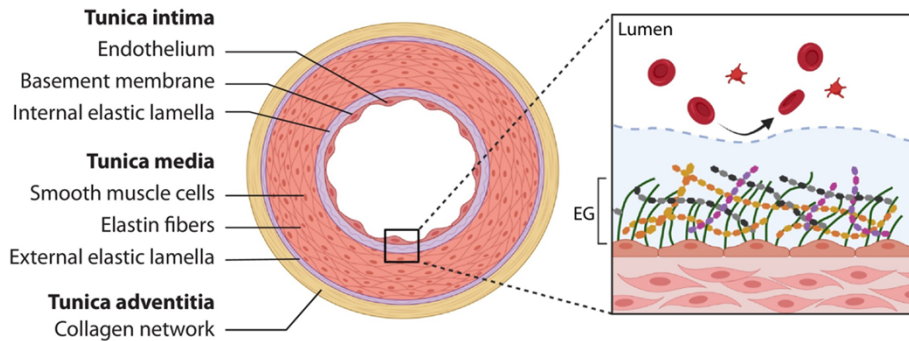
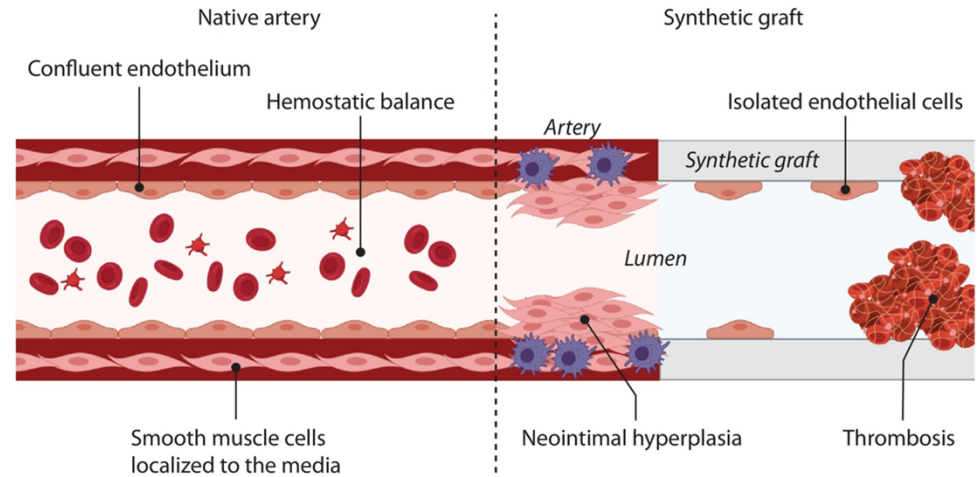
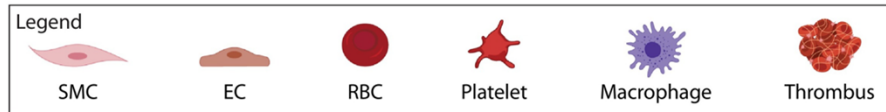
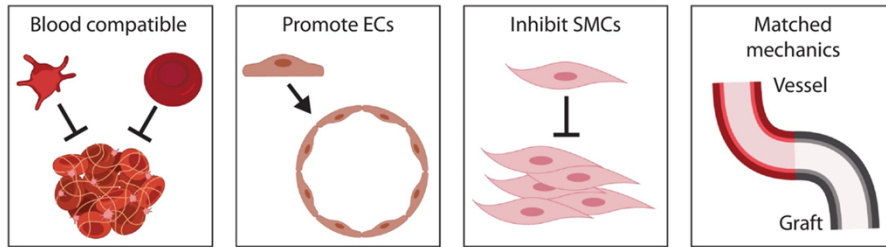


Figure 1. Vascular graft failure modes and design criteria.
(A) General structure of an artery.

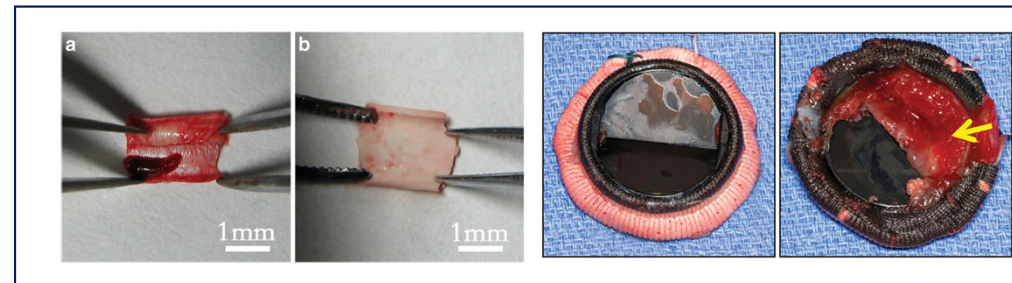


(B) Factors contributing to the failure of synthetic vascular grafts. The delayed formation of an endothelium leaves the hydrophobic graft surface exposed. Blood plasma proteins rapidly adsorb to the exposed graft, followed by platelet adhesion and activation, which results in the formation of a platelet-rich thrombus. The biologically incompatible graft material provokes an immune response, resulting in macrophage infiltration and expression of inflammatory cytokines that drive smooth muscle cells to over-proliferate, developing neointimal hyperplasia.

Moore 2021, Bioengineering artificial blood vessels from natural materials. Trends in Biotechnology, 40(6): P693-707, 2022.

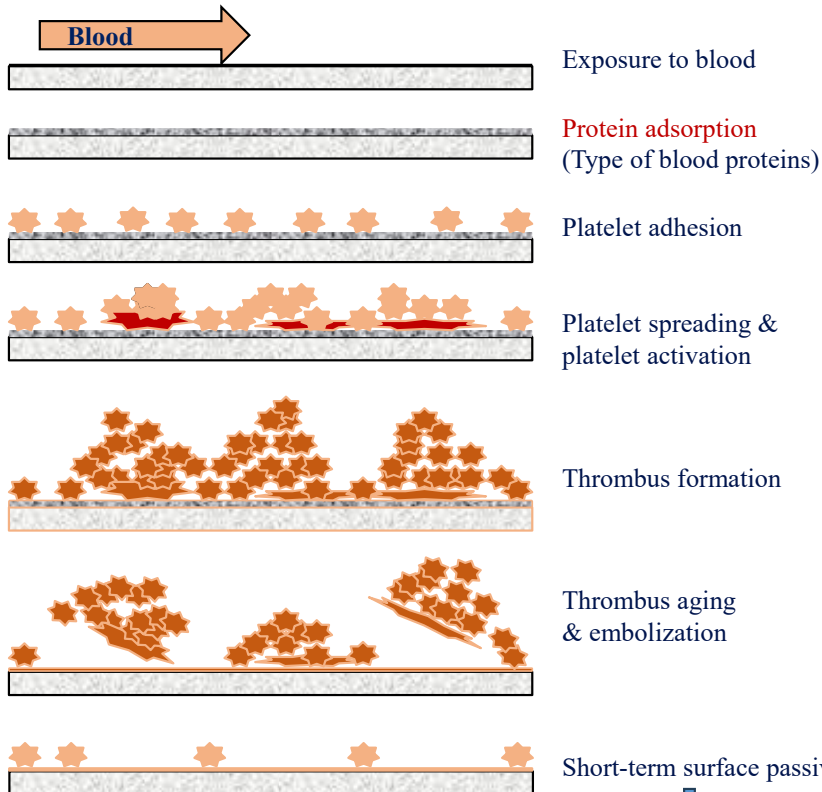


(C) Criteria for the rational design of artificial blood vessels. Image not to scale. Abbreviations: EC, endothelial cell; EG, endothelial glycocalyx; RBC, red blood cell; SMC, smooth muscle cell.



Problems Associated With Biomaterials

Surface-induced thrombosis with blood-contacting biomaterials



Vroman effect

- Proteins rapidly adsorb onto the surface $\sim 10 \mu\text{sec}$.
- Then, competitive displacement of earlier adsorbed proteins with a higher affinity for the surface occurs.
- Protein adsorption can alter the protein conformation and overall function.
- Fibrinogen, fibronectin, and von Willebrand factor are main proteins attracting platelets to the biomaterial surface.

Long-term surface passivation?
Slow progress in developing blood-compatible materials
 Control of platelet aggregation by drugs, e.g., Plavix (clopidogrel), Eliquis (apixaban), and Warfarin (Coumadin).

Hydrophobic materials:

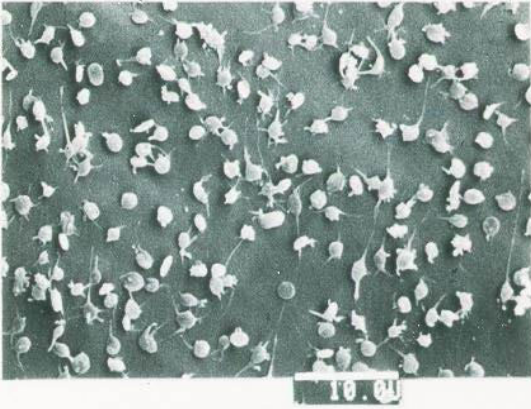
Fast adsorption which is largely irreversible
 Most change in protein conformation (reduced bioactivity)

Hydrophilic materials:

Slower adsorption, with significant desorption - Protein exchange
 Least change in protein conformation (maintains bioactivity)

Surface-Induced Thrombosis

Platelet adhesion



Platelet spreading and platelet activation



Thrombus formation

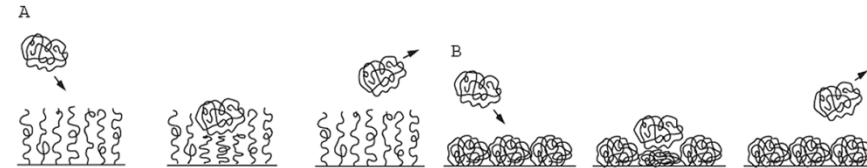


Short-term surface passivation

Successful long-term applications of implantable materials requires **prevention or minimization of surface-induced thrombosis** and/or **fibrous** encapsulation (or isolation) of implants by the body.

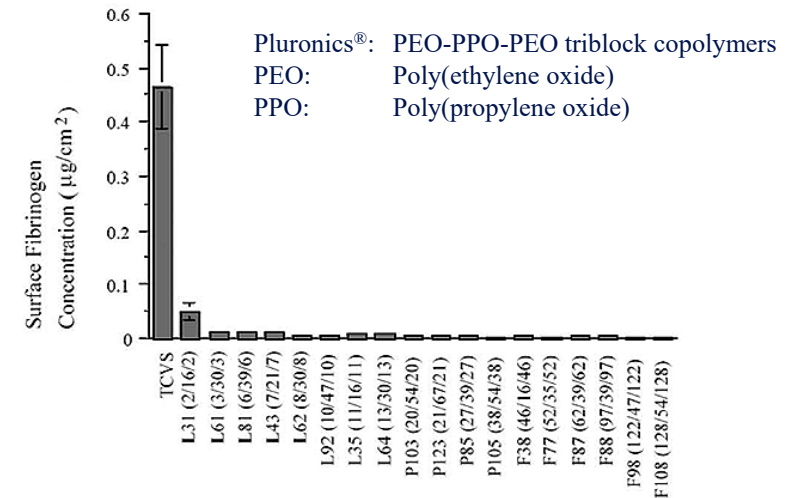
While the surface modification of biomaterials with PEO, heparin, albumin, and other hydrophilic polymers appears to be promising, further systematic studies on the long-term effects of surface modification of biomaterials are necessary for the development of truly biocompatible materials.

Prevention of (Platelet-Activating) Protein Adsorption



Schematic description of steric repulsion exerted by the surface-grafted linear polymers such as poly(ethylene oxide) or heparin (A) and globular proteins such as albumin (B).

Steric repulsion by surface-grafted PEO chains

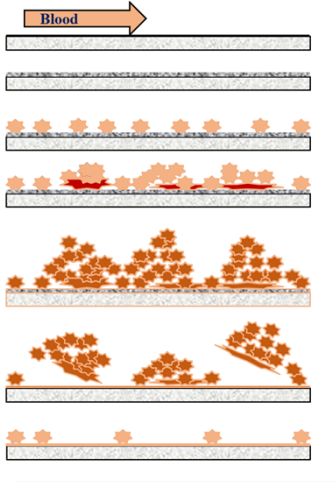


Pluronic®: PEO-PPO-PEO triblock copolymers
 PEO: Poly(ethylene oxide)
 PPO: Poly(propylene oxide)

Fibrinogen adsorption to glass surfaces grafted with various Pluronic® surfactants (L, P, and F series). The control surface was trichlorovinylsilane-modified glass. The three numbers in parentheses indicate the numbers of repeating units of ethylene oxide (EO) and propylene oxide (PO) in the poly(EO)/poly(PO)/poly(EO).

Related topic: Antifouling surfaces

Protein Adsorption and Desorption

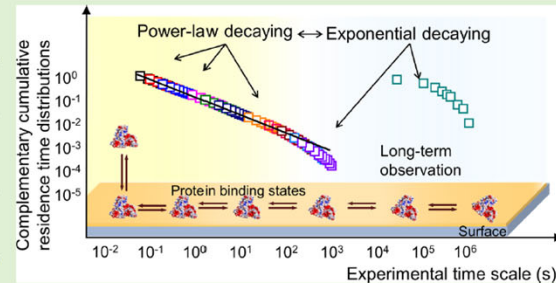


Vroman effect

- Proteins rapidly adsorb onto the surface ~ 10 μ sec.
- Then competitive displacement of earlier adsorbed proteins with a higher affinity for the surface occurs.
- Protein adsorption can alter the protein conformation and overall function.
- Fibrinogen, fibronectin, and von Willebrand factor are main proteins attracting platelets to the biomaterial surface.

Lyu et al., Protein desorption kinetics depends on the timescale of observation

ABSTRACT: The presence of so-called reversible and irreversible protein adsorption on solid surfaces is well documented in the literature and represents the basis for the development of nanoparticles and implant materials to control interactions in physiological environments. Here, using a series of complementary single-molecule tracking approaches appropriate for different timescales, we show that protein desorption kinetics is much more complex than the traditional reversible–irreversible binary picture. Instead, we find that the surface residence time distribution of adsorbed proteins transitions from power law to exponential behavior when measured over a large range of timescales (10^{-2} – 10^6 s). A comparison with macroscopic results obtained using a quartz crystal microbalance suggested that macroscopic measurements have generally failed to observe such nonequilibrium phenomena because they are obscured by ensemble-averaging effects. These findings provide new insights into the complex phenomena associated with protein adsorption and desorption.



- Fluorescent probe-labeled albumin and transferrin.
- **Single-Molecule Tracking** by total internal reflection fluorescence microscope (TIRFM)
- **Quartz Crystal Microbalance (QCM):** The oscillation of the crystal was modified by protein adsorption to the crystal surface, shifting the resonant frequency because of a change in total coupled mass. The Sauerbrey equation was used to relate the measured frequency shift (Δf) and the adsorbed mass per unit area (M): $M = -C (\Delta f/n)$, where n is the frequency overtone number (1, 3, ...) and C is the mass sensitivity constant with a value of $17.7 \text{ ng cm}^{-2} \text{ Hz}^{-1}$ at 5 MHz.

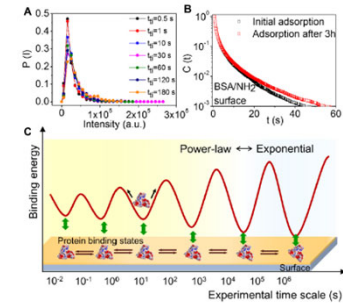
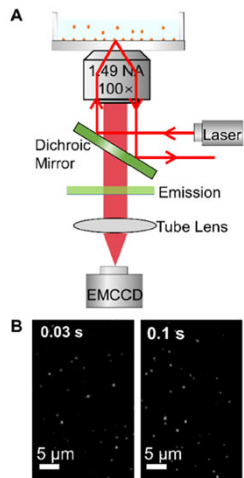


Figure 4. Protein desorption exhibiting aging. (A) Fluorescence intensity distributions of adsorbed BSA measured at different t_{ij} . (B) Complementary cumulative residence time distributions of BSA on amine-functionalized surfaces measured immediately after sample preparation or after 3 h. (C) Schematic illustration for surface protein aging originated from the reversible conversion of various binding states with distinct binding energies.

From an experimental point of view, each type of measurement was biased to recognize one or several adsorbed states in a given range of timescales. One might argue that the only populations of importance are those that dominate the surface coverage. However, the observation in Figure 4B indicates that the conversion from a short-lived to a long-lived population is a critical feature of protein adsorption which cannot be properly understood without the acknowledgment of the short-lived state. Moreover, it is well known that a protein layer can form rapidly (less than a few seconds) on a nanoparticle surface when in contact with a biological medium.³ A temporal evolution from a loosely attached to an irreversible attached protein on nanoparticles was also observed.^{56–58} Considering only an ensemble-average observation, it would be tempting to conclude that direct protein–surface attraction increased with time on such a surface when, in fact, the underlying mechanism, involving an aging effect, is completely different. While proteins are in rapid exchange between solution and surface, a small fraction of adsorbed proteins converts to a more stable adsorbed state. As time involves, more and more short-lived proteins convert into their long-lived counterparts, resulting in the time evolution of a protein layer.



Single-Molecule Tracking by total internal reflection fluorescence microscope (TIRFM)

Lyu 2022, Protein desorption kinetics depends on the timescale of observation

Non-Blood-Contacting Biomaterials

Non-blood-contacting Hard Tissue Replacements Biomaterials

Hard Tissue Replacements Biomaterials

Bone repair and joint implants

Metallic alloys, biodegradable polymers (PLA, PGA) for treating minimally loaded fractures.

Surgical wires

Used to reattach large fragments of bone, to provide additional stability in long-oblique or spiral fractures of long bones.

Pins

Used primarily to hold fragments of bones together and to guide large screws during insertion.

Screws

Most widely used devices for fixation of bone fragments and to attach a metallic plate to bone.

Plates

Used to facilitate fixation of bone fragment

Intramedullary nails

Used as internal struts to stabilize long bone fractures.

Joint replacements

Hip joint replacements

Dental implants

Soft Tissue Replacements Biomaterials

Sutures and allied augmentation devices

Sutures, Clips, staples, and pins, Surgical tapes, Tissue adhesives

Percutaneous and skin implants: Artificial skin, Burn dressing

Maxillofacial implants

Reconstructive surgery: Copolymers of vinyl chloride and vinyl acetate, PMMA, silicone rubber, polyurethane

Ear and eye implants: Contact lens, Intraocular lens

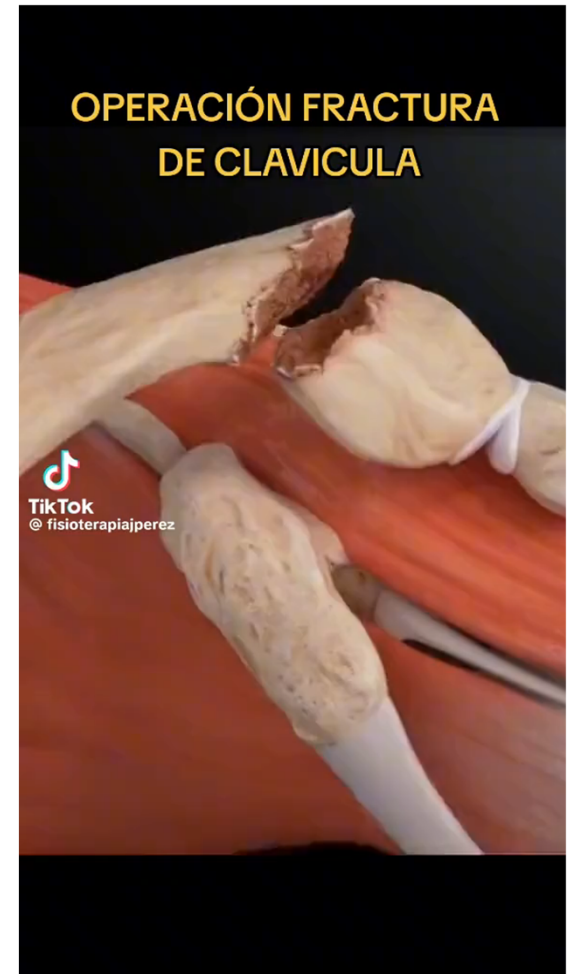
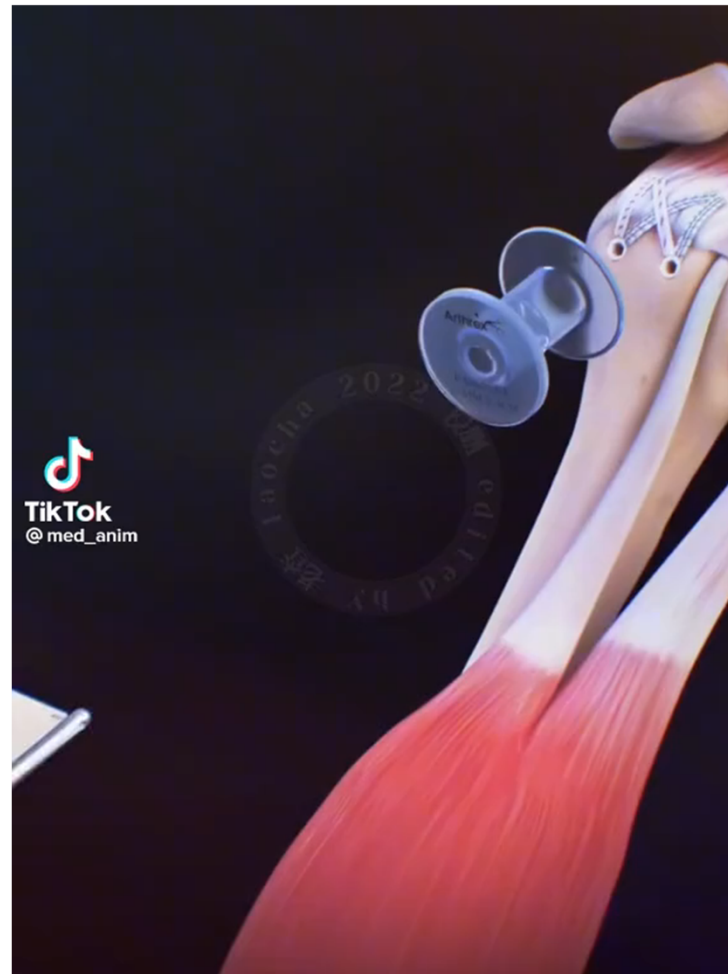
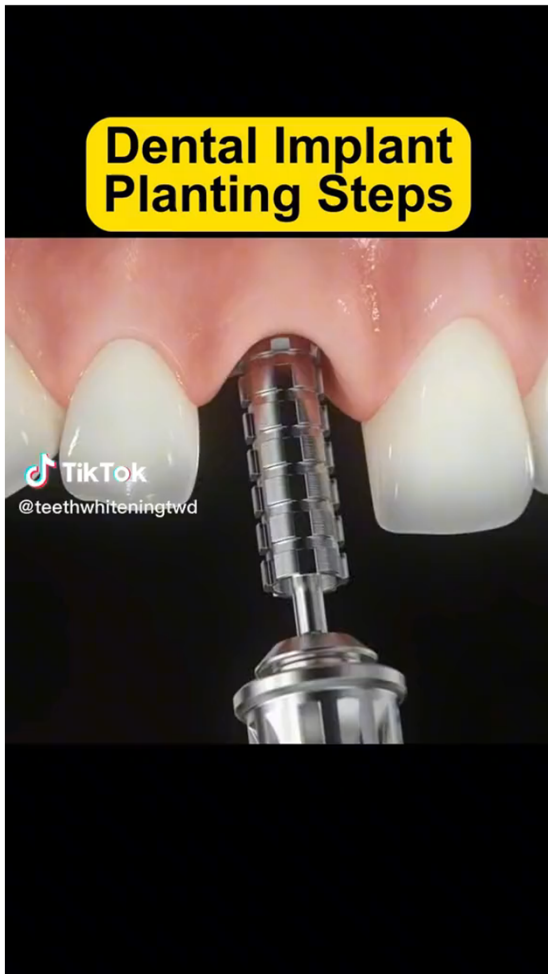
Space-filling implants: Silicone gel breast implants, tissue expanders

Fluid transfer implants: Cerebrospinal fluid shunts, Endotracheal tubes, Urinary catheter, Peritoneal dialysis catheters

Prosthetic joints

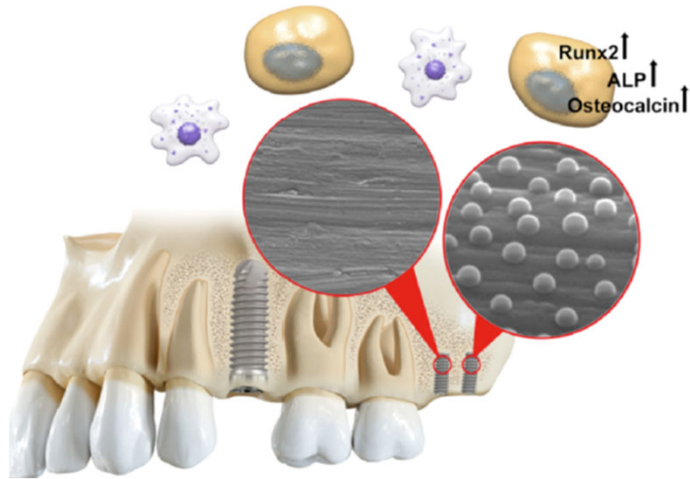
Implantable drug delivery devices

Non-blood-contacting Hard Tissue Replacements Biomaterials



Biomaterial Implants with Nanopatterns

Nanopatterned Titanium Implant



ABSTRACT: Implant surface modification by nanopatterning is an interesting route for enhancing osseointegration in humans. Herein, the molecular response to an intentional, controlled nanopography pattern superimposed on screw-shaped titanium implants is investigated in human bone. Compared to those adherent to the machined (M) implants, **the cells adherent to the nanopatterned (MN) implants demonstrate significant upregulation (1.8- to 2-fold) of bone-related genes (RUNX2, ALP, and OC).** Controlled nanopography, in the form of hemispherical 60 nm protrusions, promotes gene expressions related to early osteogenic differentiation and osteoblastic activity in implant-adherent cells in the human jaw bone.

Karazisis 2021, Molecular Response to Nanopatterned Implants in the Human Jaw Bone

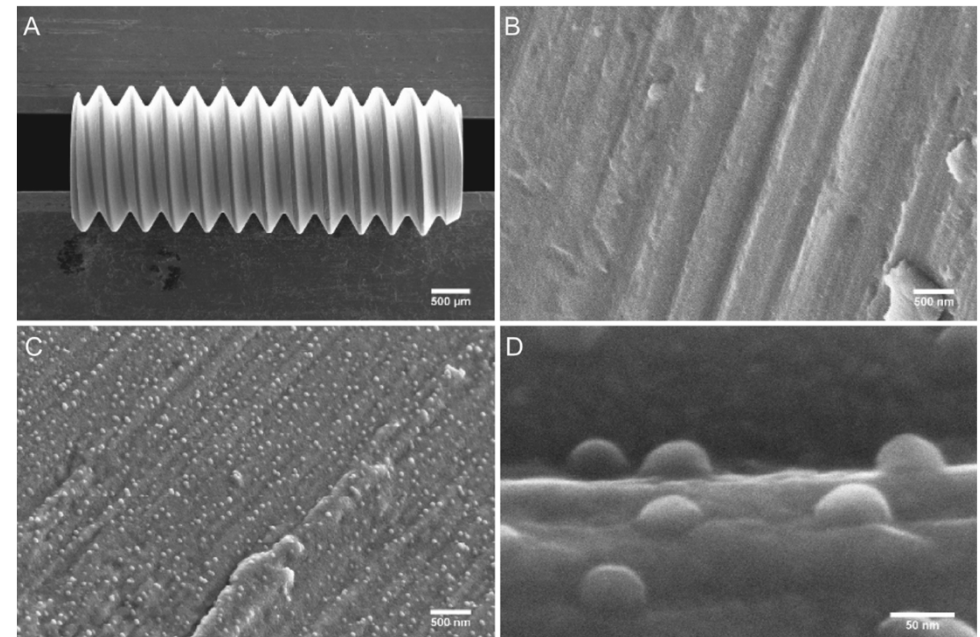


Figure 1. SEM evaluation: (A) Low-magnification overview of the mini-implant; (B) intermediate-magnification image of an implant with a machined surface; and (C) an implant with a nanopatterned surface. (D) High-magnification image of semispherical profiles on the nanopatterned surface. Images (B) and (C) were taken at the root of the implant thread. Image (D) was taken at the flank of the implant thread. All analyzed implants were sputter-coated with 30 nm titanium film and heat-treated.

Artificial Muscles

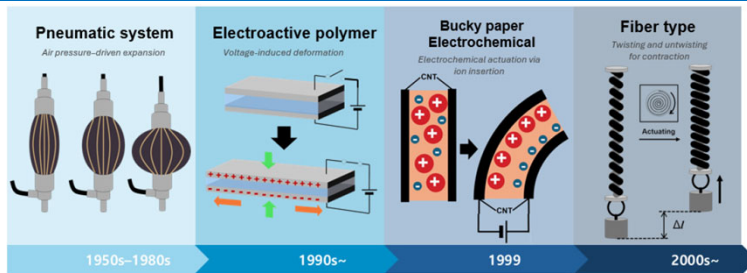


Figure 1. Historical evolution and research trends in artificial muscle technology. (A) A timeline illustrating the development of soft actuators from the 1950s to the 2000s, classifying key technologies by their actuation mechanisms: pneumatic systems (pressure-driven), electroactive polymers (voltage-induced), electrochemical bucky papers (ion insertion), and fiber-type actuators (twisting/untwisting).

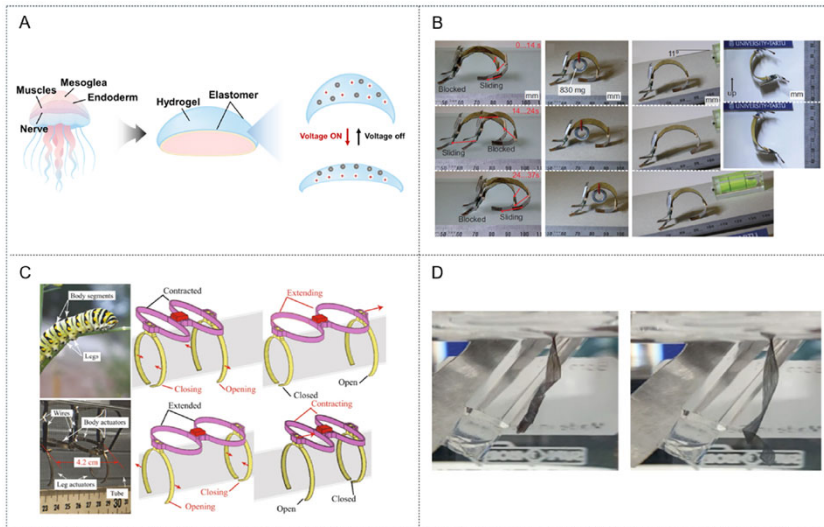


Figure 5. (A) Schematic representation of mechanism for ionic EAP artificial muscle. (B) Movement of IEAP robots imitating inchworm. (C) 3D-printed IPMC soft crawling robot inspired by a caterpillar. (D) PPy micro ribbon artificial muscle, which mimics the morphology of natural muscle fibers.

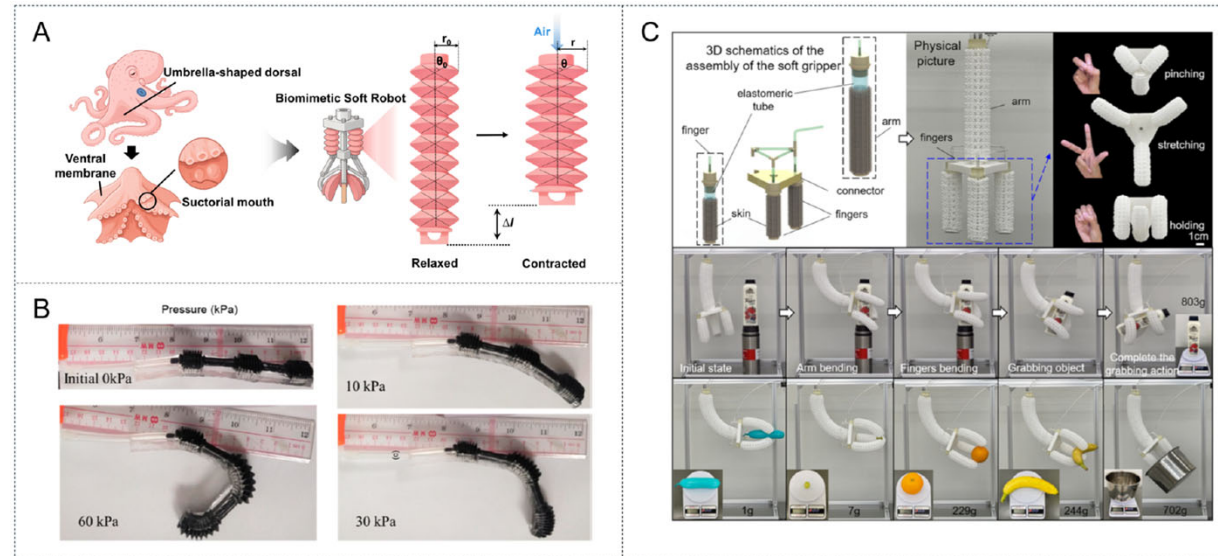


Figure 3. (A) Schematic representation of the mechanism for PAM. (B) Demonstration of digit mimicking finger action. (C) 3D assembly drawings and real-world operating photos of pneumatic tubular grippers for soft robotics applications.

Artificial Muscles



Developments in prosthetic limb technology could see them more closely mimic the function of the biological limbs they replace

BREAKTHROUGHS

Added power

A prosthesis can replace a lost limb but not the muscles in it... until now

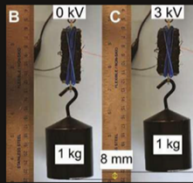
You've heard of artificial hips, knees and limbs. But what about artificial muscles? Think about it: if you lose the lower part of your leg, you can replace the bone with a piece of titanium or even carbon fibre. But how do you replace the muscles that powered that leg?

In most cases, you don't. The prosthesis isn't powered at all, except by the energy the rest of the leg puts in. A Paralympic sprinter doesn't use a battery to power their blade, so the blade must be made in such a way that the materials can utilise as much of the energy transferred from the rest of the body as possible.

Now, though, researchers are working on artificial muscles to power the next generation of artificial limbs, and not just for amputees – for robots as well. The difficulty they have in doing this is getting a lot of power out of something the size and weight of a real muscle. Traditionally, robots capable of lifting heavy loads have weighed in pretty heavily themselves and if you're already carrying around a prosthesis,

The artificial muscle can lift a 1 kg weight when an electric field is applied.

The artificial muscle can lift a 1kg weight when an electric field is applied



you don't want to be dragging along a power pack the size of a car battery to run it.

To solve the problem, scientists have been taking inspiration from nature. Many are now using soft materials, such as electroactive polymers, which change shape and size in response to an electric current but don't weigh a huge amount. There have also been slow-twitching prototypes based on twisting together slender synthetic threads in such a way that they contract and relax in response to temperature changes and are capable of lifting up to 7 kg. Most recently, researchers at Harvard University used very thin, very strong materials called elastomers to create artificial muscles that contracted as fast as natural muscles when supplied with electricity. **NE**

by HAYLEY BENNETT (@gingerbreadlady)
Hayley is a science writer specialising in biology, chemistry and the environment. She is one of the authors *The Big Questions In Science*.

A prosthesis can replace a lost limb but not the muscles in it... until now

You've heard of artificial hips, knees and limbs. But what about artificial muscles? Think about it: if you lose the lower part of your leg, you can replace the bone with a piece of titanium or even **carbon fibre**. But how do you replace the muscles that powered that leg?

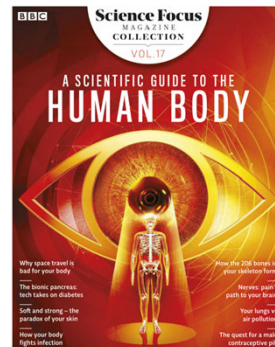
In most cases, you don't. The prosthesis isn't powered at all, except by the energy the rest of the leg puts in. A Paralympic sprinter doesn't use a battery to power their blade, so the blade must be made in such a way that the materials can utilise as much of the energy transferred from the rest of the body as possible.

Now, though, researchers are working on artificial muscles to power the next generation of artificial limbs, and not just for amputees – for robots as well. The difficulty they have in doing this is getting a lot of power out of something the size and weight of a real muscle. Traditionally, robots capable of lifting heavy loads have weighed in pretty heavily themselves and if you're already carrying around a prosthesis, you don't want to be dragging along a power pack the size of a car battery to run it.

To solve the problem, scientists have been taking inspiration from nature. Many are now using so materials, such as **electroactive polymers**, which change shape and size in response to an electric current but don't weigh a huge amount. There have also been slow-twitching prototypes based on twisting together slender synthetic threads in such a way that they contract and relax in response to temperature changes and are capable of lifting up to 7 kg. Most recently, researchers at Harvard University used very thin, very strong materials called elastomers to create artificial muscles that contracted as fast as natural muscles when supplied with electricity.

By Hayley Bennett (@gingerbreadlady)

BBC SCIENCE FOCUS MAGAZINE COLLECTION p. 57



Non-blood-contacting Hard Tissue Replacements Biomaterials

Hard Tissue Replacements Biomaterials

Bone repair and joint implants

Metallic alloys, biodegradable polymers (PLA, PGA) for treating minimally loaded fractures.

Surgical wires

Used to reattach large fragments of bone, to provide additional stability in long-oblique or spiral fractures of long bones.

Pins

Used primarily to hold fragments of bones together and to guide large screws during insertion.

Screws

Most widely used devices for fixation of bone fragments and to attach a metallic plate to bone.

Plates

Used to facilitate fixation of bone fragment

Intramedullary nails

Used as internal struts to stabilize long bone fractures.

Joint replacements

Hip joint replacements

Dental implants

Soft Tissue Replacements Biomaterials

Sutures and allied augmentation devices

Sutures, Clips, staples, and pins, Surgical tapes, Tissue adhesives

Percutaneous and skin implants: Artificial skin, Burn dressing

Maxillofacial implants

Reconstructive surgery: Copolymers of vinyl chloride and vinyl acetate, PMMA, silicone rubber, polyurethane

Ear and eye implants: Contact lens, Intraocular lens

Space-filling implants: Silicone gel breast implants, tissue expanders

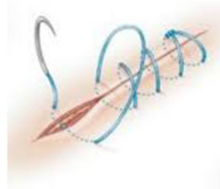
Fluid transfer implants: Cerebrospinal fluid shunts, Endotracheal tubes, Urinary catheter, Peritoneal dialysis catheters

Prosthetic joints

Implantable drug delivery devices

Sutures

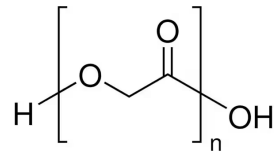
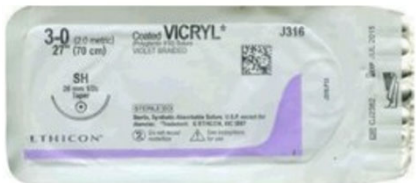
Transition from Silk to Nylon



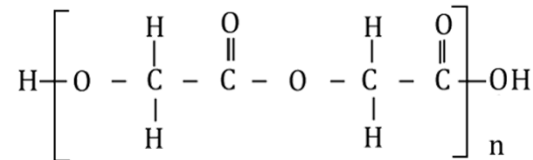
- 1950s: Polymeric Vascular Prostheses
-Nylon, Orlon, and Dacron
-Orlon and Dacron found to be superior
Both had high patency rates in large arteries



- 1974: Vicryl[®] Sutures were introduced to the market



Poly(glycolic acid)



Biomedical Polymers

Current: Existing polymers
Find application.
(e.g., Teflon - nuclear bomb)

Future: Find problems and needs
Develop new polymers

Teflon was used in various biomedical devices, but it is not used as widely anymore due to many unjustified lawsuits against the company.



Zipper Band-Aids speed up healing and does not leave a scar.
TikTok, @cooltechnology2021

Dermabond uses 2-octyl cyanoacrylate as its primary monomer, which polymerizes into a strong, flexible, and sterile tissue adhesive upon contact with skin moisture. It is a long-chain cyanoacrylate designed to provide higher strength and lower toxicity compared to shorter-chain alternatives.
https://www.accessdata.fda.gov/cdrh_docs/pdf/P960052b.pdf



Biodegradable Block Copolymer–Tannic Acid Glue

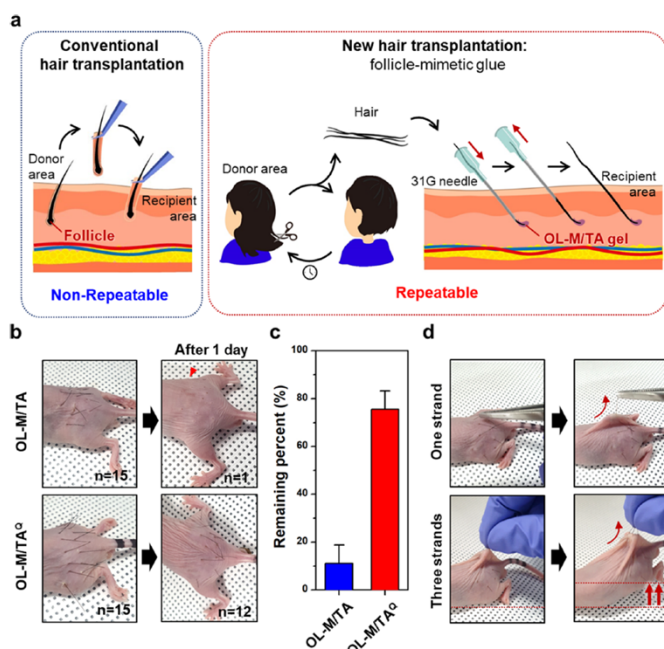


Figure 6. Application of PEO-b-PLA (OL)/tannic acid (OL/TA) glue for hair transplantation surgery. (a) Schematic illustrations of the conventional hair transplantation procedure (left box) and the new hair transplantation approach using OL/TA as follicle-mimetic glue (right box). (b) Photographs of the remaining hair strands 1 day after hair transplantation using as-prepared OL-M/TA (top) and heat-treated OL-M/TAQ (bottom). A red arrowhead indicates the remaining single strand in the OL-M/TA case. (c) Percentage of remaining hair strands 1 day postoperation using OL-M/TA (blue) and OL-M/TAQ (red). The error bar indicates standard deviations ($n = 3$). (d) Photographs showing the adhesiveness of OL-M/TAQ by pulling the transplanted hair strands 1 day after hair transplantation.

Preparation of OL/TA Glue: Three PEO-b-PLAs were prepared via ring-opening polymerization of D,L-lactide (LA) in the presence of methoxy-terminated PEO with a number average molar mass of 20 kg/mol. They were designated OL-L, OL-M, and OL-H according to the PLA volume fraction (f_{PLA}) of 6, 13, and 20%, respectively.

Park 2022, Biodegradable block copolymer–tannic acid glue

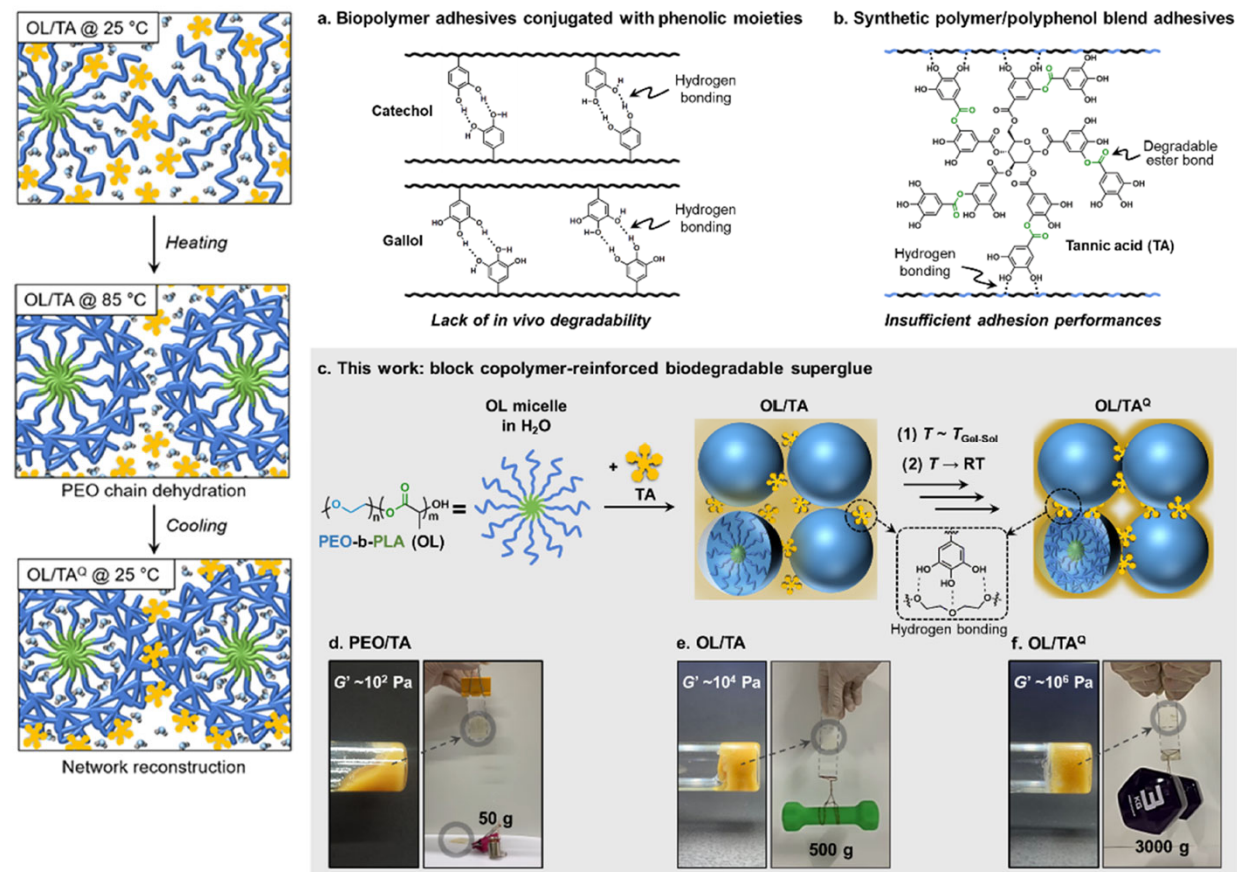
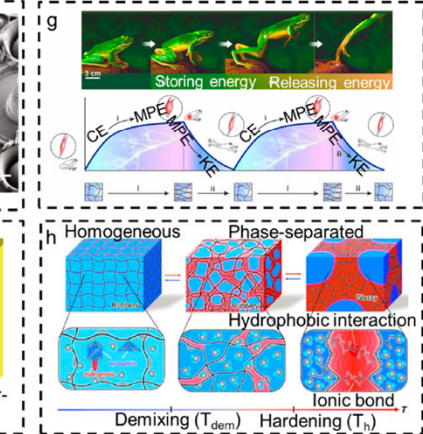
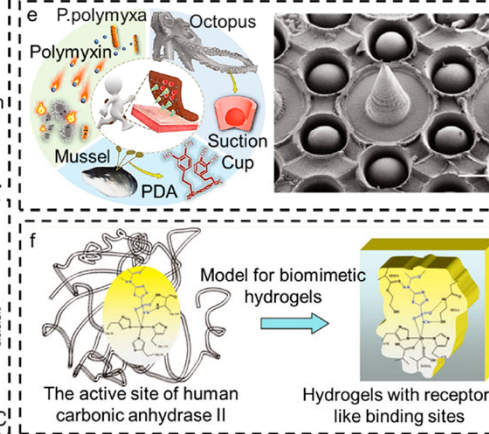
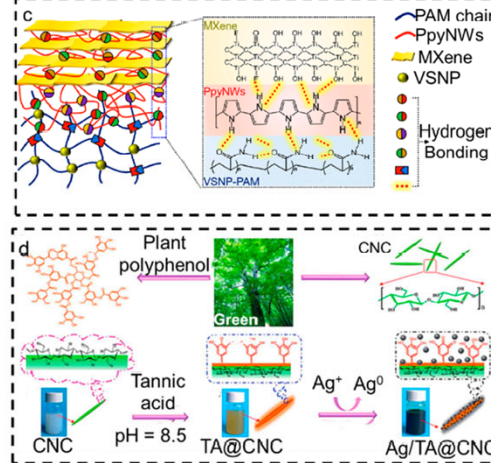
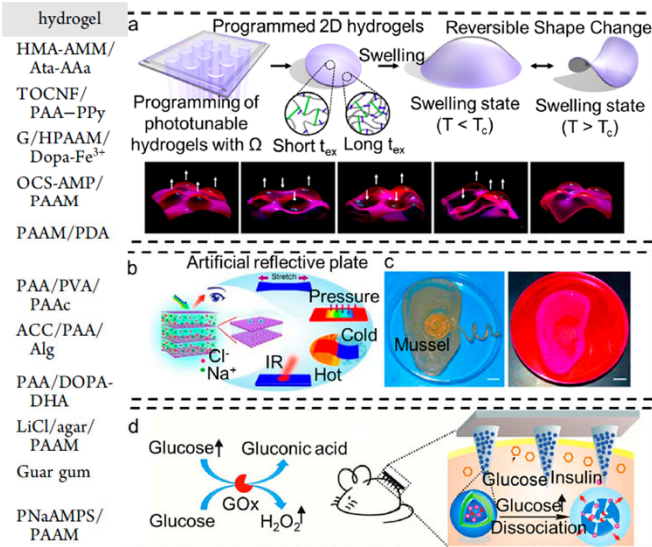
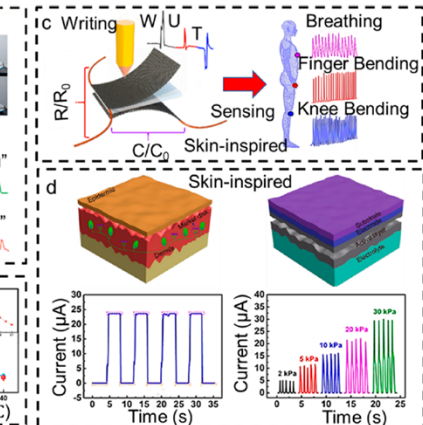
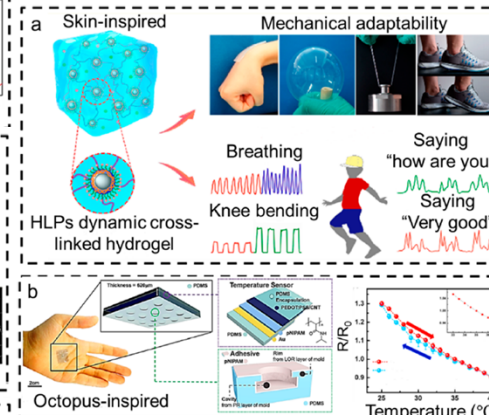
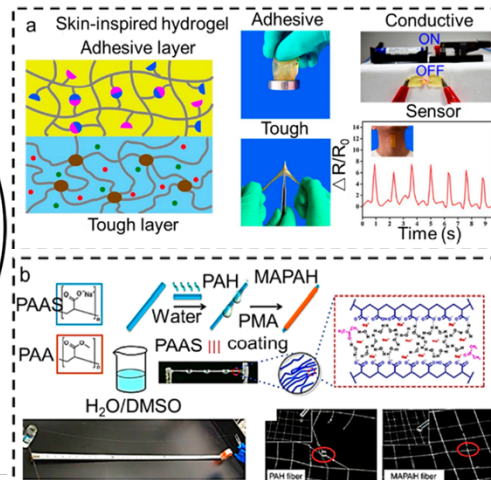
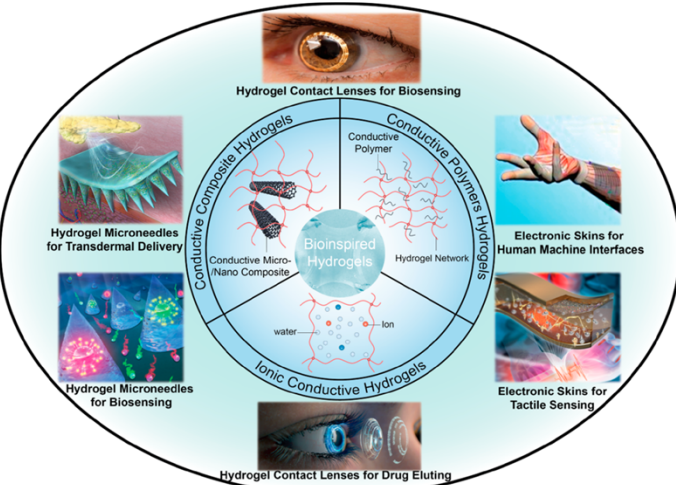


Figure 1. Block copolymer-reinforced biodegradable superglue. (a, b) Previously studied classes of bioadhesives based on phenolic moieties. (a) Catechol- and gallol-conjugated biopolymers. (b) Blend of synthetic water-soluble polymers with polyphenols. Tannic acid (TA) is given as a representative polyphenol, and the degradable ester linkage is shown in green. (c) Blend of an amphiphilic diblock copolymer with TA in this study. PEO-b-PLA (OL) consisting of hydrophilic and temperature-sensitive poly(ethylene oxide) (PEO) and hydrophobic poly(lactic acid) (PLA) was chosen as a biocompatible and biodegradable block copolymer. OL micelles form in water driven by hydrophobic interaction and associate with TA via hydrogen bonding of phenolic hydroxyl groups with PEO corona to produce an OL/TA gel at a high concentration. Repeatedly heating the gel close to the gel–sol transition and cooling back to room temperature strengthens the material by reorganizing the hydrogen-bonded network with the dehydration–rehydration process of the PEO corona. (d–f) Photos of OL/TA and heat-treated OL/TA^Q compared to the blend of TA with the PEO homopolymer (PEO/TA). G' values obtained at $\omega = 10 \text{ rad s}^{-1}$ and $\gamma = 1\%$ are shown within the photos. Adhesion strength was demonstrated by dumbbell lifting for 15 s. (d) PEO/TA. (e) OL-M/TA. (f) OL-M/TA^Q.

Hydrogels as Biomaterials

Hydrogels



Injectable Cryogels for Biomedical Applications

Cryogelation produces macroporous hydrogels without the need to use toxic organic solvents. Cryo-hydrogels (or cryogels) are typically formed in water (solvent) at subzero temperatures. **When the solvent freezes, ice crystals form and subsequently expel the gel precursors (monomers, polymer, crosslinker, and initiator), which concentrate into an unfrozen phase** (Figure 2). The cryopolymerization or gelation occurs around ice crystals generating a dense, highly crosslinked polymer network. When thawed, ice crystals leave behind a continuous and interconnected macroporous system (Box 1)

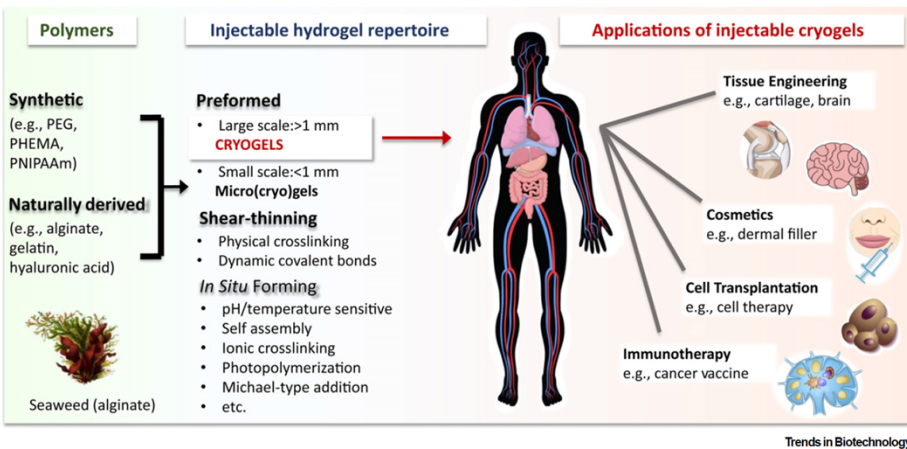


Figure 1. Hydrogels can be fabricated using synthetic or naturally derived polymers. Within the injectable hydrogel repertoire, many in situ forming gels such as shear-thinning and small-scale gels have been developed. Cryogels are the only readily available large-scale, preformed, and injectable microporous hydrogels with shape-memory properties, making them suitable for applications in tissue engineering, cosmetics, cell/drug delivery, and immunotherapy. Abbreviations: PEG, Polyethylene glycol; PHEMA, poly(2-hydroxyethylmethacrylate); PNIPAAm, poly(N-isopropylacrylamide).

Eggermont 2020, Injectable cryogels for biomedical applications

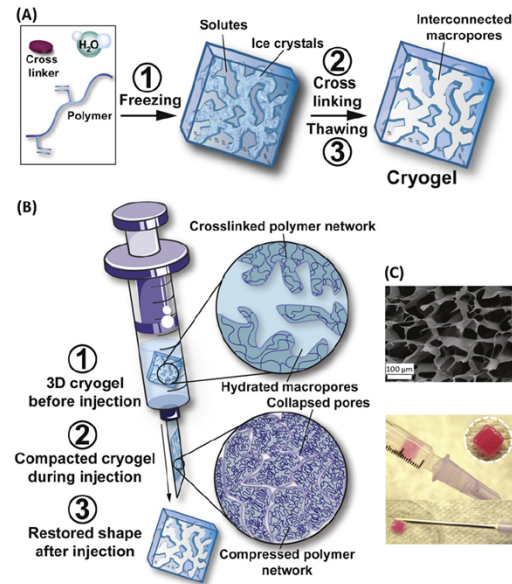


Figure 2. Fabrication Process and Injection of Cryogels. For a Figure360 author presentation of Figure 2, see the figure legend at <https://doi.org/10.1016/j.tibtech.2019.09.008>. (A) For the formation of cryogels, (1) a hydrogel precursor solution is frozen ($T < 0^{\circ}\text{C}$). This process leads to a phase separation of the solvent (e.g., water) into a frozen phase (ice crystals) and a nonfrozen phase around ice crystals, where the gel precursors (monomers, polymer, crosslinker, and initiator) are expelled. (2) Next, concentrated gel precursors are crosslinked around ice crystals (porogens). (3) Following cryogelation, thawed ice crystals give rise to a microporous sponge-like hydrogel, known as a cryogel. (B) Syringe injection of cryogels with shape-memory properties. (1) Free water within the macropores of cryogel scaffolds is released during injection and (2) the polymer network is reversibly collapsed to a fraction of its original size, enabling the gel to be pushed and travel through the needle. (3) Following injection, the initial shape and dimension of the gel are rapidly restored upon rehydration and spontaneous swelling. (C) Scanning electron microscope image of the macroporous architecture of cryogels and photos showing cryogel injection. Images were adapted with permission from [18,19].

Box 1. What Are Cryogels Really?

Cryogels, a subclass of hydrogels, are biomaterials with unique physical properties [23]. They are characterized by a highly interconnected macroporous and elastic structure, resulting in a sponge-like morphology with high mechanical stability [74]. Cryogels (or freeze-thawed cryogels) are formed via cryogelation at subzero temperatures (typically between -5 and 20°C). Freeze-dried hydrogels, conventional hydrogels that undergo cryostructure through several cycles of freeze-drying [75], are often inadvertently referred to as cryogels [17]. The process of freeze-drying leads to the formation of ice crystals within the gel matrix, creating pores in regions previously occupied by polymers. Although this technique enables the formation of an open macroporous structure [76], freeze-dried hydrogels tend to have a loss of structural integrity leading to weaker mechanical properties. As a result, freeze-dried cryogels are usually not syringe injectable [17]. In contrast, the physical or chemical crosslinking of cryogels takes place under freezing conditions, resulting in the formation of ice crystals that act as nontoxic porogens. Polymerization occurs in a liquid phase around ice crystals where the monomers/polymers and crosslinking systems are concentrated [18]. When the cryogelation is completed, a simple thawing at room temperature causes ice melting and unveils an interconnected macroporous network. The resulting cryogels are soft and elastic, can be compressed up to 90% of their initial volume without any permanent mechanical damage, and can withstand the compressive stress experienced during syringe injection [18]. Furthermore, cryogels are capable of rapid swelling and expansion, facilitating cellular infiltration, cell organization, and proliferation [17], as well as promoting angiogenesis [77].

A number of parameters can be adjusted to control the physical features and properties of cryogels [35]. For instance, lowering the polymerization temperature or increasing the cooling rate prior to cryogelation typically induces fast ice crystal nucleation and growth. As a result, cryogels display smaller pore sizes. The method of crosslinking is also an important parameter to take into account when fabricating cryogels. Injectable cryogels are generally chemically crosslinked, as physically crosslinked cryogels tend to be considerably weaker and easy to damage. Increasing the molecular weight and/or concentration of polymers have been associated with cryogels exhibiting decreased pore sizes and enhanced mechanical stability to some degree [17,35].

In summary, cryogels are versatile biomaterials that that can be selectively tailored depending on the intended application. They can be fabricated from synthetic and/or naturally derived polymers, and other materials can be integrated within their polymer walls (nano- and macroparticles) to form composite or hybrid cryogels [17]. Cryogels can be ionic, nonionic, amphoteric, or zwitterionic [17,78,79] and can be engineered to be responsive to external stimuli such as electric [80], magnetic [63,81], or thermic [82], as well as other signals such as pH variations [83].

Hydrogels

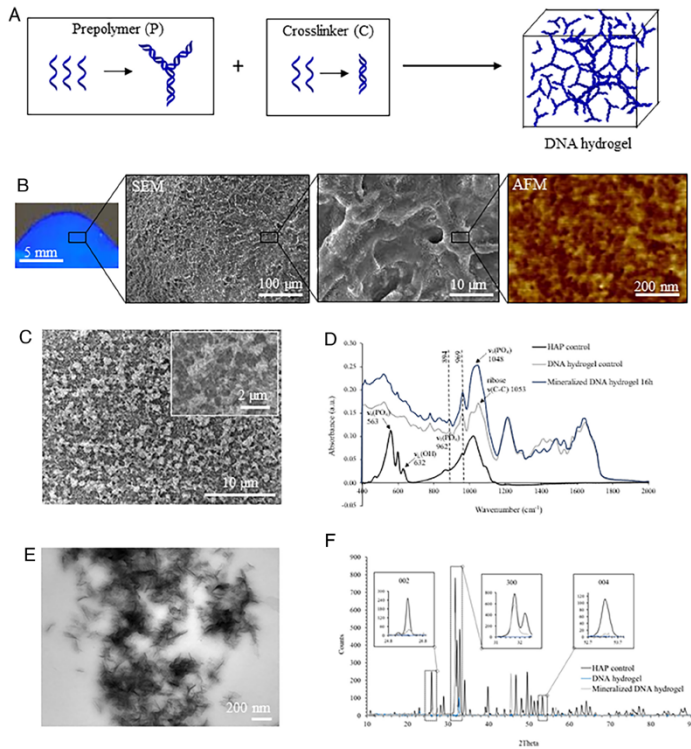


Fig. 1. DNA hydrogel synthesis and characterization. (A) Schematic representation of DNA hydrogel formation after mixing DNA prepolymer (P) with the DNA cross-linker (C). (B) Picture of the DNA hydrogel under UV irradiation (Left), and SEM along with AFM imaging showing a fibrous porous morphology at microscale and nanoscale, respectively. (C) SEM imaging of DNA hydrogels after 16 h of mineralization. (D) Infrared spectra of mineralized DNA hydrogels confirming that the observed mineral phase is HAP. (E) TEM imaging of DNA hydrogels after 16 h of mineralization. (F) XRD spectra of DNA hydrogels after 16 h mineralization confirming that the observed mineral phase is HAP.

Athanasidou 2023, DNA hydrogels for bone regeneration

Synthesis of DNA Hydrogel

DNA hydrogels were assembled in a two-step reaction, as described previously (30). Briefly, **single-stranded DNA sequences complementary to each other** were purchased from GeneLink Inc. (SI Appendix, Fig. S1). DNA prepolymer (composed of Y1, Y2, and Y3) and DNA cross-linker (L1 and L1') solutions were prepared in $1\times$ Tris(hydroxymethyl)aminomethane (Tris)- Ca^{2+} buffer (pH 7.4) in separate tubes. The DNA prepolymer and DNA crosslinker solutions were mixed in a ratio of 1:3, respectively, with the DNA hydrogel (2.25 mM) forming within seconds. The samples were characterized by denaturing experiments, which were run at 15 mA and 300 V for 1.5 h, and by native gel experiments, which were run at 15 mA and 80 V for 16 h, after which the gel was stained with GelRed[®] (Biotium). Gel imaging was performed using a Gene Genius Bioimaging System (Syngene). Quantification of the gel panels was performed using ImageJ software (version 1.53e).

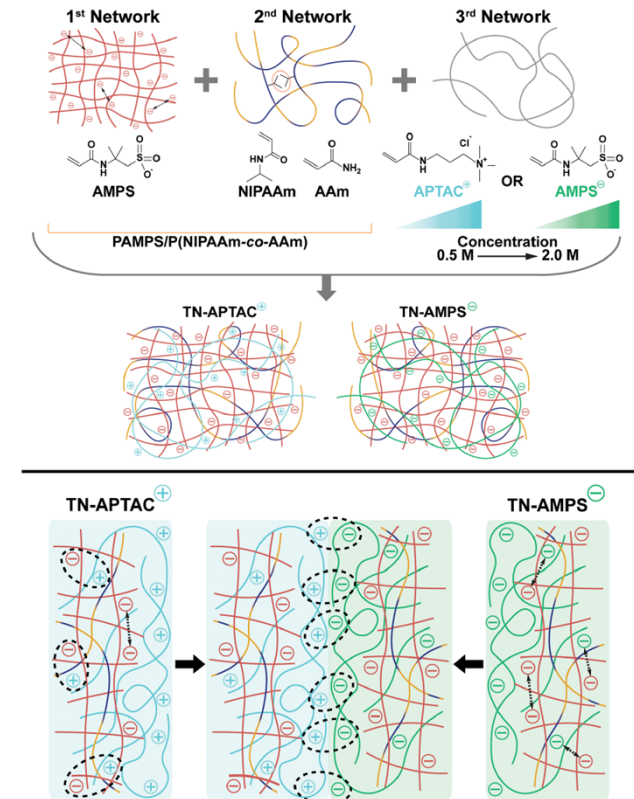


Figure 2. Top: Triple network (TN) hydrogels were fabricated with either a cationic (TN-APTAC) or anionic (TN-AMPS) 3rd network, wherein the concentration of APTAC or AMPS was tuned (0.5–2.0 M). Bottom: the 3rd network in TN hydrogels drives surface charge, enabling adhesion between the two types via electrostatic attractive forces.

Demott 2023, Adhesive hydrogel building blocks to reconstruct complex cartilage tissues

Immunomodulatory Hydrogels

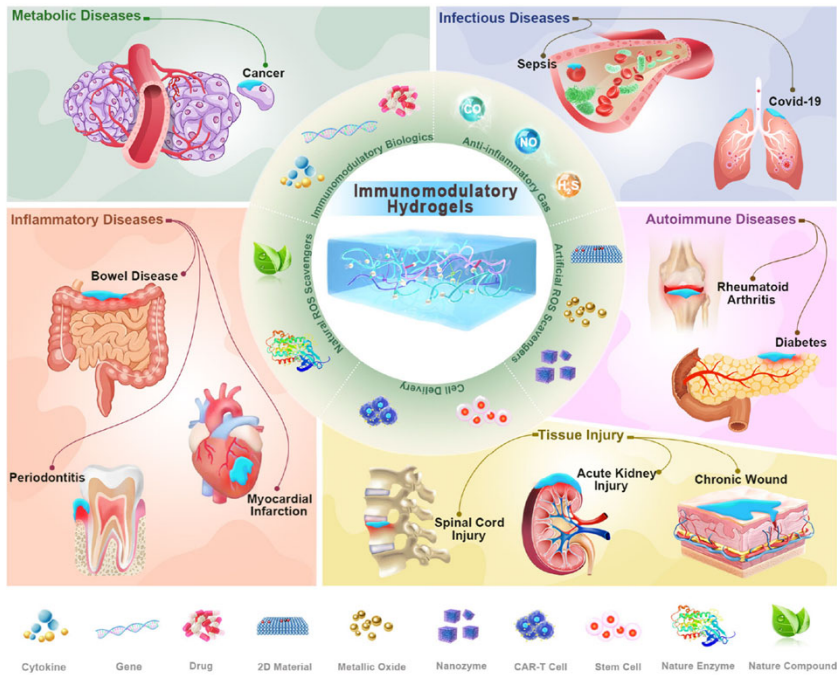


Figure 1. Scheme illustration of typical strategies for designing immunomodulatory hydrogels and their further application for defending against other pathological abnormalities, such as infectious diseases, metabolic diseases, autoimmune diseases, inflammatory diseases, and tissue injuries.

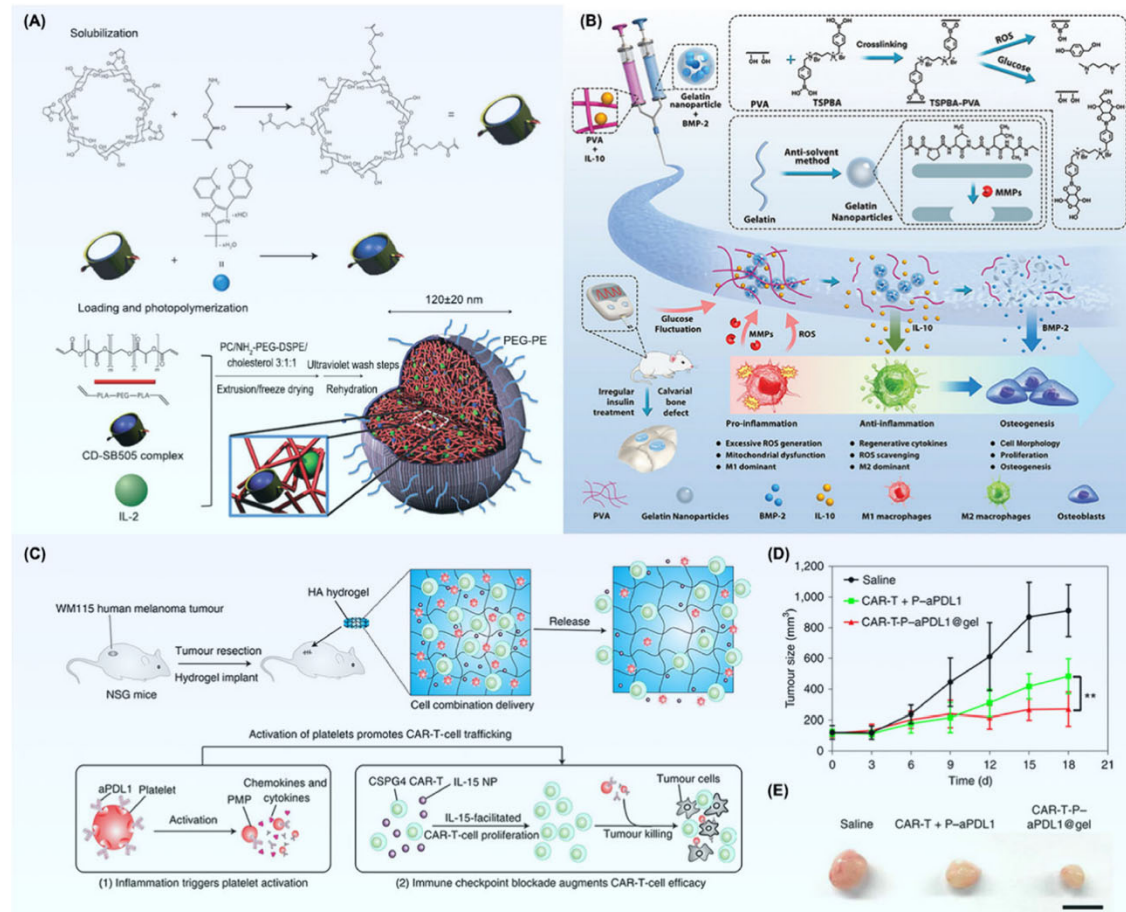


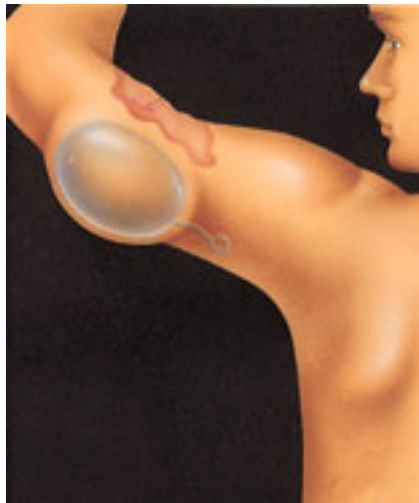
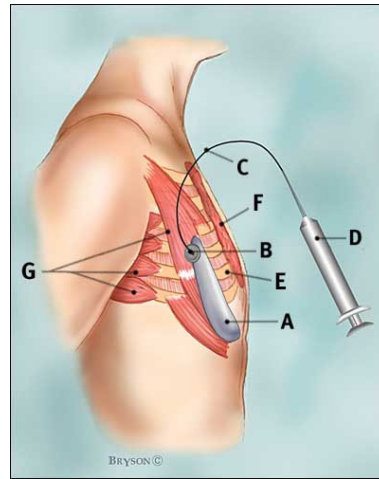
Figure 3. (A) Schematic diagram showing the synthesis approach for the nanoscale liposomal polymeric hydrogels and exert enhanced tumor immunotherapy efficiency. Reproduced with permission from ref 127. Copyright 2012 Springer Nature. (B) Schematic illustration showing the design rationale of logic-based diagnostic and therapeutic hydrogel for diabetic bone regeneration. Reproduced with permission from ref 129. Copyright 2022 Wiley-VCH Verlag GmbH & Co. (C) Schematic diagram showing the implantation of multifunctional hydrogel encapsulating the cytokine IL-15 and platelets for inhibition of tumor recurrence. (D) Tumor growth curves after treatment with different experimental groups. (E) Representative images of tumors on the 18th day. Scale bar: 1 cm. Reproduced with permission from ref 131. Copyright 2021 Springer Nature.

Zhao 2025, Hitchhiking delivery systems- Therapeutic hydrogels as advanced tools for immunomodulatory applications

Tissue Expander

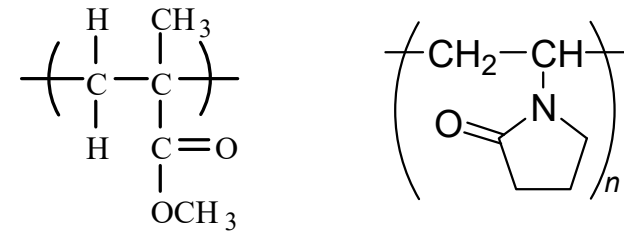


Figure 1. A conventional silicon balloon expander (left) and a hydrogel expander (right) with the same nominal final filling volume (scale in cm).



Manual delayed expansion.
 Predefined size and shape.
 No ability to reshape by surgeons.

Hydrogel Tissue Expanders



Copolymers of methyl methacrylate and N-vinylpyrrolidone
 The volume increase of 3-12 folds.
 Hydrogel in silicone shell to reduce the swelling speed.



Predefined size and shape.
 No ability to reshape by surgeons.



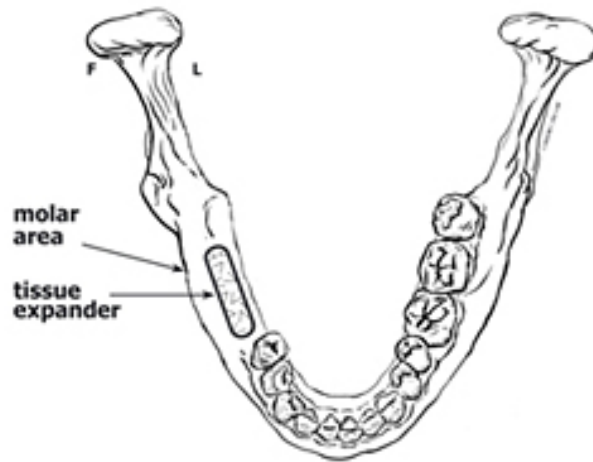
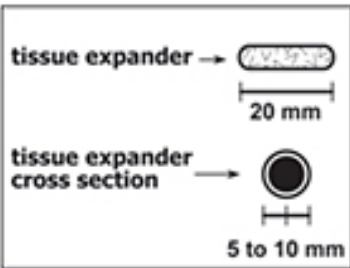
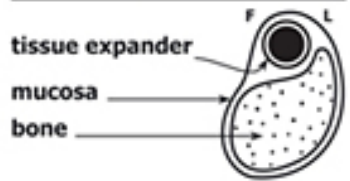
http://www.osmed.biz/html_e/produkte/produkte.html

New Tissue Expanders: Hydrogels

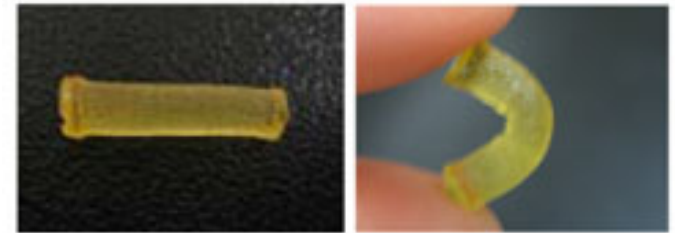


Tissue Expander

mandible cross section



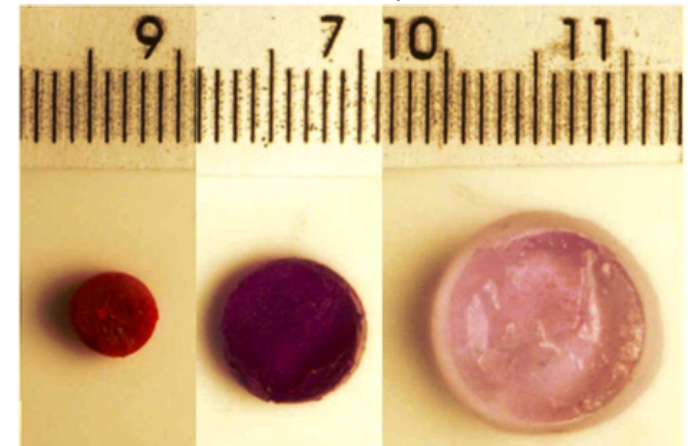
Restiex® (Re-Shapable Tissue Expanding Hydrogel)



A hydrogel expander normal and being flexed between fingers. Note its elasticity.

Delayed Swelling Hydrogel

Stained with Nile Red to improve visibility. Imaged at specified times.



Dry

1 Day

Fully Degraded
After 2 Weeks

<http://polyscitech.com/currentResearch/restiex/>

Hard Tissue - Soft Tissue Interface

Design and Fabrication of Bone-to-Soft Tissue Interfaces



Professor Sherry Harbin

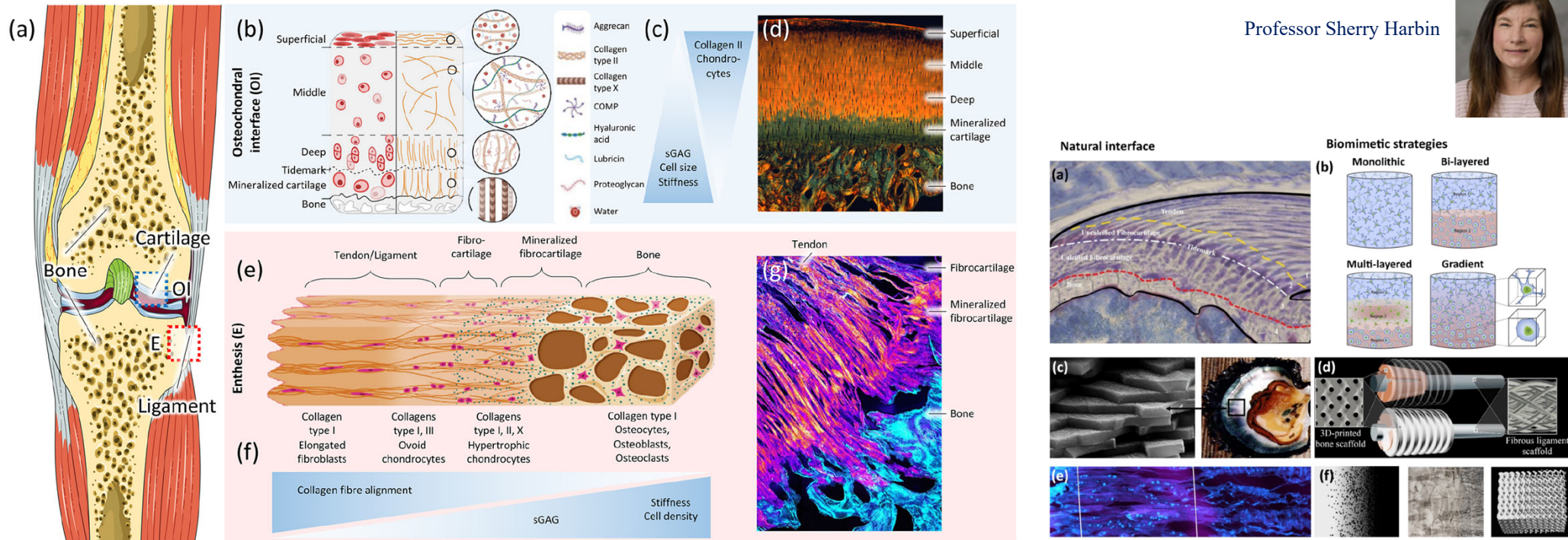


Figure 1. Structure of bone-to-soft interfaces in the human knee joint. (a) Human knee (from Servier Medical Art) illustrating a blue box for the osteochondral interface (OI) and a red box for the enthesis (E). (b) Schematic of the osteochondral interface divided into the morphology and distribution of the cells (left) and the matrix organization (right) within the different zones in the OI. Panel b is reproduced with permission from ref 72. Copyright 2021 MDPI. (c) Diagram showing the gradients observed in the OI. (d) Histological image of the osteochondral unit showing the different zones in the OI. The subfigure corresponds to a picrosirius red stained sample, imaged with a polarized light filter that shows the collagen distribution (aligned in orange and random in green). Panel d is reproduced with permission from ref 137. Copyright 2021 Elsevier. (e) Schematic of the ligament/tendon interface (enthesis, E) showing the predominant type of collagen and its orientation, and the type and morphology of the cells present in each zone. Panel e is reproduced with permission from ref 83. Copyright 2021 MDPI. (f) Diagram showing the gradients observed in the enthesis. (g) Histological image of the enthesis showing the different zones connecting the tendon and bone. The subfigure corresponds to a fluorescence microscope image showing the fibers of collagen type II in bright orange. Subfigure g is from ph.tum.de/latest/news/tendon-boneinsertion and reproduced with permission from ref 5. Copyright 2021 Nature.

Biomimetic Design and Fabrication of Bone-to-Soft Tissue Interfaces

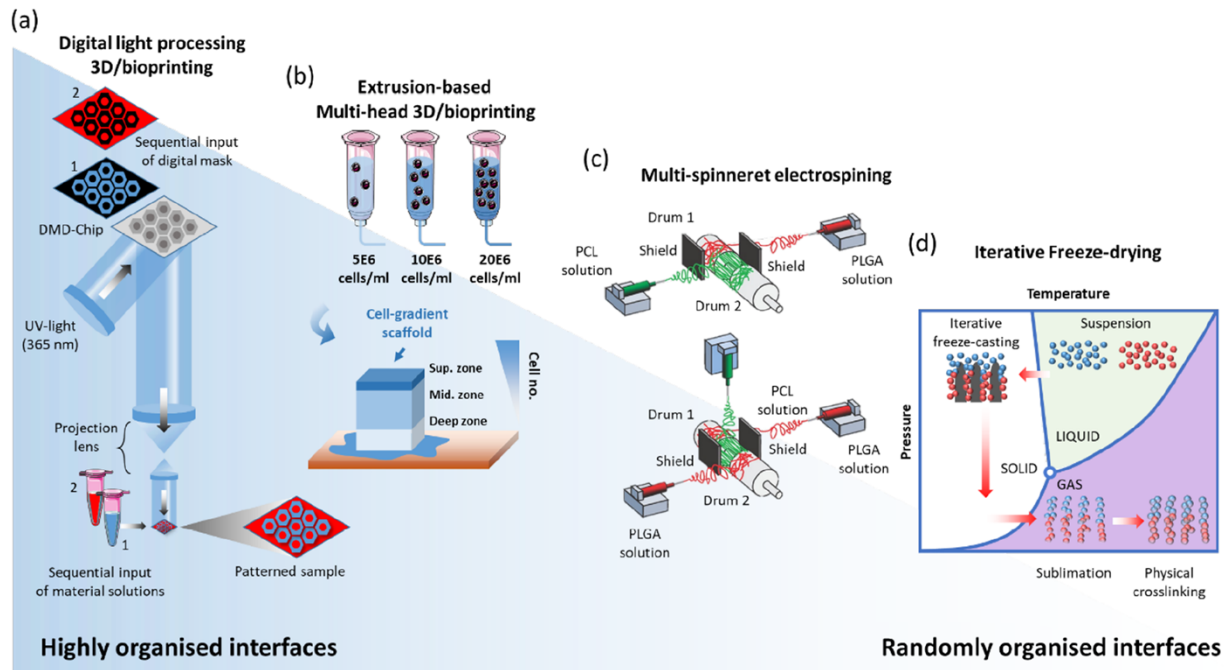


Figure 3. Schematics of different fabrication methods that can be used for bone-to-soft interfaces, from highly organized interfaces (left) to randomly organized interfaces (right).

- (a) Digital light processing-based 3D/bioprinting showing that sequential input of different digital masks can be used to generate patterns with interfaces of **different materials**.
- (b) Extrusion-based 3D/bioprinting showing that the combination of multiheads containing different bioinks can be used to generate scaffolds with **gradients** (in this example, cell gradients mimicking articular cartilage cell density).
- (c) Electrospinning setup with two spinnerets creating **a transitory region**.
- (d) Iterative freeze-casting (or ice-templating) can be combined with freeze-drying to achieve **bilayered structures** with a defined interface.

Kruize 2021, Biomimetic Approaches for the Design and Fabrication of Bone-to-Soft Tissue Interfaces

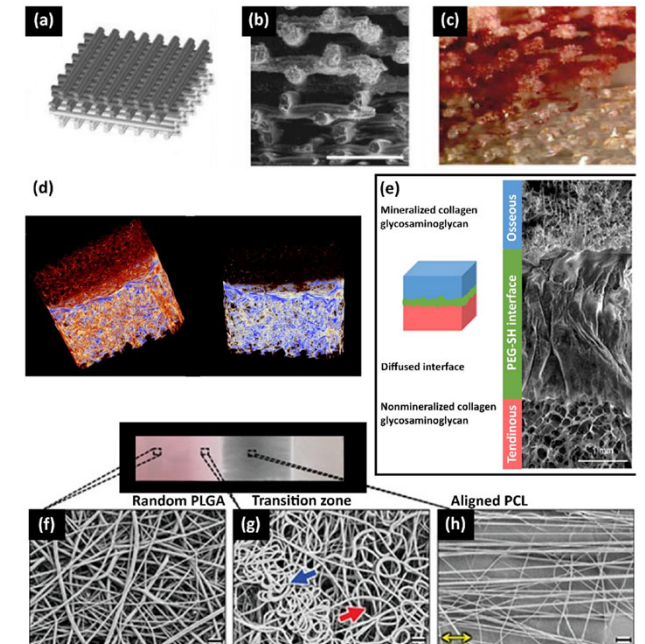
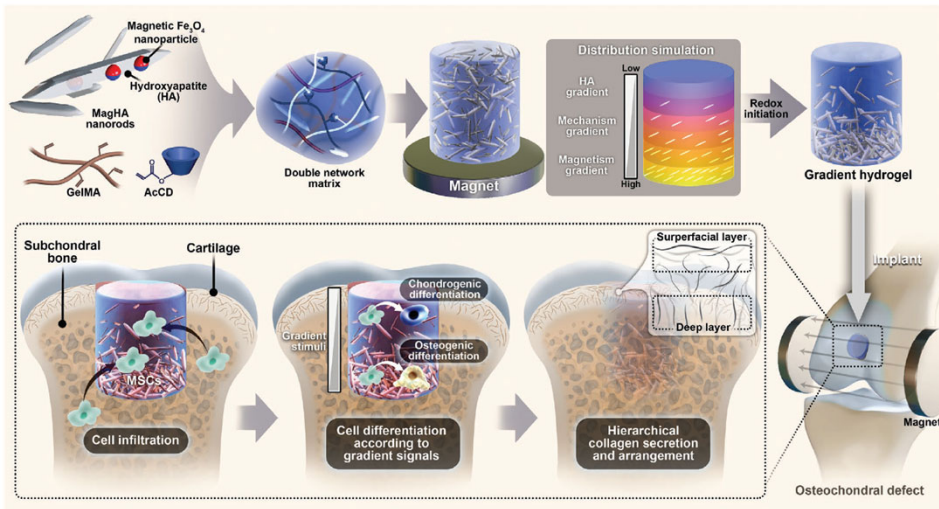


Figure 4. (a–c) Extrusion-based 3D printing of osteochondral interface scaffold: (a) CAD design, (b) interface of **PLA and a PLA/bioglass bilayer**, (c) scaffold microstructure stained with alizarin. (d) Freeze-dried **bilayered silk and silk-nano CaP scaffolds** for the osteochondral interface. (e) Freeze-dried **triphasic structural-continuous scaffolds** made of the mineralized, diffused region and nonmineralized collagen glycosaminoglycan for the bone–tendon interface. (f) the random PLGA region, (g) **the transition of PLGA to the PCL region**, to (h) the aligned PCL region.

Multileveled Continuous Gradient Hydrogel



Scheme 1. The design and application of a multileveled continuous gradient hydrogel for the repair of osteochondral defects. A) A schematic illustration shows that a gradient hydrogel consists of inorganic superparamagnetic HA nanorods (MagHA) having superparamagnetic nanocores and an organic gelatin methacryloyl (GelMA)/acrylate β -cyclodextrin (AcCD) double-network adaptable matrix. This composite hydrogel was fabricated based on gradient patterning driven by a magnet and redox-initiated crosslinking in sequence. The smooth gradient distribution was predicted and optimized before fabrication via computer simulation based on magnetic resonance imaging (MRI) and histological data. Continuous MagHA gradation contributes to the natural generation of mechanical and magnetism gradients to gain a multileveled continuous gradient hydrogel. Subsequently, such a gradient hydrogel is implanted into an osteochondral defect. This comprehensive strategy achieves an ideal regeneration for the full-thickness cartilage-to-subchondral bone interface that facilitates cell infiltration and guided depth-dependent cell differentiation.

Zhang 2023, Multileveled hierarchical hydrogel with continuous biophysical and biochemical gradients for enhanced repair of full-thickness osteochondral defect

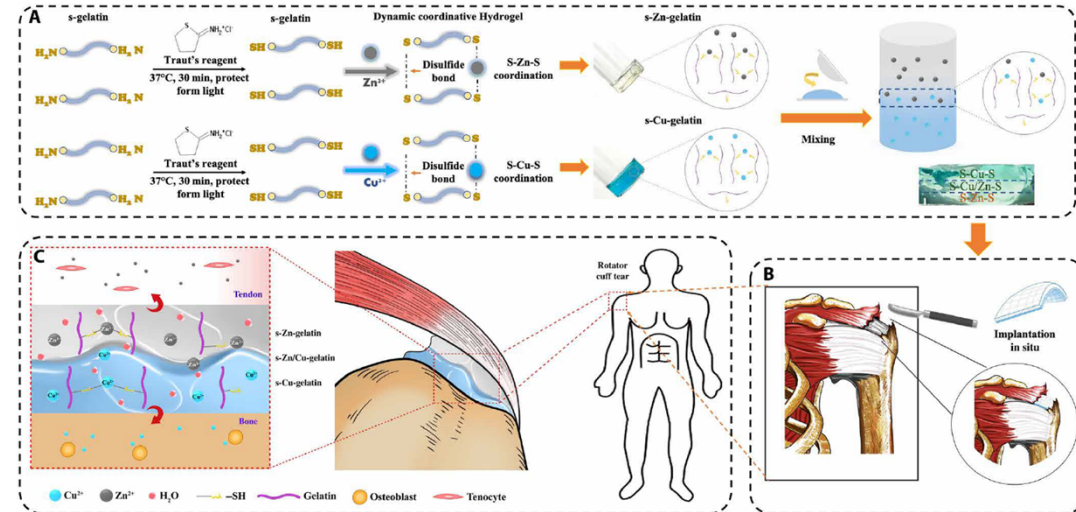


Fig. 1. The principle and fabrication of the gradient bimetallic ion-based hydrogels and the operation diagram. (A) The principle and fabrication of the novel gradient bimetallic hydrogels and the exhibition of the gradient structure. (B) The in situ implantation of the novel hydrogel for rotator cuff tear (RCT). (C) The mechanism of the gradient hydrogel for synchronous regeneration in the tendon-to-bone insertion.

Yang 2021, Gradient bimetallic ion-based hydrogels for tissue microstructure reconstruction of tendon-to-bone insertion

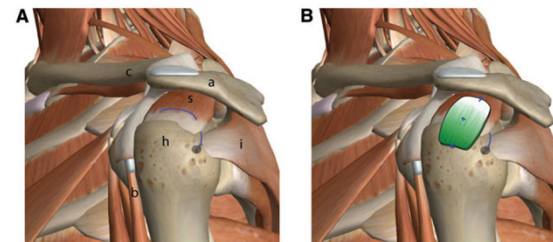


FIG. 1. A schematic of the human shoulder is shown (A) with the proposed placement of the scaffold (B).

Lipner 2015, In vivo evaluation of adipose-derived stromal cells delivered with a nanofiber scaffold for tendon-to-bone repair.

Hao 2026, Functionally graded surfaces and materials- From fabrication to biomedical applications

Making Tough Hydrogels

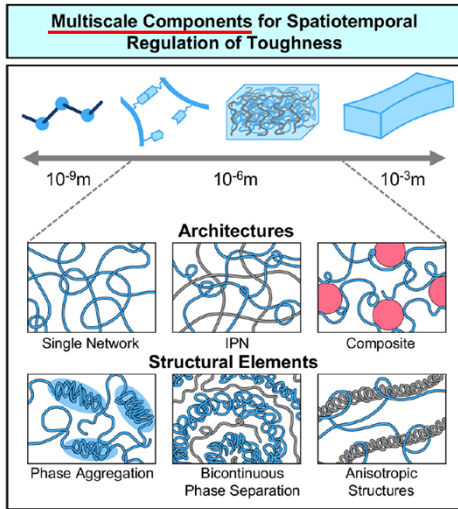


Figure 27. Toughness can result from synergy that occurs across the multiscale regime.

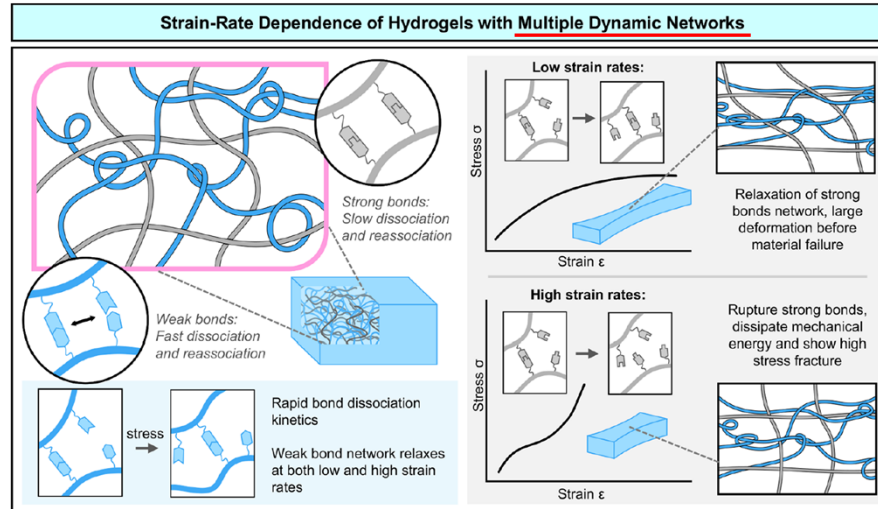
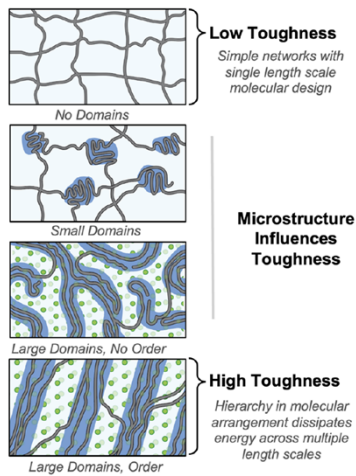
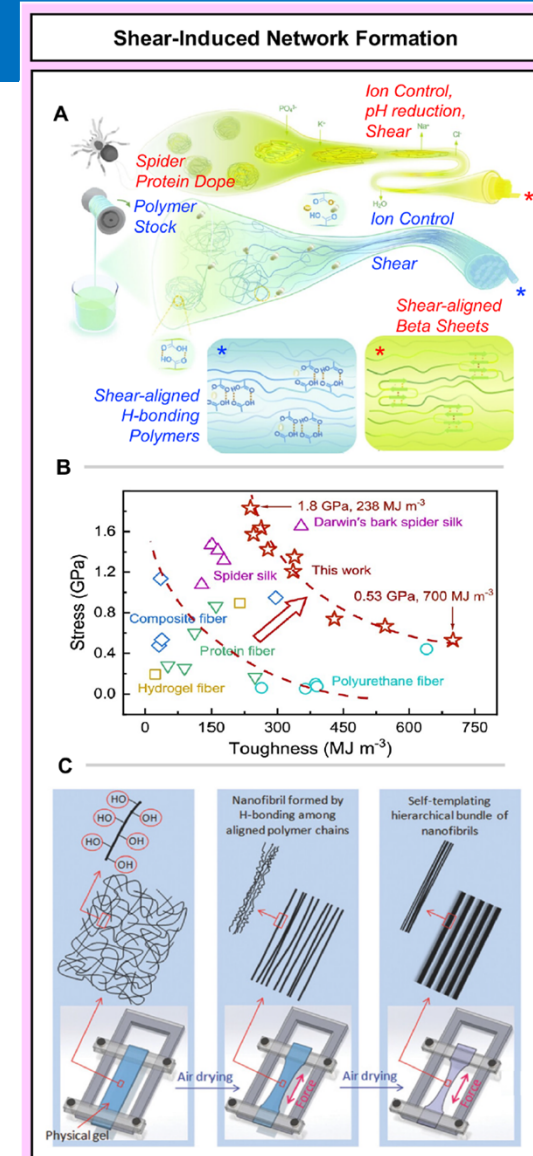


Figure 28. Strain-rate dependence of dynamic networks containing **bonds with distinct reformation timescales and bond strengths**. Weaker bonds with fast reformation timescales act as dynamic crosslinkers that relax quickly across strain rates. **Strong bonds with slow reformation timescales** act as dynamic crosslinkers under slow strain rates, allowing a large amount of deformation. Under fast strain rates, these bonds act as static crosslinkers that rupture and dissipate mechanical energy, resulting in high stress fracture and strain-induced toughening.

Figure 50. A) Schematic of the spinning of spider silk and the PAA fiber artificial spider silk system, where modulation of the nanofibrils of the PAA fiber can be achieved by tuning the polymer chain flexibility, and B) the breaking stress and toughness of the artificial spider silk fibers using PAA fiber can be compared with those of typical robust fiber materials reported in the literature. C) Schematic of drying in confined conditions method for creating **aligned fibrous hydrogels** with hierarchical superstructures. A rectangular piece of hydrogel with fiber-forming H-bonding sites is clamped to a sample holder. During air drying, the gel's width and thickness shrink, and it experiences tension that aligns the polymer chains along its length. Thin fibrils are formed along the tensile direction through H-bond formation as drying increases the concentration of polymer. Further drying induces aggregation of nanofibrils to form thick fibers, and reswollen gels maintain their structure due to the formation of stable H-bonds.

Tabit 2026, Tailoring crosslinks through time- A paradigm for tough hydrogels



Polymers in Wound Healing

Polymers for Wound Healing

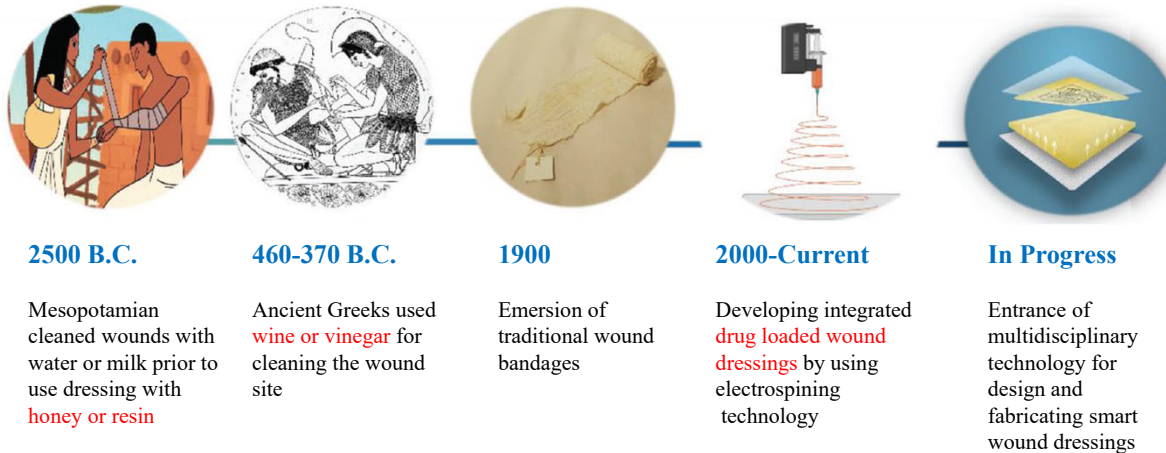


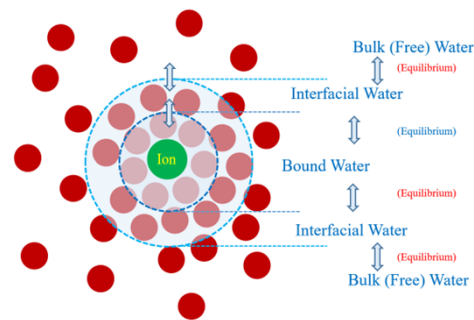
Figure 1. Historical timeline of wound dressing evolution.

Sugars are the major component of honey (>85%)

Valverde 2022, Recent trends in the analysis of honey constituents

Only free water can be used by cells.

Bound water does not freeze when cooled below 0 °C.



Moisture Content

- Quantitative amount of free water and bound water in a food system.
- Measured using moisture meter.
- Can be measured in wet or dry basis.

Water Activity

- Quantitative and qualitative amount of free water in a food system.
- Measured using water activity meter.
- Microbes use free water for their growth.

The Water Activity

The water activity (a_w) of a food is the ratio between the vapor pressure of the food itself (p), when in a completely undisturbed balance with the surrounding air media, and the vapor pressure of distilled water under identical conditions (p^*), i.e., $a_w = p/p^*$. A water activity of 0.80 means the vapor pressure is 80 percent of that of pure water. The water activity increases with temperature. The moisture condition of a product can be measured as the equilibrium relative humidity (ERH) expressed in percentage or as the water activity expressed as a decimal.

Most foods have a water activity above 0.95 and that will provide sufficient moisture to support the growth of bacteria, yeasts, and mold. The amount of available moisture can be reduced to a point which will inhibit the growth of the organisms. If the water activity of food is controlled to 0.85 or less in the finished product, it is not subject to the regulations of 21 CFR Parts 108, 113, and 114.

The water activity level of 0.85 is used as a point of definition for determining whether a low-acid canned food or an acidified food is covered by the regulations. Low-acid canned foods can be preserved by controlling water activity at levels above 0.85. The minimum a_w level for the growth of *C. botulinum* is approximately 0.93. Depending on various product characteristics this minimum level can be as high as 0.96. The regulations (21 CFR 113.3(e) (1) (ii)) state that commercial sterility can be achieved by the control of water activity and the application of heat. The heat is generally necessary at a_w levels above 0.85 to destroy vegetative cells of microorganisms of public health significance (e.g., staphylococci) and spoilage microorganisms which can grow in a reduced a_w environment.

FDA 1984, Water activity (a_w) in foods (<https://www.fda.gov/inspections-compliance-enforcement-and-criminal-investigations/inspection-technical-guides/water-activity-aw-foods>)

Rifna 2022, Role of water activity in food preservation (pp. 39-64)

Polymers for Wound Healing

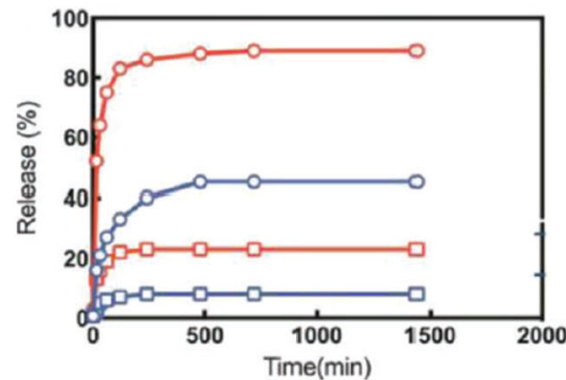
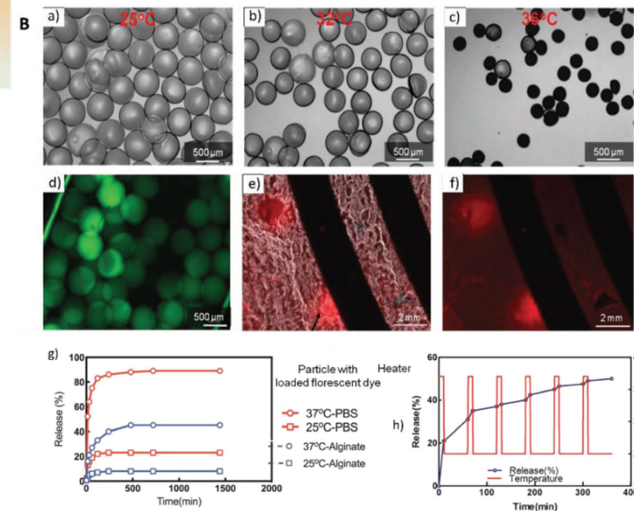
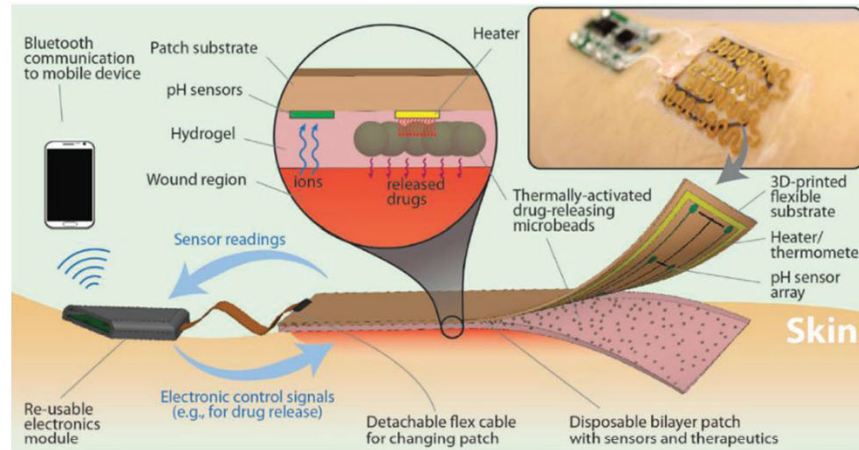
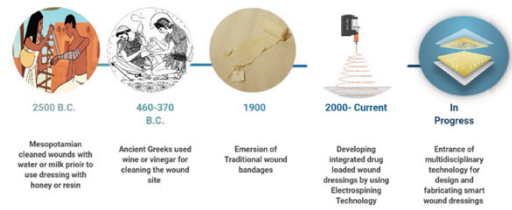


Figure 3. A–C) Schematic of the smart wound bandages with wound markers sensing capabilities and on-demand delivery of therapeutic molecules for the treatment of chronic wounds. A) Conceptual view of the automated smart bandage. The bandage comprised a **multilayer flexible pH sensor and a flexible heater for on-demand release triggering thermoresponsive drug carriers containing antibiotics** in the wound site with wireless communication capabilities to smartphones. B) Schematic view of integrated drug-releasing microparticles within the dressing. a–c) Optical image of the temperature-responsive microparticles at different temperatures. d–f) Fluorescence images of embedded drug microcarriers inside the smart microheater attached hydrogel dressing. Rhodamine B was used for better visualization of drug carriers inside the dressings. g) Release profile of cefazolin as a model antibiotic drug in different temperatures. h) Controlled release profile of cefazolin.

Figure 8. Schematic demonstration of a smart hydrogel-based wound dressing. A) An intelligent hydrogel wound dressing for the early detection of wound infection. B) Schematics of the stages of the smart wound dressing fabrication process. C) A close-up view of the final prototype of the smart wound dressing. D) Assessment of the function of treated dressing by using Triton under UV light exposure.

Farahani 2021, Wound healing. From passive to smart dressings

Wound Healing

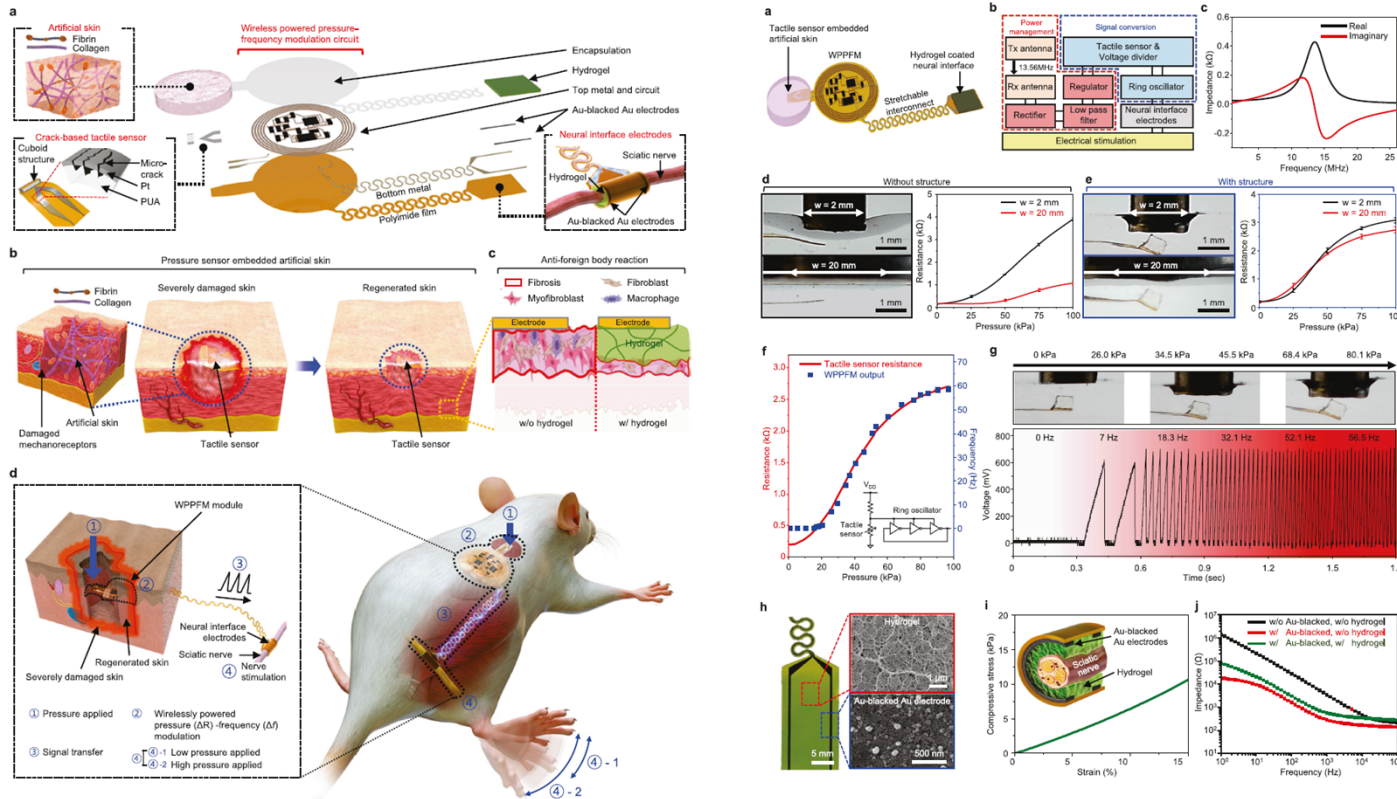


Fig. 1 | Overall schematic of the WTSA and converted tactile signal transfer process to stimulate the sciatic nerve. a) An exploded view schematic of WTSA composed of artificial skin, crack-based tactile sensor, WPPFM circuit, neural interface electrodes and fibrin coating to minimize foreign body reaction. b) Accelerated skin regeneration process through an ECM-based artificial skin composed of collagen and fibrin. c) Suppression of the foreign body reactions by the hydrogel layer for an effective neural stimulation. d) Schematic image of tactile signal modulation and signal transfer process for stimulating the sciatic nerve with respect to the different intensities of applied pressure.

Fig. 2 | Characteristics of the WPPFM and neural interface electrodes.

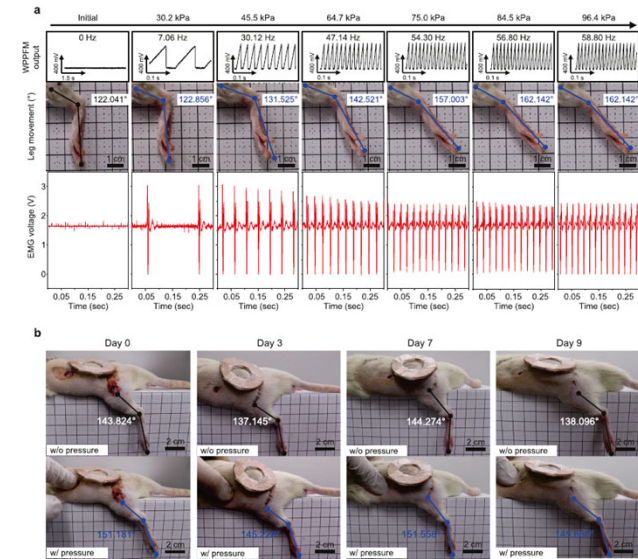


Fig. 5 | In vivo demonstration of implanted WTSA and precise analysis of leg movements according to the externally applied pressure

Kang 2024, Heparin-network-mediated long-lasting coatings on intravascular catheters for adaptive antithrombosis and antibacterial infection

Antifouling Surfaces

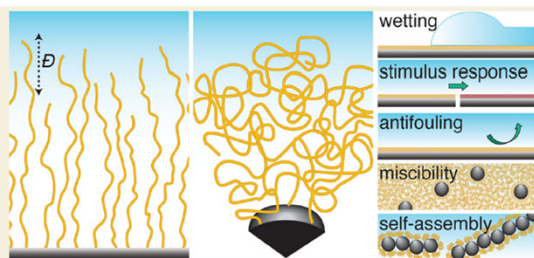
ABSTRACT: Antifouling properties are indispensable for ensuring the efficiency of biomedical applications in biotechnology. Bioinspired antifouling surfaces have undergone significant development. The adhesive interactions of nanopatterns supply localized force-related data. In this study, a precisely defined conducting polymer (CP), poly(3,4-ethylenedioxythiophene) (PEDOT), was enriched with antifouling phosphorylcholine moieties (PEDOT-PC) for comparison with hydroxyl-functionalized PEDOT (PEDOT-OH) to investigate their effects. Well-defined nanopatterned PEDOT films can be precisely created by controlling the electropolymerization process on a polystyrene (PS) monolayer template using a colloidal lithography approach. Electropolymerized PEDOT coatings have emerged as a surface modification strategy for bioelectrodes due to their facile functionalization and fabrication. The patterns are versatile, depending on the sizes of PS beads and electropolymerization conditions. Atomic force microscopy (AFM) allows for the examination of the adhesion effects of periodic nanostructures in aqueous solutions. Real-time and quantitative assessment of adhesion between the AFM tip and the sample was conducted through force–volume mapping. Furthermore, the study involved the examination of protein adsorption behaviors at these interfaces using a quartz crystal microbalance with dissipation (QCM-D), including bovine serum albumin (BSA), cytochrome *c* (cyt *c*), lysozyme (LYZ), and C-reactive protein (CRP). AFM probing near the interface revealed that surface morphology induced higher adhesion forces than pristine polymer films, whereas the PEDOT-PC coating exhibited minimal interaction during tip scanning. Additionally, protein adsorption tests indicated that the nanostructures compromised the antifouling properties of PEDOT-PC films, aligning with water contact angle measurements. The periodic structure enhances the energy barrier, disrupting the preservation of a continuous water layer captured by the PC moieties. Our research offers a straightforward approach to creating a nano CP template suitable for various systems. Moreover, it provides a deeper understanding of the physical investigation and the implications of biomolecule responses of the nanostructure effects using AFM and QCM-D.

KEYWORDS: nanostructure, AFM, conducting polymer, PEDOT, adhesive force, biointerface

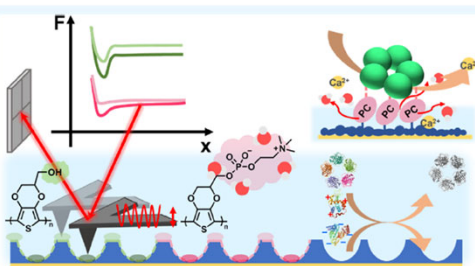
Lin 2023 Nanostructured effect on antifouling conducting polymers through interfacial adhesive interaction and protein adsorption

ABSTRACT: Breadth in the molecular weight distribution is an inherent feature of synthetic polymer systems. While in the past this was typically considered as an unavoidable consequence of polymer synthesis, multiple recent studies have shown that tailoring the molecular weight distribution can alter the properties of polymer brushes grafted to surfaces. In this Perspective, we describe recent advances in synthetic methods to control the molecular weight distribution of surface-grafted polymers and highlight studies that reveal how shaping this distribution can generate novel or enhanced functionality in these materials.

KEYWORDS: surface-grafted polymer, dispersity, molecular weight distribution, polymer-grafted nanoparticle, polymer conformation, stimulus response



Conrad 2023, Shaping the structure and response of surface-grafted polymer brushes via the molecular weight distribution



Surface Hydration and Antifouling Activity of Zwitterionic Polymers

Zhan Chen*

Cite This: *Langmuir* 2022, 38, 4483–4489

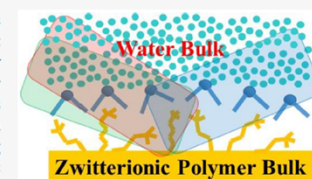
Read Online

ACCESS |

Metrics & More

Article Recommendations

ABSTRACT: It is believed that the strong surface hydration of zwitterionic polymers leads to excellent antifouling properties. This Perspective presents the recent developments in studies on such surface hydration in situ using sum frequency generation (SFG) vibrational spectroscopy. SFG research provides direct molecular level evidence that zwitterionic polymers have strong surface hydration, which prevents protein adsorption and marine animal attachment. The salt effect and protein interaction on surface hydration of zwitterionic polymers have also been examined using SFG. Possible future research directions on surface hydration of new zwitterionic polymers including zwitterionic hydrogels, copolymers, and mixed charged polymers are discussed. It is also important to combine experimental SFG studies with computer simulations to further elucidate the surface hydration to understand antifouling mechanisms.



Chen 2022, Surface hydration and antifouling activity of zwitterionic polymers

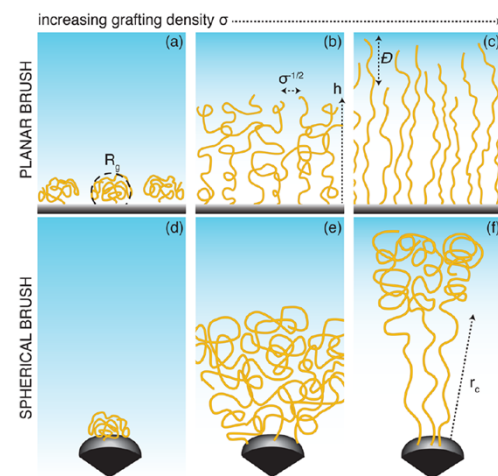


Figure 1. Schematic illustration of the conformation of (a–c) planar and (d–f) spherical polymer brushes with increasing grafting density σ . The polymer radius of gyration R_g , brush height h , and (for spherical brushes) critical radius r_c are shown. The dispersity D is the ratio of the weight-average and number-average molecular weights.

Antifouling Surfaces

ABSTRACT: Implant-associated infections arising from biofilm development are known to have detrimental effects with compromised quality of life for the patients, implying a progressing issue in healthcare. It has been a struggle for more than 50 years for the biomaterials field to achieve long-term success of medical implants by discouraging bacterial and protein adhesion without adversely affecting the surrounding tissue and cell functions. However, the rate of infections associated with medical devices is continuously escalating because of the intricate nature of bacterial biofilms, antibiotic resistance, and the lack of ability of monofunctional antibacterial materials to prevent the colonization of bacteria on the device surface. For this reason, many current strategies are focused on the development of novel antibacterial surfaces with dual antimicrobial functionality. These surfaces are based on the combination of two components into one system that can eradicate attached bacteria (antibiotics, peptides, nitric oxide, ammonium salts, light, etc.) and also resist or release adhesion of bacteria (hydrophilic polymers, zwitterionic, antiadhesive, topography, bioinspired surfaces, etc.). This review aims to outline the progress made in the field of biomedical engineering and biomaterials for the development of multifunctional antibacterial biomedical devices. Additionally, principles for material design and fabrication are highlighted using characteristic examples, with a special focus on combinational nitric oxide-releasing biomedical interfaces. A brief perspective on future research directions for engineering of dual-function antibacterial surfaces is also presented.

KEYWORDS: antibacterial, antifouling, biomedical devices, surface coatings, nitric oxide, biofilm

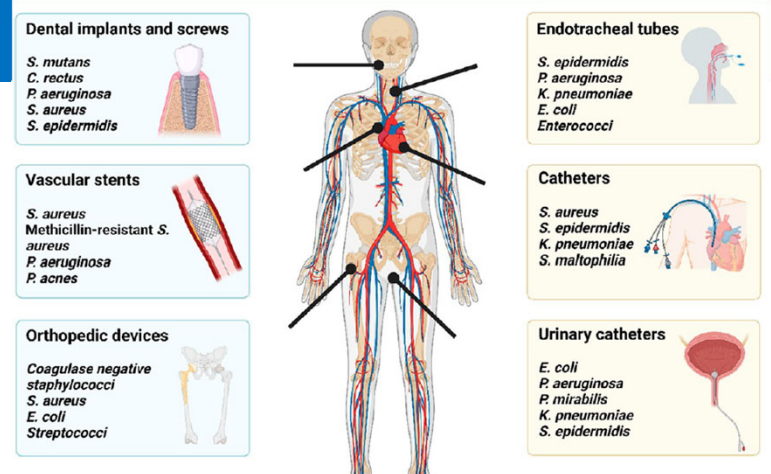
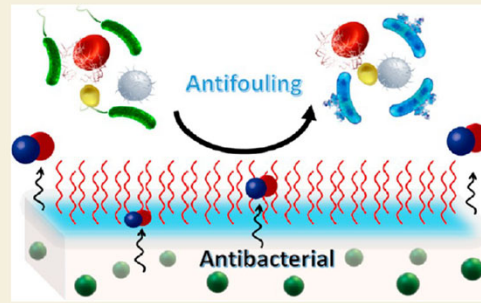


Figure 1. Examples of microbial species frequently responsible for causing biomedical-device-associated infections that arise from various implantable and indwelling medical devices. These include both short- and long-term devices, including dental implants, endotracheal tubes, vascular and peritoneal catheters, vascular stents, urinary catheters, and fracture fixation devices. The three most common infections arising from medical devices are catheter-related bloodstream infections (CRBSIs), catheter-associated urinary tract infections (CAUTIs), and ventilator-associated pneumonia (VAP). These are indicated by yellow boxes on the right.

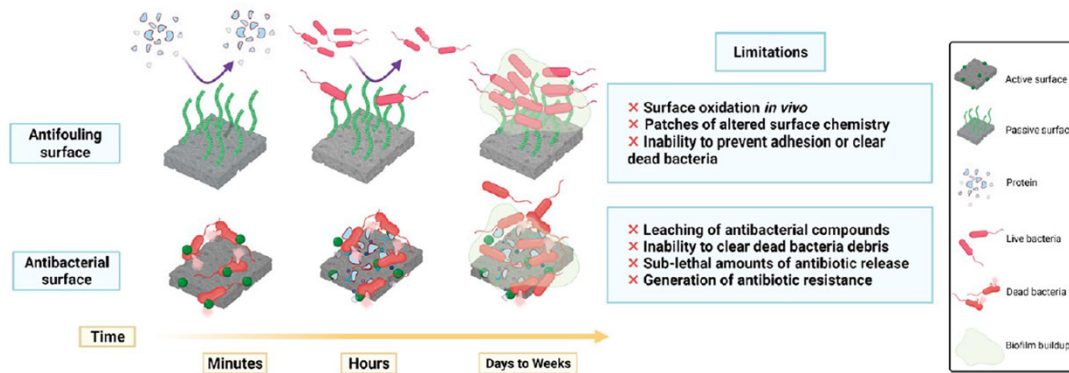


Figure 3. Progression of biofilm formation and proliferation on a medical device surface and failure of a singular approach to fully prevent infection on biomaterial surfaces. A passive surface can prevent or reduce the initial attachment of bacteria. However, the material chemistry can significantly change upon exposure to the physiological environment, which can lead to failure of the antifouling material chemistry. Ultimately, bacteria are able to breach the altered surface, colonize, and form a biofilm. Active surfaces with contact-based killing succumb to fouling from dead bacteria debris and proteins. However, the release of active agents from these biomaterials continues to eradicate pathogens until the source of the active agent becomes depleted. Both single-mechanism active and passive surfaces lead to eventual biofilm formation in long-term applications.

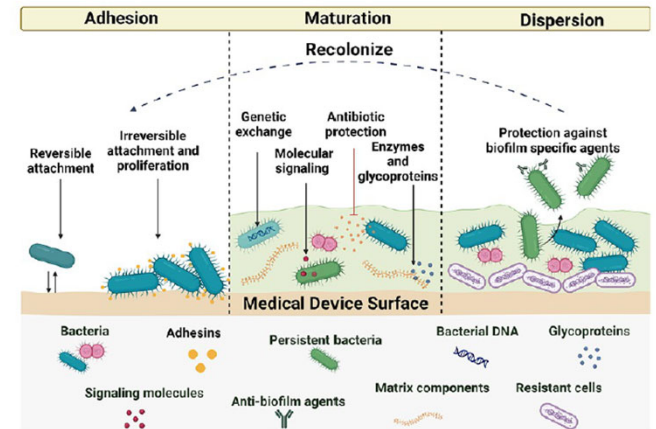


Figure 2. (A) Progression of biofilm formation and proliferation on a medical device surface.

Silly String

Poly(isobutyl methacrylate) resin in trichloromonofluoromethane (Freon-11)

United States Patent Cox et al.

[15] **3,705,669**
[45] **Dec. 12, 1972**

[54] FOAMABLE RESINOUS COMPOSITION

[72] Inventors: Robert P. Cox, Madison, Wis.; Leonard A. Fish, Chicago, Ill.
[73] Assignee: Wham-O Manufacturing Company, San Gabriel, Calif.

[22] Filed: June 8, 1970
[21] Appl. No.: 44,529

Related U.S. Application Data

[63] Continuation-in-part of Ser. No. 860,854, Sept. 24, 1969, abandoned.

[52] U.S. Cl. 222/394, 260/2.5 P, 260/2.5 E, 260/2.5 R, 260/23 R, 260/31.8 H, 260/86.1 E, 260/33.8 UA, 260/89.5 A, 272/1

[51] Int. Cl. C08f 47/10, C08f 29/46
[58] Field of Search ... 260/2.5 E, 2.5 P, 23 R, 23 AC, 260/33.8 UA, 31.8 H, 272/1, DIG. 1; 273/1, DIG. 16; 222/394

[56] References Cited

UNITED STATES PATENTS

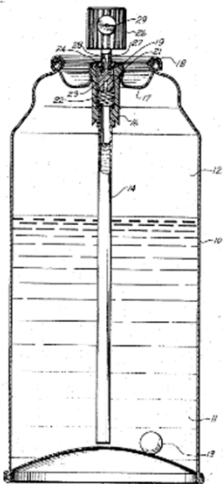
3,419,506 12/1968 Gander.....260/33.8 UA
3,413,387 11/1968 Ohol.....260/2.5 E
2,773,855 12/1956 Hochberg et al.260/33.8 UA

Primary Examiner—Murray Tullman
Assistant Examiner—Wilbert J. Briggs, Sr.
Attorney—Christie, Parker & Hale

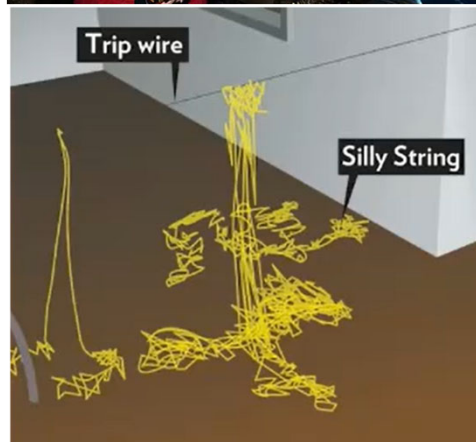
[57] ABSTRACT

A pressurized or "aerosol" can containing a composition of matter for producing a string of plastic foam is described. The plastic foam produced from the aerosol can is in the form of a cohesive plastic body sufficiently tacky to adhere to inert surfaces such as walls, windows or the like to support the weight of the foam, however, of insufficient tackiness to adhere with a force greater than the cohesive strength of the foam so that the foamed body can be readily removed from surfaces to which it lightly adheres. Such a combination has substantial play and decorative utility.

14 Claims, 1 Drawing Figure



Cox 1972, Foamable resinous composition



Original Intended Application

Silly String was originally intended to be a medical product - specifically an instant spray-on bandage. In 1969, inventors Leonard A. Fish and Robert P. Cox were working on a way to provide **immediate, sterile coverage for wounds by forming smooth, thin, and uniform film with fine mist spray of elastomeric polymers**. They were experimenting with a mixture of resins and propellants in an aerosol can, hoping to create a fine mist that would settle into a thin, protective film over the skin.

During a test with a specific nozzle, the device didn't produce a mist. Instead, it shot out a long, continuous, slightly sticky plastic foam string that could travel across a room.

While **it was a total failure as a medical bandage (since it didn't coat the wound evenly)**, Fish and Cox realized they had accidentally invented a highly entertaining projectile.

Wham-O licensed the technology and branded it as "Silly String," launching it into the toy market in 1972.

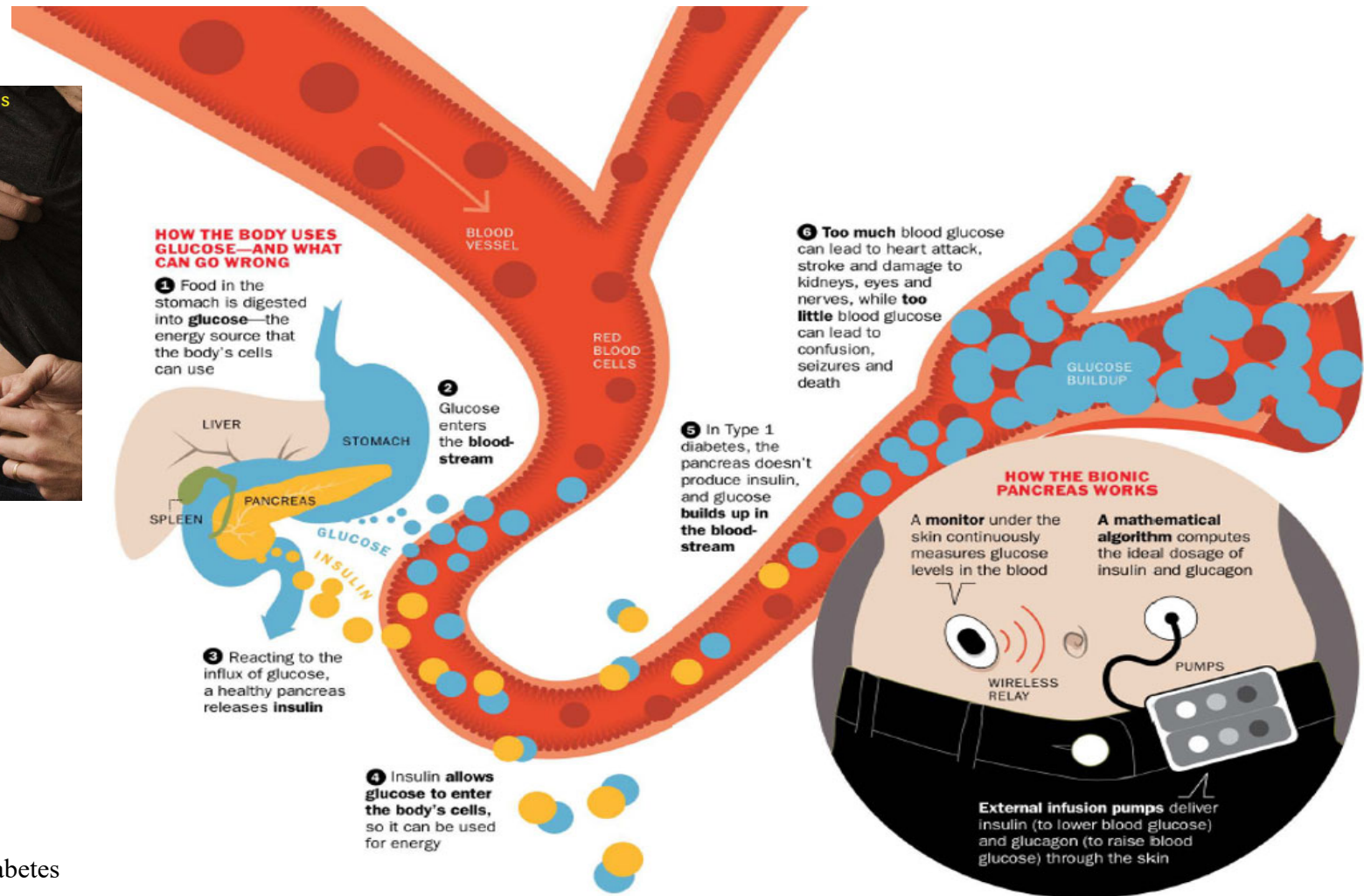
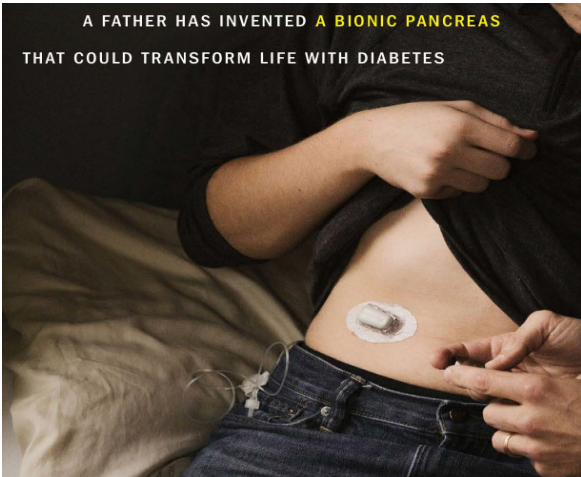
An example of serendipity (as with the invention of the Post-it Note adhesive or Play-Doh, which started as a wallpaper cleaner).

Military Application

One of the most unique "serious" references for Silly String is its use by United States forces during the Iraq War. Soldiers discovered that Silly String was lightweight enough to be sprayed over a room to **detect invisible tripwires**. If the string draped over a wire without triggering the explosive, it alerted the soldiers to the danger. Charity Efforts: In the mid-2000s, several high-profile "Silly String drives" saw civilians mail cans of the toy to troops overseas for this tactical purpose.

Hybrid Closed-Loop Systems for Insulin Delivery

Bionic Pancreas



The Next Best Thing to a Cure for Diabetes
 Alexandra Sifferlin . TIME 2015

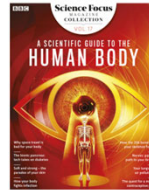
Continuous Glucose Monitoring and Insulin Delivery

Records glucose levels every five minutes.
Replace the sensor after three days of use. Required to take finger sticks twice a day order to calibrate the glucose sensor.



Computer-controlled diabetes Managing diabetes means an ever-changing daily regime of multiple, self-administered insulin injections. But what if there was a device that could do the managing for you? (SARA RIGBY)

For someone living with type 1 diabetes, monitoring and maintaining glucose levels can be a chore, requiring, on average, an injection of insulin between two and six times a day. A team at Imperial College London is aiming to make their lives easier by developing a device dubbed the 'bionic pancreas'. "It will be a revolution both in terms of glucose control and quality of life for people living with diabetes," says Dr Pau Herrero-Vinas, an engineer on the team. The pancreas is a small, pear-shaped organ that controls blood sugar levels. The cells responsible for this job, beta cells, respond to spikes in glucose levels by simultaneously releasing and manufacturing the hormone insulin, which allows glucose to be absorbed into tissue. When not enough insulin is produced, glucose builds up in the bloodstream and, past a certain point, can lead to coma and death. High blood sugar levels, also known as hyperglycaemia, can cause blindness, heart disease and nerve damage over the long-term. TECHNOLOGY STEPS IN In people with type 1 diabetes, the pancreas contains only 20 to 30 per cent of the regular number of beta cells, meaning that insulin levels are dangerously low unless treated with regular injections of insulin. The bionic pancreas, or the Bio-inspired Artificial Pancreas for the Home, is designed to act like a replacement organ. The process of regulating blood sugar levels is fully automated, so the device is constantly monitoring glucose levels and making small changes to keep them under precise control. ABOVE: Dr Nick Oliver, part of the team developing the Bio-inspired Artificial Pancreas, with a prototype of the device BELOW: The MiniMed 670G 'hybrid' system is already available but requires the user to input info about the food they're consuming The device is comprised of a glucose sensor, an insulin pump and a microchip. The microchip's algorithm calculates the precise amount of insulin needed, mimicking the behaviour of beta cells. By embedding all the software onto a microchip, the team created a device that not only requires small amounts of power, but is also compatible with other medical devices the user might need. "We focussed on developing a system that is very low-power so that it can be embedded in any medical device," Dr Herrero-Vinas explains. There is another artificial pancreas system, the MiniMed 670G, already on the market, but it is known as a 'hybrid' system since it isn't fully automated. At mealtimes, the user still needs to give the device information about the carbohydrates they're about to eat so that it can calculate the correct insulin dose. When the user isn't eating, though, the MiniMed works happily on its own – meaning it is most effective overnight. "Overnight control is a problem that's already been solved, so it's not very challenging anymore," says Dr Herrero-Vinas. "But daytime control, especially after meals, that's still a problem. So that's what we're focussing on: to have a system that works at night and through the day." The bionic pancreas is currently being clinically tested. Once these tests are complete, says Dr Herrero-Vinas, the team will look at licensing the product to make it available to patients, which he estimates will happen in a couple of years. bySARA RIGBY Sara is BBC Science Focus Magazine's online assistant.



Computer-controlled diabetes

Managing diabetes means an ever-changing daily regime of multiple, self-administered insulin injections. But what if there was a device that could do the managing for you?

words by SARA RIGBY

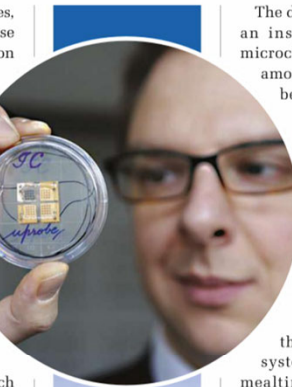
For someone living with type 1 diabetes, monitoring and maintaining glucose levels can be a chore, requiring, on average, an injection of insulin between two and six times a day. A team at Imperial College London is aiming to make their lives easier by developing a device dubbed the 'bionic pancreas'. "It will be a revolution both in terms of glucose control and quality of life for people living with diabetes," says Dr Pau Herrero-Vinas, an engineer on the team.

The pancreas is a small, pear-shaped organ that controls blood sugar levels. The cells responsible for this job, beta cells, respond to spikes in glucose levels by simultaneously releasing and manufacturing the hormone insulin, which allows glucose to be absorbed into tissue. When not enough insulin is produced, glucose builds up in the bloodstream and, past a certain point, can lead to coma and death. High blood sugar levels, also known as hyperglycaemia, can cause blindness, heart disease and nerve damage over the long-term.

TECHNOLOGY STEPS IN

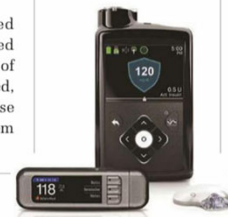
In people with type 1 diabetes, the pancreas contains only 20 to 30 per cent of the regular number of beta cells, meaning that insulin levels are dangerously low unless treated with regular injections of insulin.

The bionic pancreas, or the Bio-inspired Artificial Pancreas for the Home, is designed to act like a replacement organ. The process of regulating blood sugar levels is fully automated, so the device is constantly monitoring glucose levels and making small changes to keep them under precise control.



ABOVE: Dr Nick Oliver, part of the team developing the Bio-inspired Artificial Pancreas, with a prototype of the device

BELOW: The MiniMed 670G 'hybrid' system is already available but requires the user to input info about the food they're consuming



The device is comprised of a glucose sensor, an insulin pump and a microchip. The microchip's algorithm calculates the precise amount of insulin needed, mimicking the behaviour of beta cells. By embedding all the software onto a microchip, the team created a device that not only requires small amounts of power, but is also compatible with other medical devices the user might need. "We focussed on developing a system that is very low-power so that it can be embedded in any medical device," Dr Herrero-Vinas explains.

There is another artificial pancreas system, the MiniMed 670G, already on the market, but it is known as a 'hybrid' system since it isn't fully automated. At mealtimes, the user still needs to give the device information about the carbohydrates they're about to eat so that it can calculate the correct insulin dose. When the user isn't eating, though, the MiniMed works happily on its own – meaning it is most effective overnight. "Overnight control is a problem that's already been solved, so it's not very challenging anymore," says Dr Herrero-Vinas. "But daytime control, especially after meals, that's still a problem. So that's what we're focussing on: to have a system that works at night and through the day."

The bionic pancreas is currently being clinically tested. Once these tests are complete, says Dr Herrero-Vinas, the team will look at licensing the product to make it available to patients, which he estimates will happen in a couple of years. **SF**

by SARA RIGBY
Sara is BBC Science Focus Magazine's online assistant.

Hybrid Closed-Loop System

Closed-loop insulin (HCL) delivery systems (also known as “artificial pancreas”).

Hybrid closed loop systems (HCL systems): Integration of a closed-loop insulin delivery system with continuous glucose monitoring (CGM) and an algorithm that automates insulin delivery.

Currently, there are 2 systems: the commercial “auto-mode” and the “Do-it yourself” Artificial Pancreas System (DIYAPS) [2]. The use of technological progress is becoming an important and quite interesting point of care for diabetics, ranging from continuous glucose monitoring systems, through personal insulin pumps, and finally to the use of a combination of both systems to automate the insulin supply [3]. Citing evidence-based medicine, diabetological care in patients with T1D departs from the independent use of the CGM system and the insulin pump, replacing it with the HCL system option [4].

Commercial HCL systems

Closed-loop hybrid systems are characterized by automated algorithm-based insulin delivery and patient-initiated insulin delivery (e.g., post-meal boluses). There are several systems using hybrid closed loop technology currently offered on the global market: Medtronic’s System MiniMed™ 670G, and MiniMed™ 780G (SmartGuard™); Tandem’s T slim x2 Control IQ; Insulet’s Omnipod5®-Automated mode (HypoProtect™)[5]; and CamAPS FX DanaRS or Ypso pump [6].

Technology is moving forward, so advanced systems are being developed that include a developed algorithm with individualization of primary target points, an automated correction bolus function, and improved stability of the automated mode. The automated correction bolus feature is an innovation, which is why we refer to these systems as advanced hybrid closed-loop (AHCL).

Seget 2023, Commercial hybrid closed-loop systems available for a patient with type 1 diabetes in 2022

Table I. Characteristics of the commercial HCL and AHCL systems in a table of the research paper by Leelarathna et al. [2], Cobry et al.[8], and Braune et al. [9], with authors’ modification

Name of HCL system	Medtronic Minimed™ 670G [10]	Medtronic Minimed™ 780G [11]	Tandem’s T slim x2 Control IQ [12–14]	CamAPS FX DanaRS or Ypsomed pump [6, 15]	Insulet’s Omnipod5-Automated mode (HypoProtect™) [8, 16]
Name of Pump	670G	780G	Tandem T. Slim x2	Dana RS pump, Ypsomed pump	Omnipod (Pod + PDM - Personal Diabetes Manager)
Name of Sensor	Guardian 3	Guardian 3, Guardian 4	Dexcom G6, Dexcom G7 (coming soon [17, 18])	Dexcom G6	Dexcom G6, Dexcom G7 (coming soon [17, 18])
Duration of the Sensor (days)	7	7	10	10	10
Number of finger calibrations	Minimum 2 or even 4	Guardian 3: Minimum 2 (every 12 hours) Guardian 4: No finger calibration required	No finger calibration required	No finger calibration required	No finger calibration required
Pump insertion replacement time	Every 3 days	Every 3 days	48–72 hours	2–3 days [19]	Every 3 days
Working principle	<ol style="list-style-type: none"> SmartGuard™ technology¹ Manual mode: same as 640G [20] Automatic mode: <ul style="list-style-type: none"> Base: automatically adjusted basal insulin dose every 5 minutes based on real-time CGM values Bolus: required to manually administer a bolus by entering carbohydrate information into the insulin pump 	<ol style="list-style-type: none"> SmartGuard™ technology Manual Mode: Same as 640G [20] Automatic Mode: <ul style="list-style-type: none"> Base: precise, automatically selected basal insulin dose (every 5 minutes) based on rCGM values Bolus: automatic bolus correction based on rCGM value 	<ol style="list-style-type: none"> Using CGM values in conjunction with other variables (“insulin on board”) to predict glucose levels 30 minutes in advance and adjust insulin delivery accordingly If glucose levels fall < 112.5 mg/dl, basal insulin delivery is reduced When glucose is predicted to fall < 70 mg/dl, basal insulin delivery is stopped If glucose values > 160 mg/dl within the next 30 minutes, basal insulin increases If glucose values > 180 mg/dl, Control-IQ technology calculates a correction bolus to a target of 110 mg/dL and delivers 60% of this value as needed, up to once every 1 hour 	<ol style="list-style-type: none"> Model Predictive Control (MPC) – targeted treatment Automatic mode “Off” (open loop) is the mode in which the pump operates according to the programmed basic profile Automatic mode “On” (closed loop) is an operating mode in which insulin delivery is directed by the application, overriding the pre-programmed basal insulin delivery Automatic mode “Attempting” is a mode in which the application attempts to go into Auto mode but some condition prevents it from doing so. In “Attempting” mode, the insulin infusion will revert to the programmed basal infusion after approximately 30 minutes “Boost” mode is a mode that can be used when more insulin is needed. You can set the duration (from 0 to 13 hours) and the start time of Boost mode 	<ol style="list-style-type: none"> MPC algorithm to calculate microboluses of insulin delivered every 5 minutes based on CGM glucose data and predicted glucose values over a 60-minute prediction horizon The user is responsible for delivering bolus doses to meals using bolus settings programmed in PDM HypoProtect function – allows temporary reduction in basal insulin delivery during exercise Manual mode – only then are the basic doses used Automatic mode: <ul style="list-style-type: none"> basal control of the algorithm is based on the patient’s total daily insulin dose (TDDI) and does not require user intervention TDDI is estimated from the programmed basal doses during system startup the system assumes that the user needs 50% TDDI from basal insulin and 50% from bolus to estimate TDDI, the system calculates the total daily insulin dose resulting from the programmed basal doses and then doubles this value basal doses are modulated every 5 min based on TDDI the system tracks and updates the actual TDDI provided to the user.
Exercise mode	Appears	Appears	Appears	Appears	Appears (HypoProtect function for use during exercise (provides temporary reduction in basal insulin delivery)
Options for glucose targets	120 mg/dl – default setting for automatic mode 150 mg/dl – option for use during exercise	100 mg/dl, 110 mg/dl, 120 mg/dl, 150 mg/dl – during exercise	112.5–160 mg/dl 112.5–120 mg/dl – during sleep, 140–160 mg/dl – during exercise	(105 mg/dl) with an adjustable range of (80 to 200 mg/dl)	A user-programmable glucose value between 110–150 mg/dl (110, 120, 130, 140, and 150 mg/dl)
System limitations	Dedicated for patients with T1D ≥ 14 years old System use ≥ 7 years of age TDDI [2] ≥ 8 units per day.	Patients with T1D aged 7–80 years TDDI ≥ 8 units per day	Intended for people aged ≥ 14 years T1D in patients ≥ 6 years of age. TDDI ≥ 10 units of insulin per day Body weight ≥ 55 lbs	Patients with T1D aged 1 year and over using HCL Additional age restrictions may apply depending on the chosen continuous glucose monitor and insulin pump	The system has been designed and tested in patients with T1D aged 2 years and older
Use by pregnant women	Safety has not been studied in pregnant women	The safety of using the MiniMed™ 780G system in pregnant women has not been evaluated	Technology is not indicated for use in pregnant women	Can be used	Lack of data

Biomaterials for Encapsulation of Cells

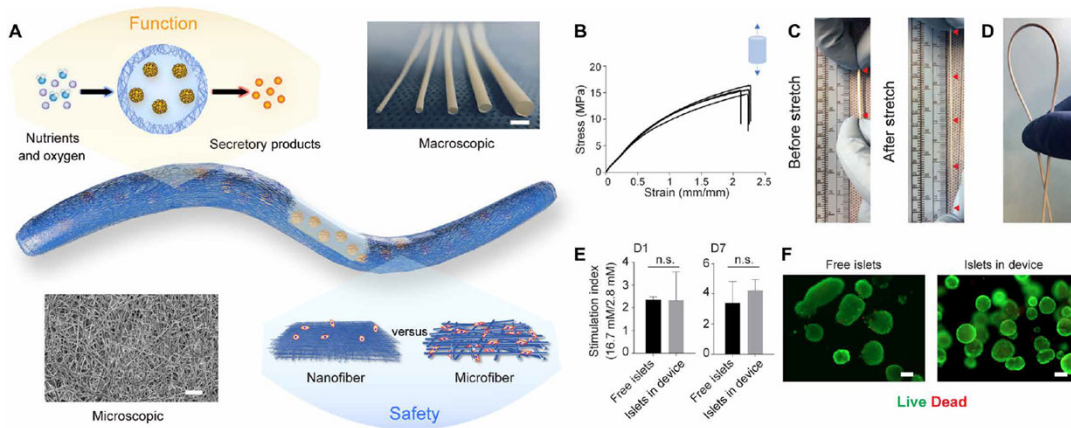


Fig. 1. Design and characterization of the NICE device including mechanical properties, permeability, and cell compatibility. (A) Schematics of the device showing the islet-laden hydrogel core surrounded by the nanofibrous skin that prevents cell penetration while allowing maximum mass transfer, along with a photo of nanofibrous tubes with different diameters (from left to right: 0.5, 1, 1.5, 2, and 3 mm) and a scanning electron microscope image of the nanofibers. (B) Tensile test (stress-strain curves) of the nanofibrous tubes ($n = 4$). (C and D) Photographs showing the device being stretched more than three times in length (C) and bent without kink (D). (E) SI of mouse islets (the ratio of insulin secretion in the buffers of high- and low-glucose concentrations) encapsulated in the device, compared to that of free-floating islets after 1 and 7 days of culture; mean \pm SD ($n = 3$). (F) Live (green) and dead (red) staining of free-floating islets and islets encapsulated in device after 1-day culture. The data were compared using the two-tailed Student's *t* test. Scale bars, 3-mm (A) macroscopic image and 100- (F) and 5- μ m (A) microscopic images. n.s., nonsignificant.

Wang 2021, A nanofibrous encapsulation device for safe delivery of insulin-producing cells to treat type 1 diabetes

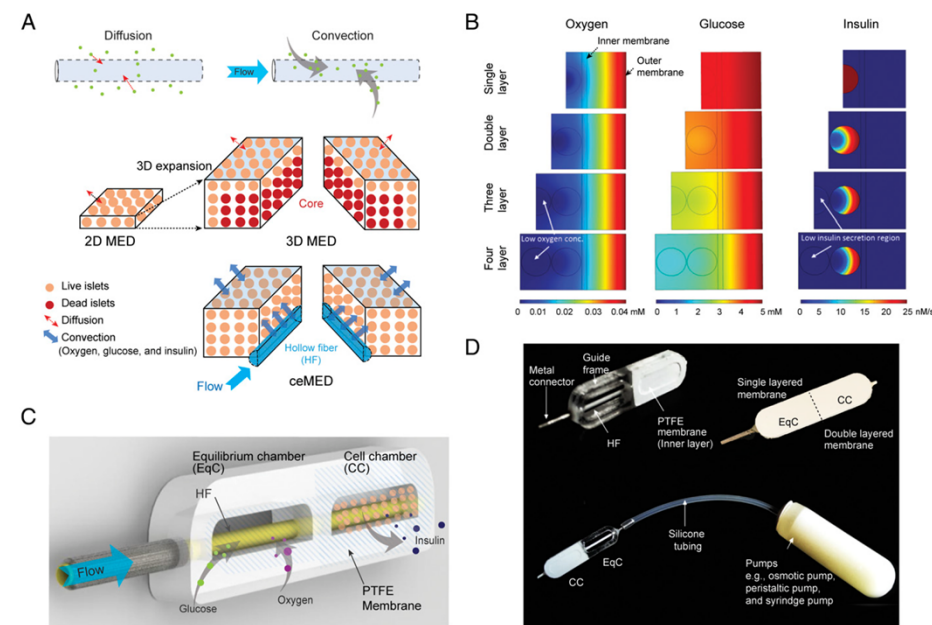


Fig. 1. Design of a ceMED for increasing mass transport, β cell viability, and insulin secretion sensitivity. (A) Illustration comparing diffusion-based versus convection-enhanced approaches. Expanding MEDs from a typical two-dimensional (2D) wafer static system to a 3D MED brings forth mass transport limitations and cell death. These limitations motivate the introduction of a HF in a 3D expanded MED to allow increased nutrient delivery by perfused flow in the ceMED. (B) Simulation showing the gradient of oxygen (millimolar), glucose concentration (millimolar), and insulin secretion rate (anomolar per second) as a function of position inside a static macroencapsulation with multiple layers of islets. The color bars indicate the concentration of each variable. White arrows indicate the hypoxic regions in the islet due to diffusion-limited transport of the oxygen in the device. (C) Scheme of the ceMED, consisting of an EqC, a CC, and a connecting HF. EqC captures glucose and oxygen from the surroundings; HF transports these solutes to the encapsulated cells in the CC. Inside the CC, positive pressure facilitates flow and improved mass transport to and from the encapsulated cells. The CC is enclosed by a PTFE membrane for protection from immune attack while allowing for nutrient transfer. (D) Gross view of a fully assembled, transplantable ceMED and its components. The ceMED can be connected to various pump systems, exemplified here by an osmotic pump.

Yang 2021, A therapeutic convection-enhanced macroencapsulation device for enhancing β cell viability and insulin secretion

Foreign Body Reaction

Foreign Body Reaction

Composed of multinucleated giant cells (= foreign body giant cells), macrophages, fibroblasts, and capillaries.

Surface topography will dictate the extent of the foreign body reaction.

- Smooth surfaces have a foreign body reaction composed of macrophages and foreign body giant cells at the surface.
- Rough surfaces have foreign body giant cells, macrophages, and granulation tissue sub-adjacent to the surface response.

High-surface-to-volume implants have a higher ratio of macrophages and foreign body giant cells at the implant site, which increases fibrosis.

The foreign body reaction may persist for the entire life of the implant.

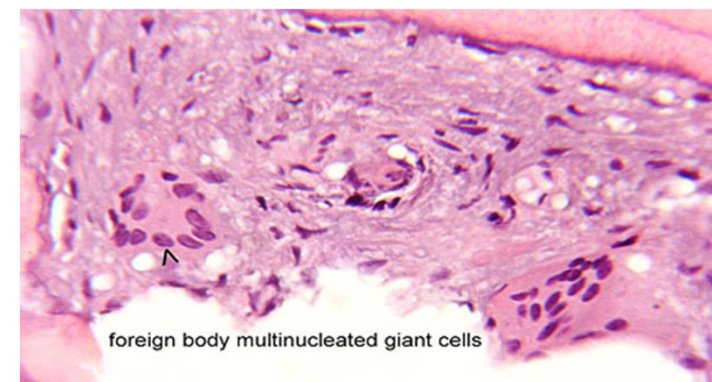
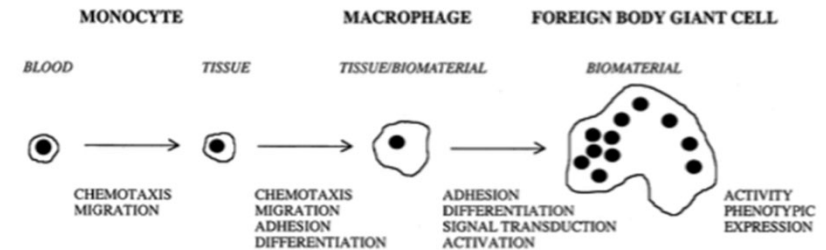
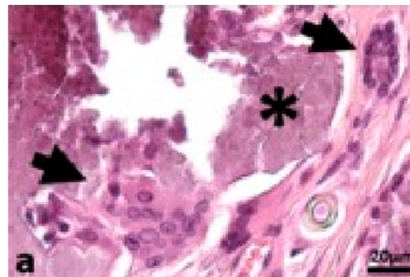
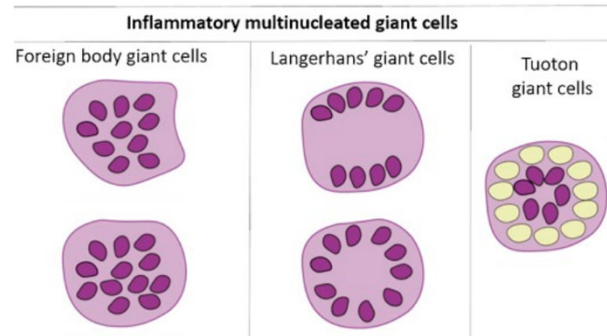


Figure 1. Schematic representation of the histopathological features of multinucleated giant cell subtypes. (a) Foreign body giant cells with heterogeneously distributed nuclei (black arrows) within the implantation site of a bone replacement material (*) on day 15. (Eslami-Kaliji 2023, Mechanisms of foreign body giant cell formation in response to implantable biomaterials)

Immune Response to an Implanted Biomaterial

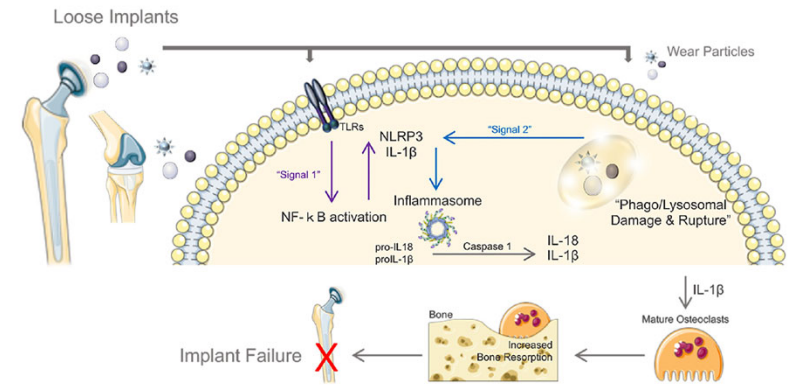
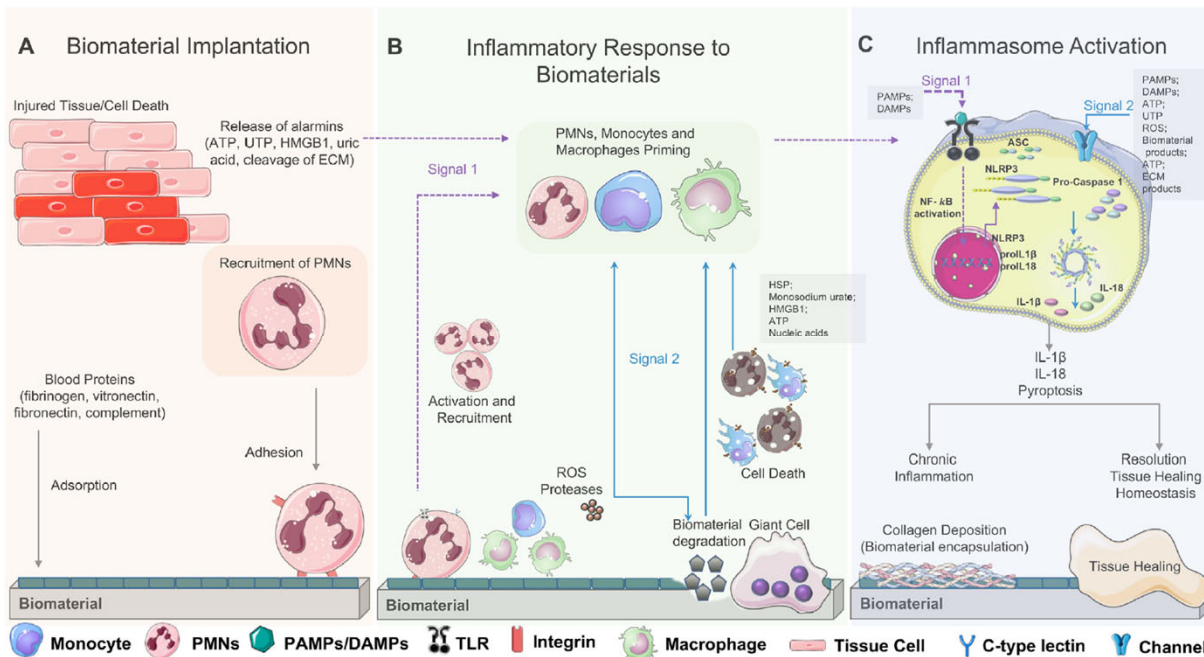


Fig. 5. Wear particles released from loose implants lead to inflammasome activation. Wear particles are recognized as such or after phagocytosis (lysosomal rupture), by PRRs including TLRs and NLRs leading to the assembly of NLRP3 inflammasome. Once assembled the NLRP3 inflammasome cleaves pro-IL-1 β into the active IL-1 β . Secreted IL-1 β can promote the maturation of osteoclasts into bone-resorbing cells increasing bone resorption and consequently impairing implant function.

Fig. 1. The inflammasome in the immune response to an implanted biomaterial. (A) Biomaterial implantation: The process of implantation of a biomaterial causes injury to cells. Danger signals released from injured cells (such as alarmins, HMGB1, ATP and UTP) results in the recruitment and activation of polymorphonuclear leukocytes (PMNs), monocytes and resident macrophages, via pattern recognition receptor (PRRs) engagement. Well-known damage associated molecular patterns (DAMPs) include ATP, nucleic acids, HSP, monosodium urate, HMGB1 and inflammatory cytokines. The adsorption of blood proteins to material surface will further recruit immune cells. (B) Acute inflammatory response to biomaterials: Immune cells secrete proteolytic enzymes and reactive oxygen species (ROS) that will degrade the biomaterial surface and ECM components. Endogenous danger signals are usually released from stressed or necrotic cells and also damaged ECM during acute inflammation. (C) Inflammasome activation: Activation of NLRP3 inflammasome, composed of NLRP3, ASC, and pro-caspase-1, is regulated by two-step signals: The first signal (signal 1) can be danger signals released from injured tissues and immune cells that will enhance the expression of inflammasome components and target proteins via activation of NF- κ B. The second “activation” signal (signal 2) promotes the assembly of inflammasome components, that involves three major mechanisms, including generation of ROS, lysosomal damage (phagocytosis of biomaterial degradation products), and the potassium efflux. Inflammasome assembly leads to caspase-1 activation that in turn cleaves the pro-forms of cytokines IL-1 β and IL-18 as well as gasdermin D that induce the pyroptotic inflammatory cell death. The perpetuation of the inflammatory cascade culminates either in resolution of inflammation, return to homeostasis and tissue healing or in chronic inflammation and biomaterial encapsulation

Vasconcelos 2019, The inflammasome in host response to biomaterials-Bridging inflammation and tissue regeneration

Immune Response to an Implanted Biomaterial

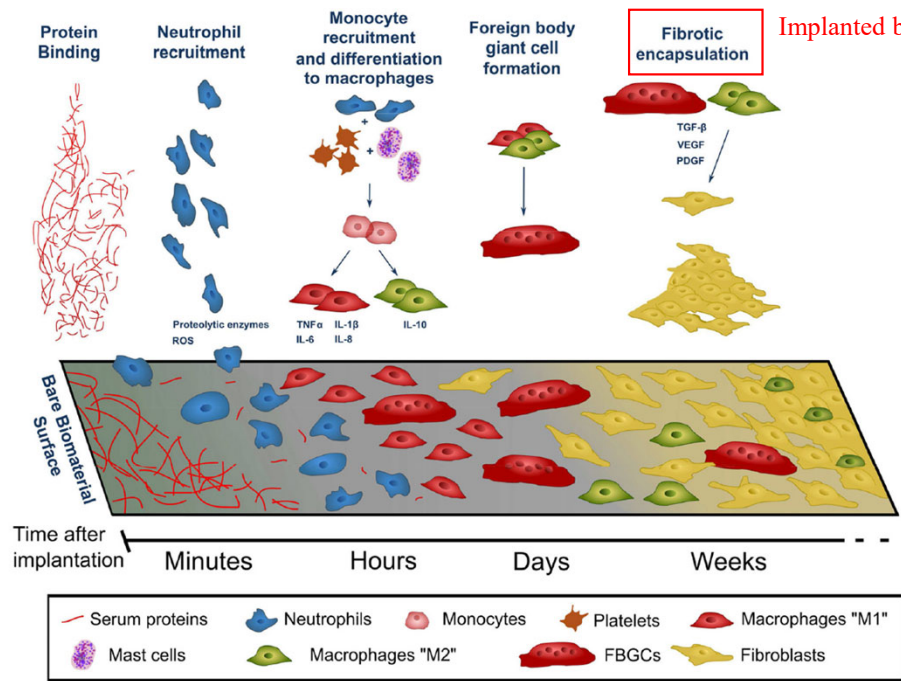


FIGURE 1 | Timeline of the events leading to the development of the foreign body reaction to a material following its implantation into the body. The composition of the cell population adhered to the surface of the implant evolves over time following the initial implantation. Factors released by cells (indicated by blue text) contribute to the recruitment of further cells and progression of FBR. ROS, reactive oxygen species.

Implanted biomedical devices and drug delivery systems

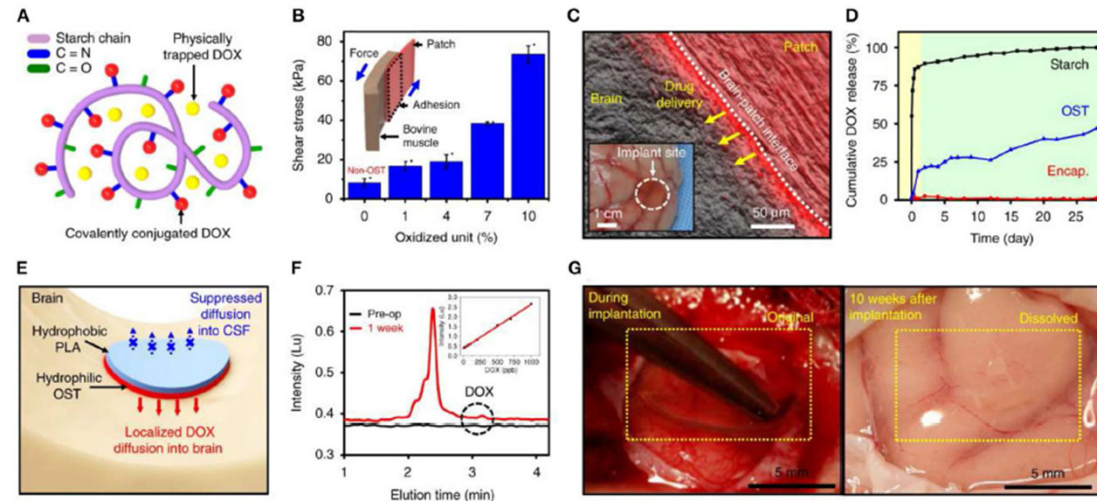
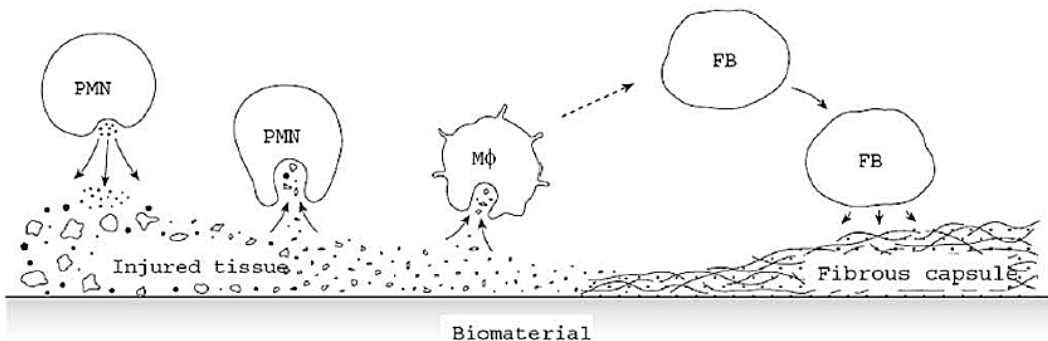
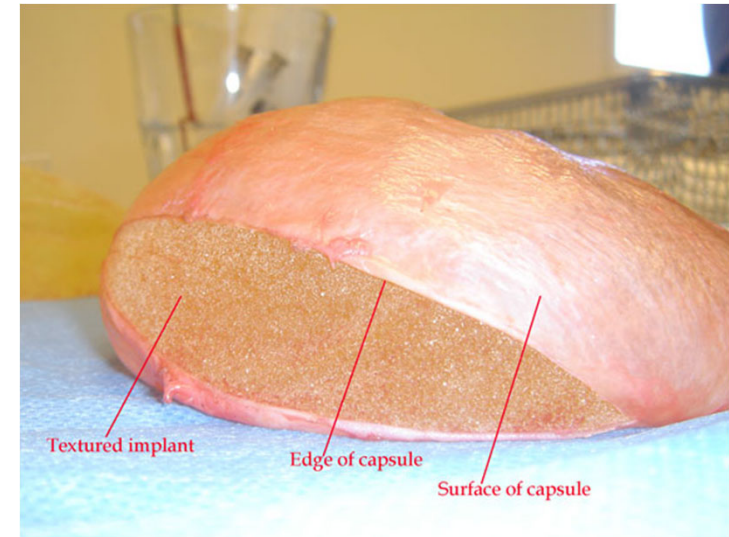


FIGURE 6 | Bioresorbable electronic patch (BEP) implant for controlled drug release. Reproduced under the terms of the Creative Commons Attribution License (Lee et al., 2019). (A,B) The patches are fabricated from a drug-loaded (doxorubicin) oxidized starch (OST) reservoir, and an electronics-containing compartment made from Mg (conductor), PLGA (dielectric), and PLA (encapsulation) which is bound to it. (C) Wireless control mediates drug delivery into neural tissue. (D-F) Doxorubicin release into tissue occurs over a period of days. (G) The entire implant becomes fully resorbed within 10 weeks of implantation, leaving no adverse reaction in the nearby tissue.

Fibrosis/Fibrous Encapsulation

- Fibrosis surrounds the biomaterial with an interfacial foreign body reaction
- Consists of connective tissue
- Isolates the biomaterial from the local tissue environment
- End stage healing response
- **Exceptions to the rule**
- Implant site repair involves 2 processes:
 - regeneration, replacement of injured tissue by parenchymal cells of the same type
 - replacement by connective tissue (fibrous capsule)
- Extent of the injury and framework of the tissue (bone vs nervous system) determines process
 - cells are labile (stem cells), stable (can replicate, but not typical), or permanent (static)
 - all injuries to permanent cells give rise to fibrosis/loss of tissue function)



Description of fibrous capsule formation around the implanted biomaterial. Activated polymorphonuclear leukocytes (PMN) release enzymes to remove dead cells, and macrophages (Mφ) participate in the phagocytosis of foreign and cellular debris, Mφ also stimulate fibroblasts (FB) to secrete collagen and other extracellular matrix components to form a fibrous capsule around the implanted biomaterial.

Side Effects of Biomaterials and Biomedical Devices

FDA reports new cases of cancer linked to textured breast implants

More women have been diagnosed with a deadly lymphoma caused by breast implants, according to a report released Wednesday from the Food and Drug Administration.

In a statement, the FDA's Dr. Binita Ashar said there are now 457 women in the U.S. diagnosed with breast implant-associated anaplastic large cell lymphoma (BIA-ALCL), up from 414 cases in the last report. There have been more than 600 cases of BIA-ALCL, a cancer of the immune system, reported worldwide. Sixteen women have died, nine in the U.S. "We hope that this information prompts providers and patients to have important, informed conversations about breast implants and the risk of BIA-ALCL," Dr. Ashar said in the statement. The new report comes one day before French regulatory authorities are scheduled to meet to discuss the safety of textured implants, which are used in cosmetic and reconstructive surgeries and account for 85 percent of the French market. The majority of ALCL cases have been linked to the textured devices. In December, France's National Agency for the Safety of Medicines and Health Products (ANSM) asked Allergan to recall its textured implants after the agency pulled its safety approval.

That recall followed an NBC News investigation, in conjunction with the ICIJ, finding that ALCL could be more common than previously thought. The FDA, which first alerted women to the risks from the textured breast implants in 2011, also announced today that for the first time, they are sending letters to doctors, specifically primary care physicians and gynecologists, urging them to learn about ALCL so they can better diagnose and treat women who may be at risk. ALCL patients, who have been fighting to raise more awareness of disease, applaud the FDA's efforts to better inform physicians.

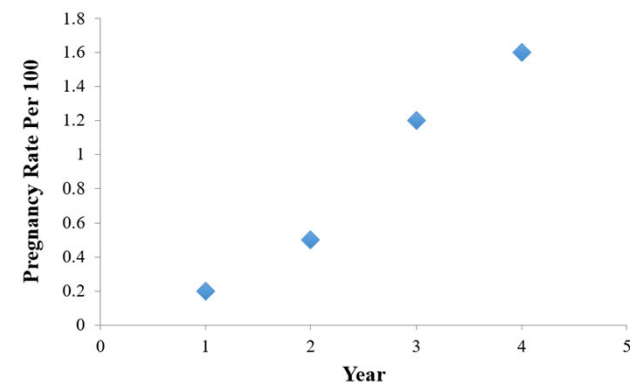
"Letters to these health care providers, like OBGYNs, ER Doctors are critical to the diagnosis of this disease. They are some of the first physicians to treat patients symptomatic for BIA ALCL and these patients are often missed and mistreated for mastitis, shingles and other conditions," said Michelle Forney, a California mother of two, diagnosed with ALCL last year. "This disease is not rare. It's emerging and should not belong in the hands of plastic surgeons." The FDA is meeting next month to review safety of all breast implants.

Feb. 6, 2019. By Lauren Dunn

<https://www.nbcnews.com/health/womens-health/fda-reports-new-cases-cancer-linked-textured-breast-implants-n968626>



Norplant: Withdrawal from the market in 2002



Foreign Body Reaction

Another key aspect, often overlooked, is **the foreign body reaction** to LADDS following administration. Tuning material properties is critical to avoid such reactions, which can lead to **the formation of a fibrous capsule** around the LADDS, thereby preventing effective drug release. (71, 72)

Minimising foreign body response requires a multidisciplinary approach, as various LADDS-related parameters are involved such as surface roughness and charge, chemical composition, material type, and the size and shape of the formulation once administered. (71) The implementation of these technologies requires regulatory clearance and clinical trials.

Regulatory approval can be particularly challenging for some of these novel strategies, as they often involve new chemical entities or unregulated approaches. To facilitate faster regulatory clearance, the use of already-approved materials in the development of new LADDS is highly recommended.

In addition to technical challenges, patient-centred design should be a priority. Co-design strategies that involve patients in the design and development process are preferred, as this approach maximises patient acceptability and adoption of the technology.

71. Capuani S, Malgir G, Chua CYX, Grattoni A. Advanced strategies to thwart foreign body response to implantable devices. *Bioeng Transl Med.* 2022;7, e10300. <https://doi.org/10.1002/btm2.10300>.

72. Capuani S et al. The effect of the foreign body response on drug elution from subdermal delivery systems. *Biomaterials.* 2025;317, 123110. <https://doi.org/10.1016/j.biomaterials.2025.123110>.

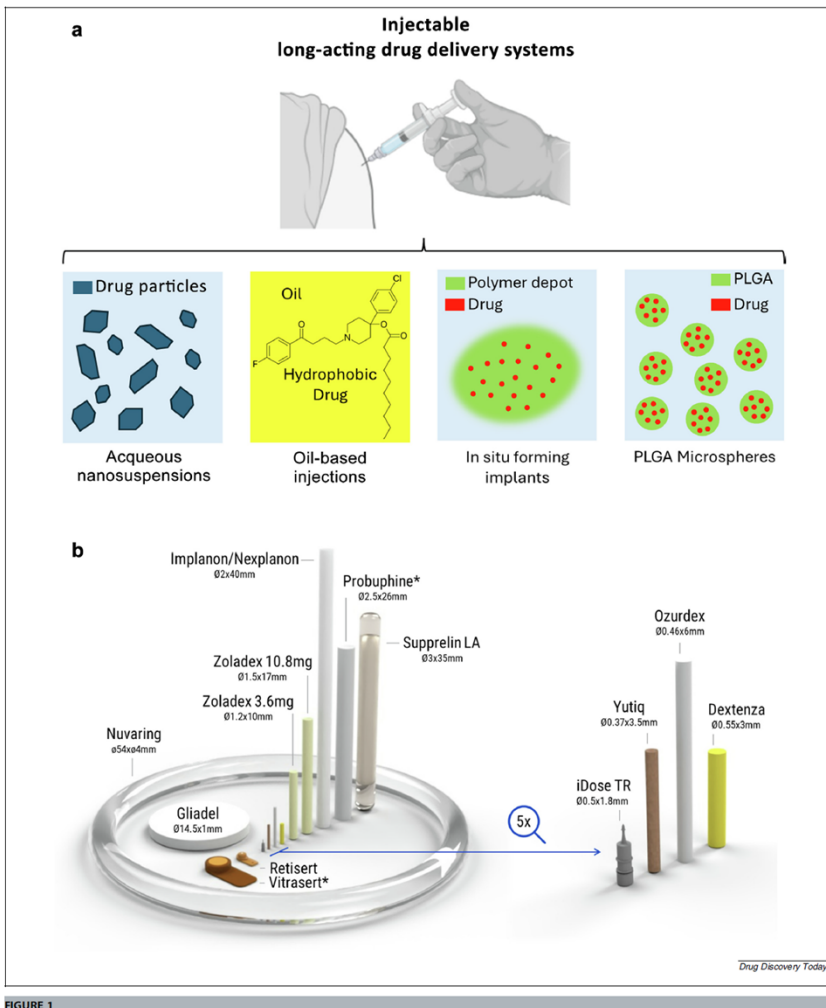
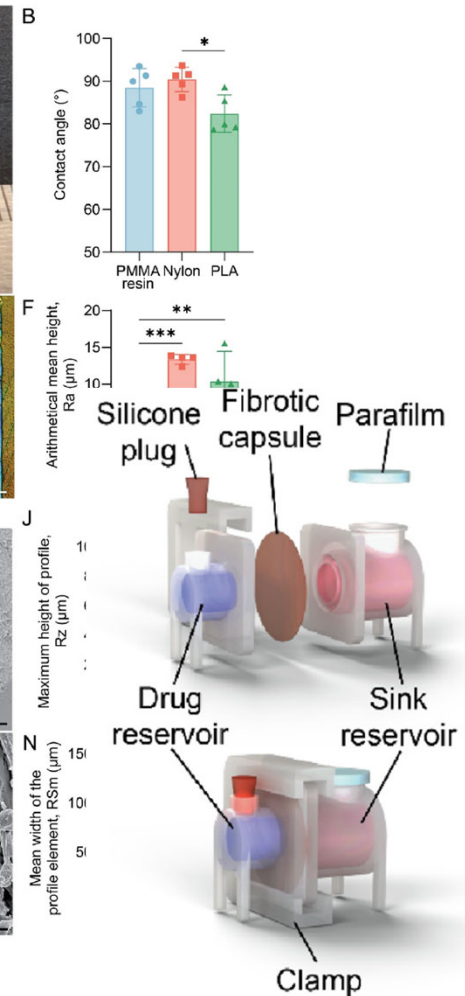
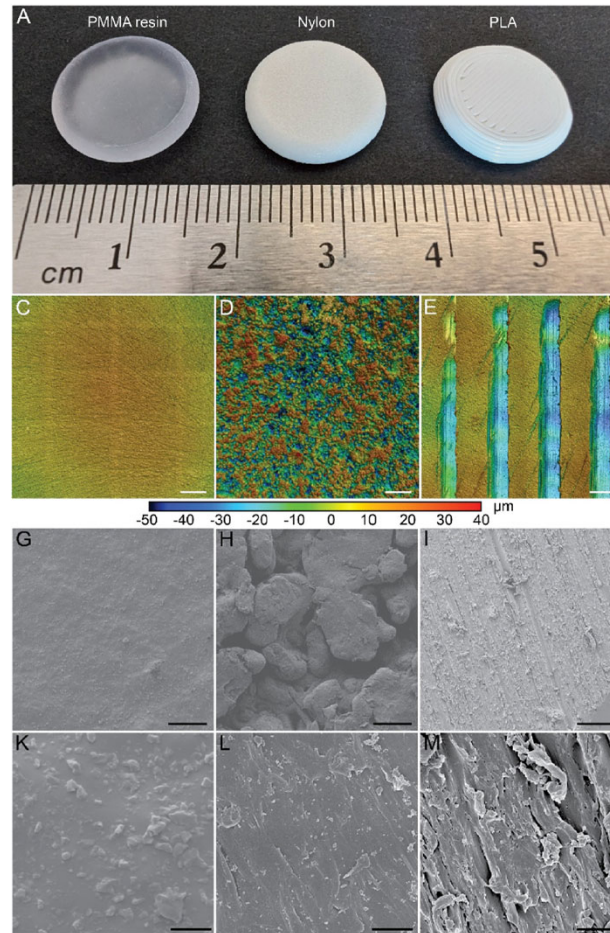
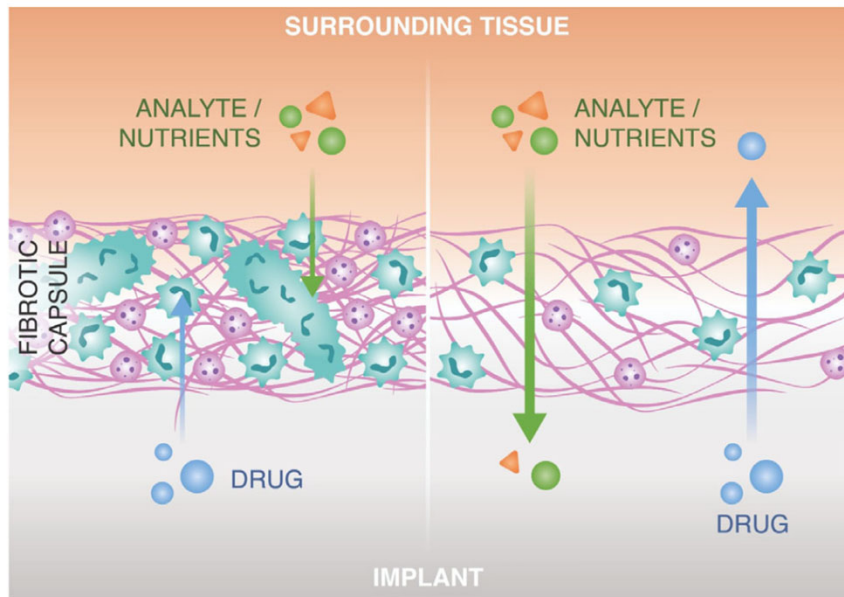
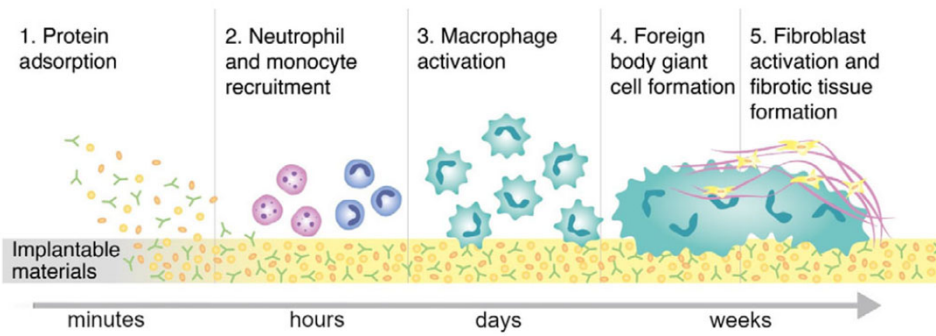


FIGURE 1
Diagram showing different types of injectable (a) and implantable (b) LADDS. Panel b image was provided by MeltPrep®.

Foreign Body Response



Capuani 2021, Advanced strategies to thwart foreign body response to implantable devices

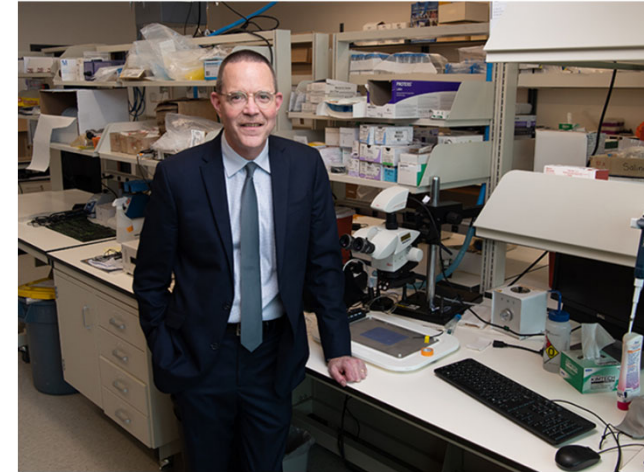
Capuani 2025, The effect of the foreign body response on drug elution from subdermal delivery systems

Biomaterials for Daily Function

Biomaterials for Sensors

About SonarMed™ Airway Monitoring System

The SonarMed™ airway monitoring system includes a bedside monitor and single-use sensor. The SonarMed™ sensor fits any brand of standard endotracheal tube (ETT) in sizes ranging from neonatal to pediatric populations (2.5 mm–6.0mm ID) and attaches by replacing the 15-mm connector at the end of the ETT, placing the sensor between the ETT and the ventilator circuit. The SonarMed™ monitor incorporates an easy-to-read color screen that continuously displays any change in ETT depth within the trachea.



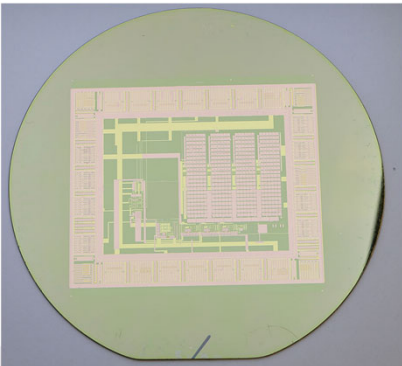
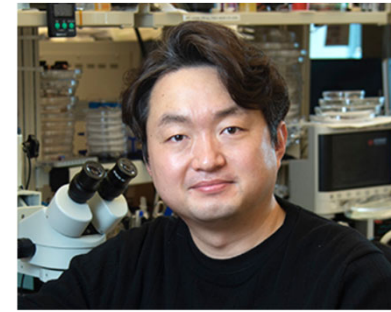
In 1990, Purdue University Professor George Wodicka conceived of a medical device that gives clinicians vital information to make more informed, life-saving decisions for their smallest patients.

<https://www.purdue.edu/newsroom/releases/2021/Q2/every-newborn-on-a-ventilator-can-now-be-better-protected,-thanks-to-technology-that-helps-prevent-a-common-breathing-tube-incident.html>

Biomaterials for Sensors

Purdue Biomedical engineer Professor Chi Hwan Lee specializes in sticktronics and custom-printed soft medical sensors.

Electronic stickers to streamline large-scale 'Internet of Things'



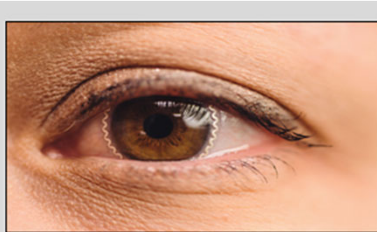
An electronic glove that simulates the sense of touch for prosthetic hands.

"Soft sensors help to map prosthetic pressure points" – Purdue News

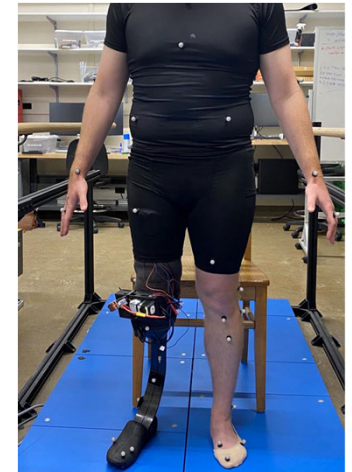
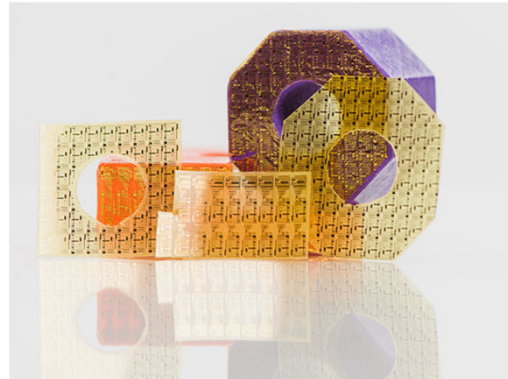
For amputees, wearing a prosthesis can be a game-changer — but it also can introduce huge pressure points which become very painful. Purdue University researchers have developed soft sensors that can be worn comfortably, providing a more accurate picture of the pressures experienced at the interface of limb and prosthesis. "There are more than 2 million people living with limb amputation in the United States, and 50 million worldwide," said Tianhao Yu, graduate student in mechanical engineering and co-lead author of the paper... [\[continue to read\]](#)



A sensor that can be placed on an over-the-counter contact lens and then used to detect glaucoma in patients.

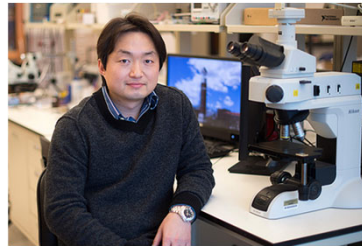


Smart Soft Contact Lens for Glaucoma Monitoring



- <https://www.purdue.edu/newsroom/releases/2021/Q3/enhancing-ordinary-items-for-addressing-health-outcomes.html>
- <https://www.purdue.edu/newsroom/releases/2018/Q3/electronic-stickers-to-streamline-large-scale-internet-of-things.html>
- <https://engineering.purdue.edu/Engr/AboutUs/News/Spotlights/2024/2024-0111-bme-me-lee>

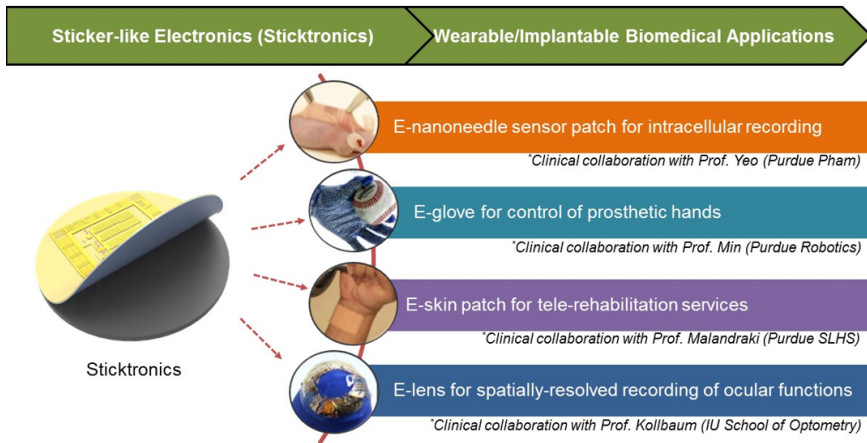
Bionic Touch



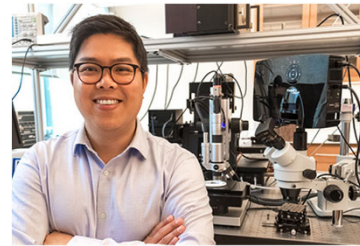
DR. CHI HWAN LEE

Areas of Research: Flexible and Stretchable Sensors for Human Body-Integrated Healthcare Systems

Projects: Our lab's research spans expertise in many disciplines including biomedical, mechanical, and materials engineering, through the fundamental understanding of the device physics, mechanics, and fabrication principles along with clinical implementations through effective communications with medical doctors, clinicians, nurses, and caregivers. The main research focus lies on developing flexible and stretchable materials for wearable biomedical devices.

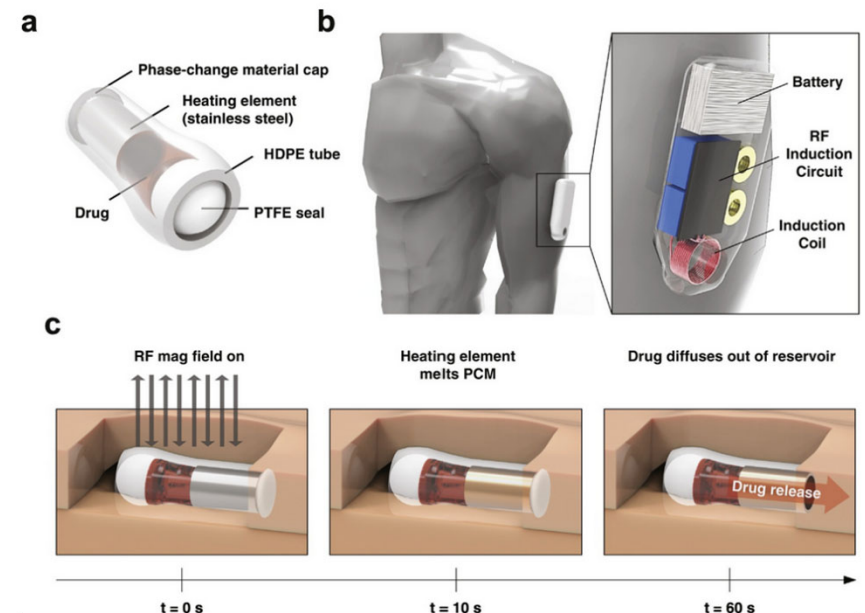
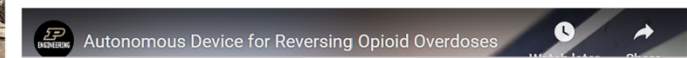


Recruitment Needs: A creative, highly motivated, self starter to enroll as a PhD student in fall 2019



Device could automatically deliver drug to reverse opioid overdose

Opioid users tend to be alone and incapacitated during an overdose. Purdue University researchers are developing a device that would automatically detect an overdose and deliver naloxone, a drug known to reverse deadly effects.



Purdue researchers are developing a wearable device that would automatically deliver an antidote upon detecting opioid overdose, buying time for emergency services to arrive. (Purdue University image/Jongcheon Lim)

<https://engineering.purdue.edu/BME/AboutUs/News/2019/Device-could-automatically-deliver-drug-to-reverse-opioid-overdose>

Bionic Touch: The Robot Revolution on the Way



www.womansday.com/life/10-incredible-real-life-robots-116174



Bionic fingers. Rewired nerves.

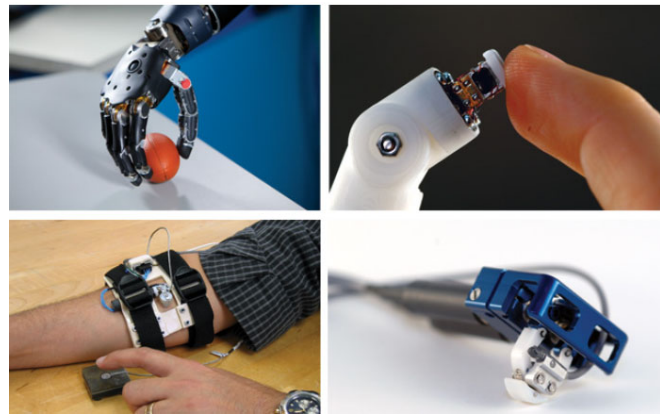
If you can't feel anything, your hand is pretty close to useless. That is basically the problem with prosthetic hands for the last century—no touch.

—Gerald Loeb, University of Southern California



The robot revolution has arrived

Machines now perform all sorts of tasks: They clean big stores, patrol borders, and help children with autism. But will they improve our lives?



TOUCH THIS: A motorized tactor developed by Kinea (bottom right) mechanically stimulates an alternative body surface (bottom left) to “playback” the sensations picked up by fingertip sensors (top left) of a prosthetic hand. The Modular Prosthetic Limb (top right and featured image), developed by the Johns Hopkins Applied Physics Laboratory, uses the Kinea sensors in its fingertips. HDT Global; Johns Hopkins University Applied Physics Laboratory

<http://the-scientist.com/2012/09/01/missing-touch/>

Bionic Connections

A new way to link artificial arms and hands to the nervous system could allow the brain to control prostheses as smoothly as if they were natural limbs

By *Il-Kyung Chul and Douglas H. Smith*

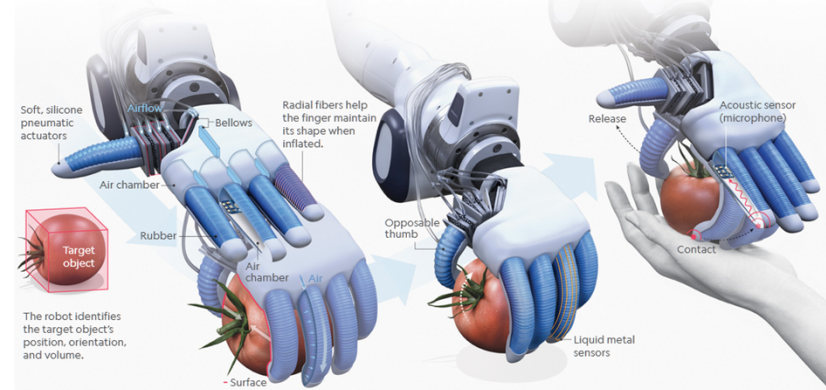
IN ONE OF THE MOST RECENT SCENES IN SCIENCE-FICTION FILMS, LERO HETZELBERGER casually examines his new synthetic forearm and hand. The star *Star Wars* here is able to move the fingers by extending and contracting plastic sleeves through an open flap along the wrist. There he senses the robotic surgeon's playful of one of his fingers. Not only can the prosthetic be moved with the wearer's thoughts, it feels to him like his own hand.

When the audience does not see, however, in the actual case, a prosthetic hand is not a simple matter of plastic sleeves and wires. In fact, researchers are trying to create a prosthetic hand that can be controlled by the brain. This is a major goal of the field of bionics, which is the study of how to combine the best of nature and the best of technology. In the case of prosthetics, the goal is to create a hand that can be controlled by the brain. This is a major goal of the field of bionics, which is the study of how to combine the best of nature and the best of technology. In the case of prosthetics, the goal is to create a hand that can be controlled by the brain.



A Helping Hand

Designers of the revolutionary RBO Hand 3, a soft robotic hand made of flexible materials, are working to give it something akin to a human's sense of touch. Features include sensors that measure strain via electrical resistance and embedded acoustics to track where fingers are in contact with objects (or humans) and the amount of force.



1. DETECT

A camera senses the target object and sends data to the software in the robot's "brain"—a desktop computer—which sends command signals to the hand.

2. GRASP

Pressurized air from a compressor activates fingers, allowing them to curl and straighten as required, while controlling any impact. Fingers mold around the object for a firm grasp.

3. MANIPULATE

A soft, compliant hand and opposable thumb allow the robot to change the position of the object to perform various tasks, such as getting a better grasp on it or putting it on.

4. INTERACT

Soft robots are safer than rigid, metal ones when it comes to working with humans. Any impact or force that could harm a human is reduced by the soft materials.

https://www.nationalgeographic.com/magazine/article/the-robot-revolution-has-arrived-feature?cmpid=org%3Dngp%3A%3Ame%3Derm-email%3A%3Asc%3Dngp%3A%3Acmp%3Dwelcome%3A%3Aadd%3DNGM_thanks&rid=FF526C1F1B0738788B420FE1D0034350&loggedin=true

Robotic Materials

The stark performance gap between living organisms and artificial machines arises from their bodies' different material compositions and physicochemical behaviors.¹ Living organisms bypass many shortcomings of modern robots due to their soft matter construction and the distributed nature and complexity of biological sensorimotor systems.

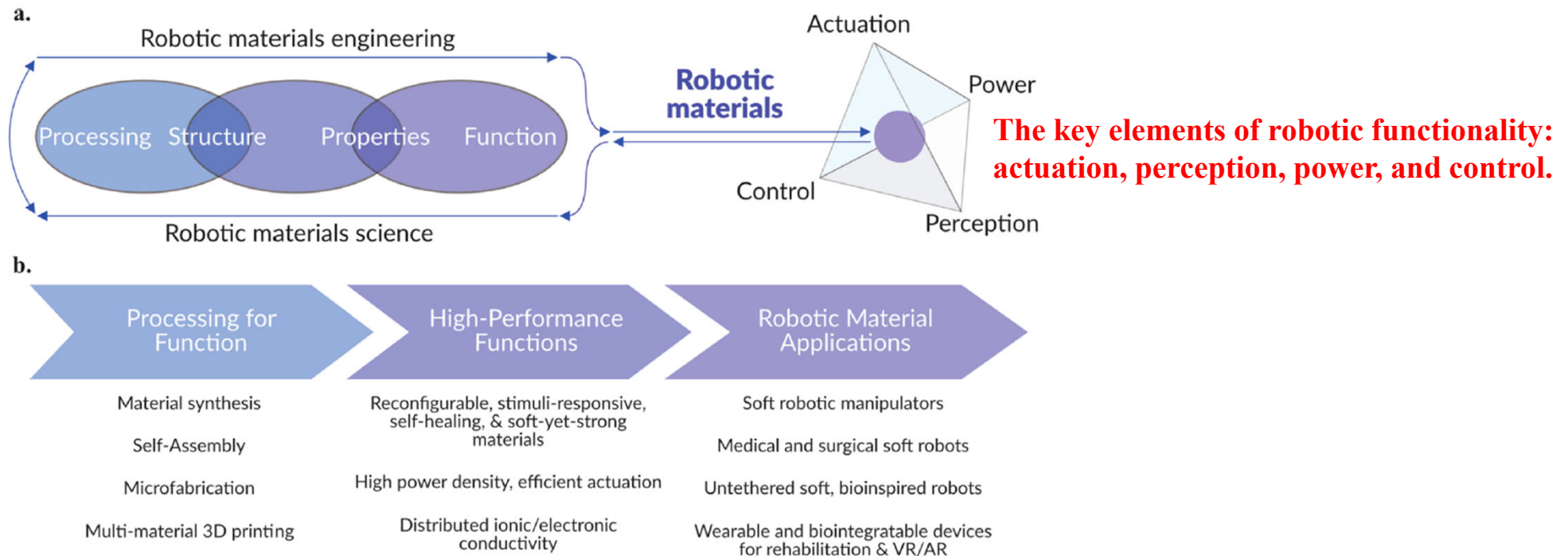


Figure 1. A paradigm for robotic materials design. (a) Inspired by design approaches in materials science and engineering, robotic materials couple robotic behaviors in self-contained material systems through considerations of material processing-structure-properties-function relationships. (b) Opportunities for robotic innovations via robotic materials are illustrated through relevant processing methods for target robotic functions in emerging applications.

Soft Robotics

Soft materials

1. Passive materials primarily serve structural purposes without undergoing external stimulus-induced changes.
2. Active materials exhibit responses to external stimuli (e.g., temperature, pH, light, and magnetic fields) to perform actuation or sensing functions.

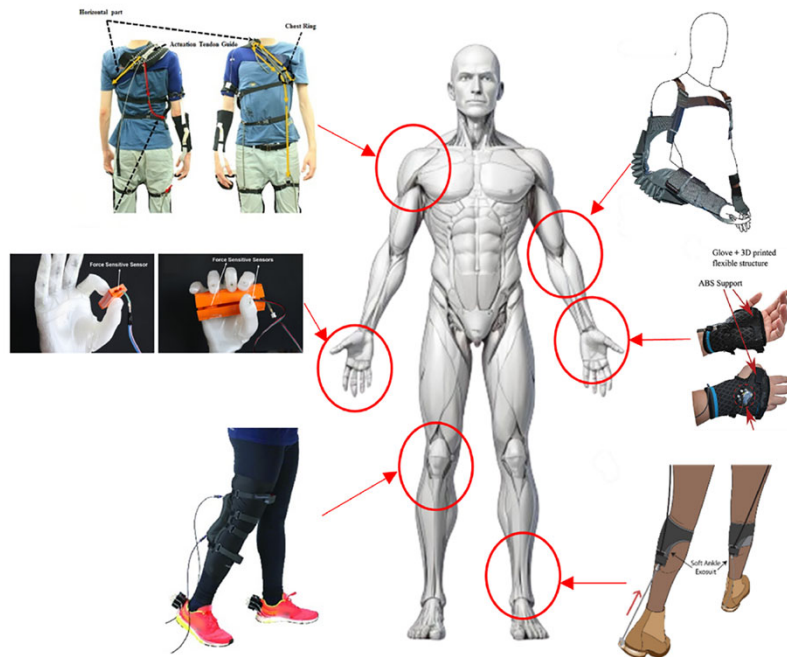
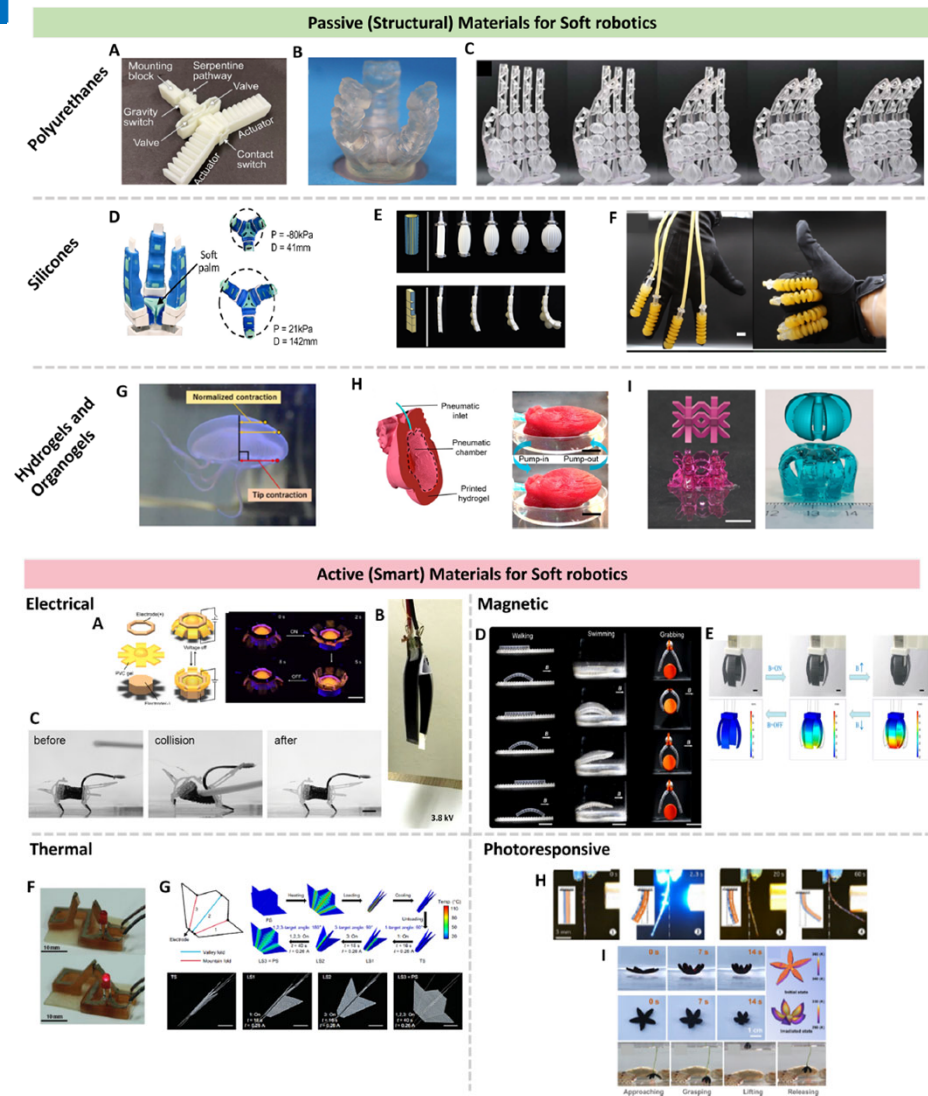


Figure 7. Schematic illustration of the application of soft robotics exoskeletons and prosthetic devices for almost every joint in the body, including the elbow, wrist, ankle, knee, prosthetic hand, and shoulder.

Blihan 2025, Fabrication of soft robotics by additive manufacturing- From materials to applications



Biomaterials for Sensors

Baumgartner 2020, Resilient yet entirely degradable gelatin-based biogels for soft robots and electronics

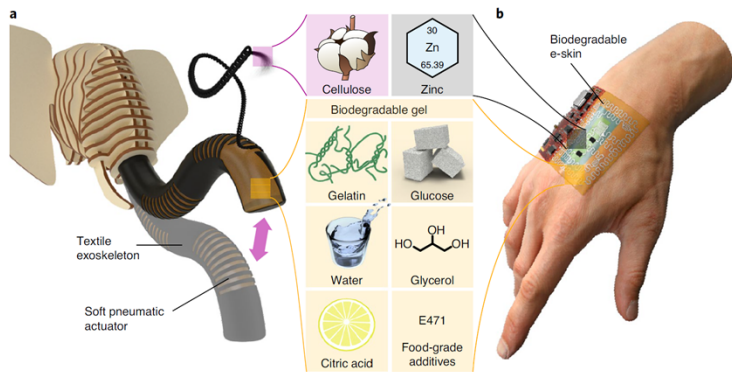
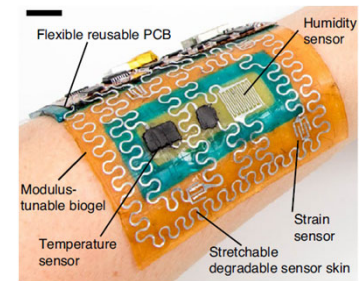
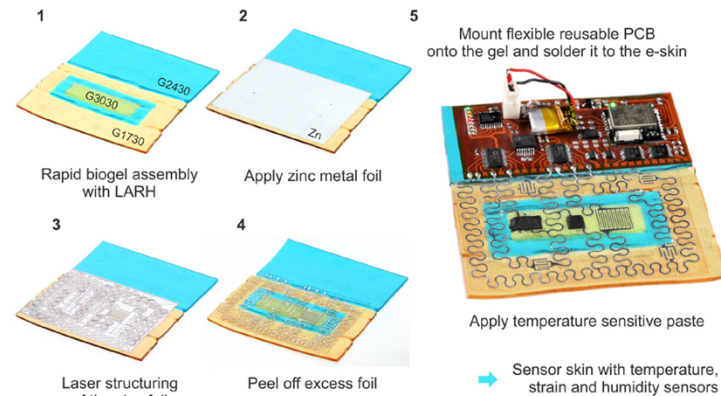


Fig. 1 | A resilient yet fully degradable biogel. a,b, Naturally derived ingredients, such as gelatin and citric acid, enable an elastic and stable, but fully degradable, biogel. Together with cellulose fibres and zinc, soft and durable pneumatic actuators (a) and multifunctional e-skins (b) are realized.



Soft e-skin on a human arm. Scale bar, 3 cm.

Extended Data Fig. 3 | Assembly of sensor skins. Assembly process of the sensor skin consisting of degradable e-skin and reusable PCB. 1, Gels of different mechanical properties are joined by laser assisted rapid healing (LARH). 2–3, A zinc metal sheet is then applied to the gel and structured by a fiber laser. 4, After the structuring process the zinc residues are peeled off. 5, A flexible reusable PCB is mounted on the gel and soldered to the zinc foil of the e-skin. In the last fabrication step a temperature sensitive paste is placed on the gel to finalize the temperature sensor.

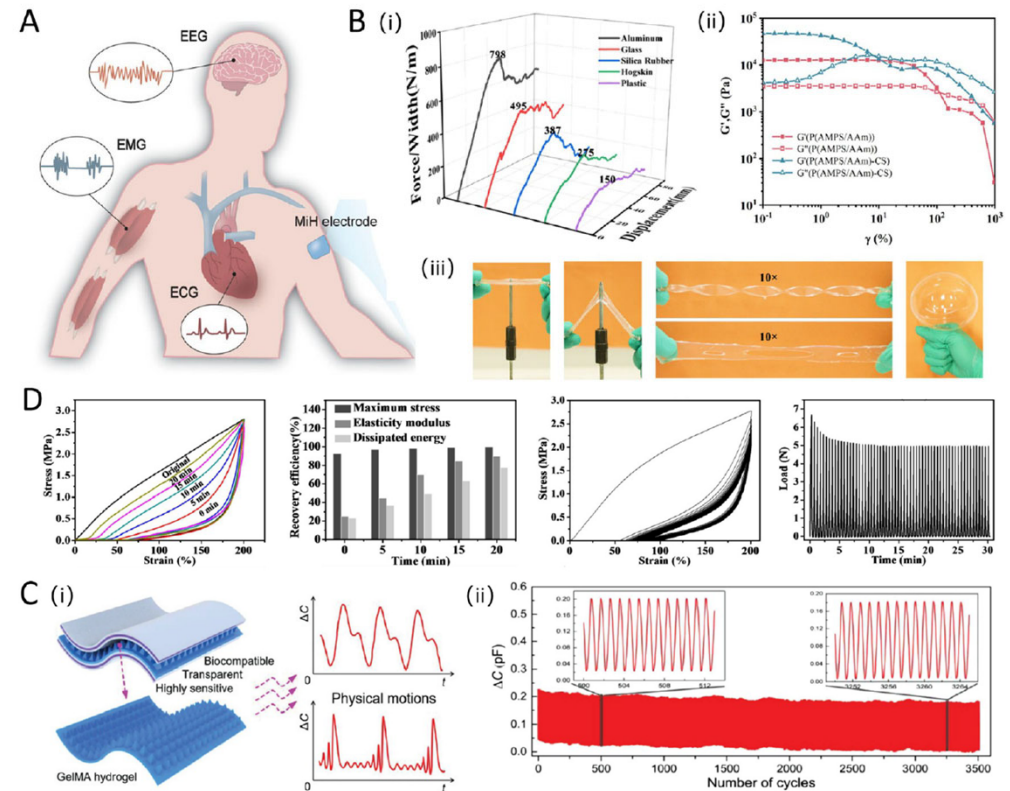
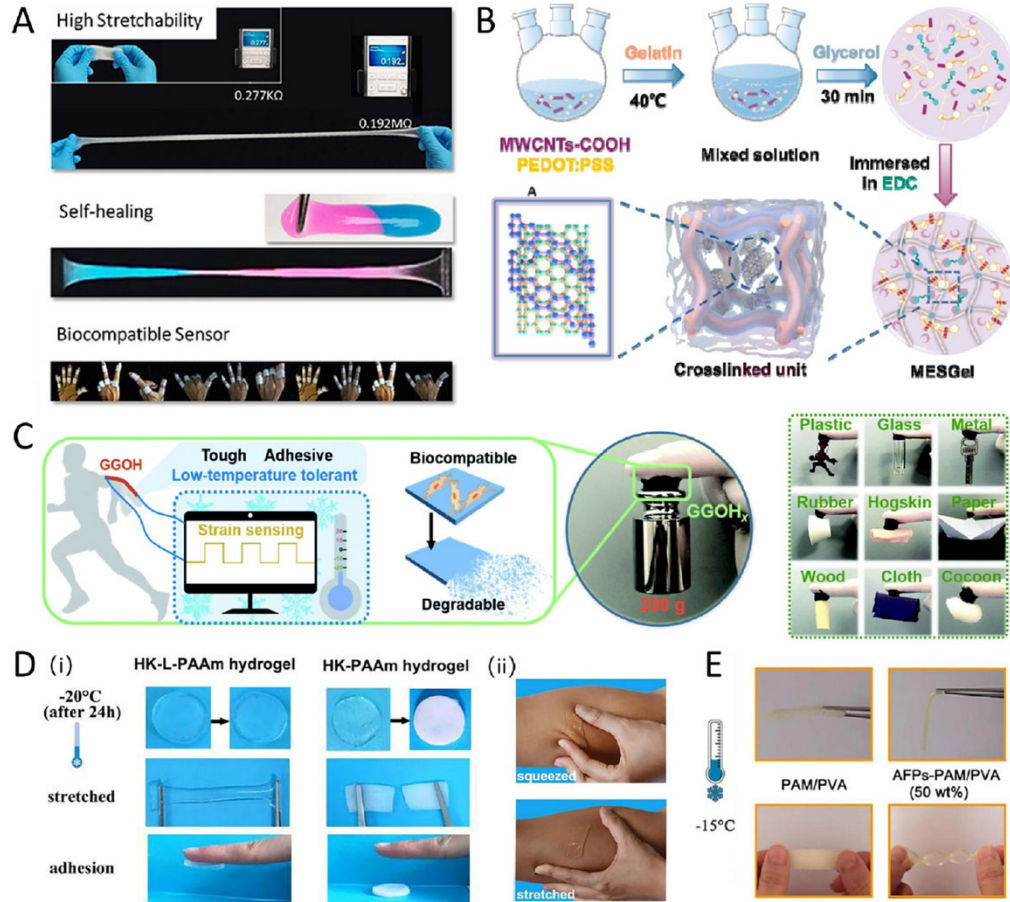
Biogel preparation. Citric acid (1 g) and glycerol (8 g) were dissolved in deionized water (8 g) and heated to 60 °C. Sugar syrup (7 g) was heated to 60 °C to reduce its viscosity and mixed to the presolution. After cooling to room temperature, gelatin powder (4 g) was added and allowed to soak for 1 h. The mixture was heated in an oven at 70 °C for 1 h and stirred in a planetary mixer (DAC 600.2 VAC-P, Hauschild Engineering) under vacuum (2,350 r.p.m., 450 mbar) for 4 min to achieve a homogeneous precursor ready for moulding. Gel recipes with varying compositions used here are listed in Supplementary Table 3.

Biogel foam. E471 powder was dissolved in deionized water (ratio 1:2) for 2 h under vigorous stirring. The dissolved E471 (8 g) was mixed with the biogel presolution and gelatin powder (4 g) and allowed to soak for 1 h. The mixture was heated at 65 °C for 1.5 h and mixed with a hand blender for 30 s at 5,000 r.p.m., which resulted in a microfoam, which was cast into acrylic glass moulds.

Biogel thin films. The prepared warm liquid biogel was poured on a Teflon plate and distributed via doctor blading. The films were left to dry for 1 h, which resulted in a thickness of 0.58 mm. Coating with talcum powder rendered non-sticky films.

Biogels with biodegradable encapsulation. Shellac solution was prepared according to Luangtana et al.⁴⁶. Schellac (36 g) was dissolved in ethanol (100 g). PEG 400 (7.2 g) was added to the shellac solution and stirred for 10 min. G2430 biogel samples were dip coated in the shellac solution four times, followed by 30 min of heating at 50 °C in an oven and a final heating at 70 °C for 1 min. We repeated this procedure to achieve a homogeneous encapsulation of thickness ~200 μm.

Biomaterials for Sensors



Biomaterials for Sensors

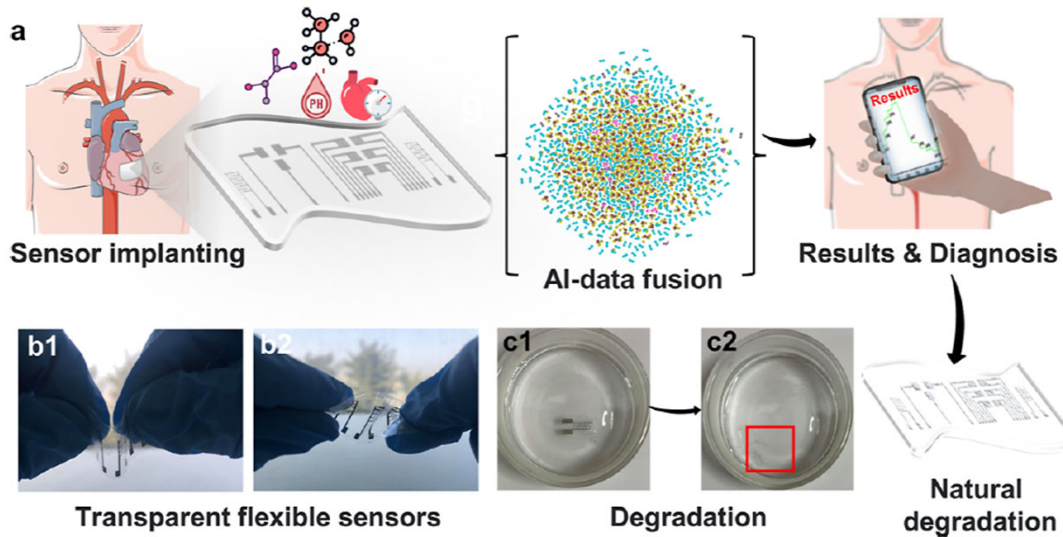


Figure 1. Overview of the biodegradable multiplex nanosensor platform for cardiac monitoring.

(a) Concept of implantable **multifunctional sensors** for cardiac monitoring, including sensor implanting for detecting multiple biomarkers: pressure, lactic acid, pH and VOCs, AI-data fusion, **results analysis**, and degradation. (b1,b2) Flexible and bendable electrodes on polylactic acid (PLA). (c1,c2) Degradation of the sensors after a period.

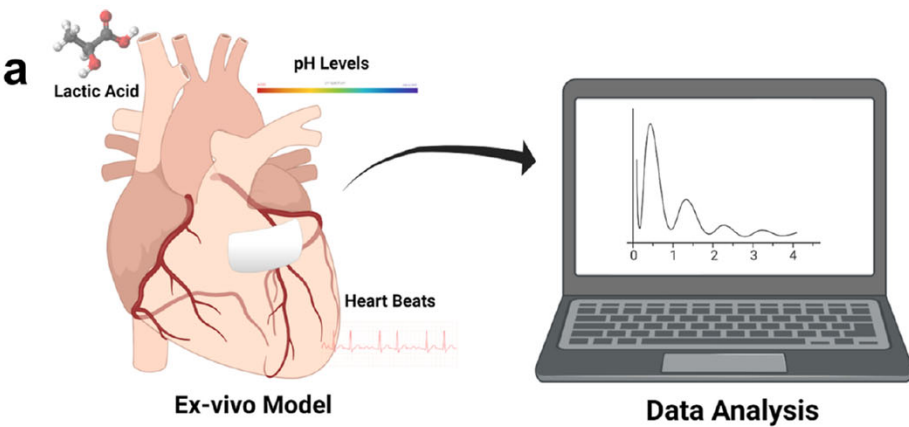


Figure 5. Ex vivo validation of the sensor using 3D printed models and AI-model development.

(a) Overview of the ex vivo experimentations set. (b) Testing the biodegradable pressure sensor with a 3D-printed silicone heart model.

Omar 2025, Biodegradable, biocompatible, and implantable multifunctional sensing platform for cardiac monitoring

Conductive Hydrogels for Implantable Bioelectronics

Hydrogels and conductive hydrogels for implantable bioelectronics

Kutay Sagdic, Emilio Fernández-Lavado, Massimo Mariello, Outman Akouissi, and Stéphanie P. Lacour

Hydrogels are a class of soft materials, which display unique biomimetic properties to biological tissues. Their mechanical properties, high water content, and porosity resemble that of extracellular matrix so that cell growth and proliferation can be reliably supported. *In vitro* studies report that mechanosensitive cells found in the central nervous system, such as astrocytes and glia, display reduced activation, thus promoting lower foreign body reaction, when cultured on hydrogel substrates of <1-kPa modulus. This observation provides an opportunity to explore whether soft hydrogels should be integrated in or form implantable neural interfaces and offer long-term biointegrated neurotechnologies. This article highlights recent progress in hydrogel materials and associated technologies for the design of implantable bioelectronics. Essential structural, mechanical, and electrical properties of hydrogels and composite hydrogels are briefly reviewed. Manufacturing methods suitable for these multiscale and multifunctional materials are presented. The final section presents hydrogel-based implantable bioelectronics for the brain and outlines current challenges and future opportunities.

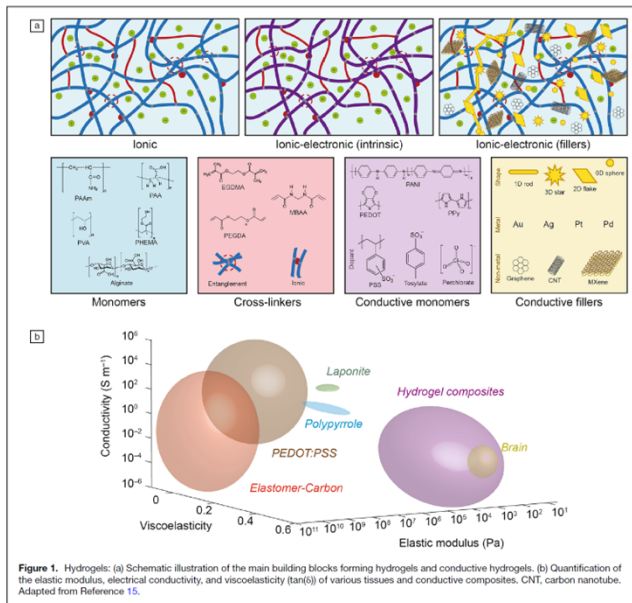


Figure 1. Hydrogels: (a) Schematic illustration of the main building blocks forming hydrogels and conductive hydrogels. (b) Quantification of the elastic modulus, electrical conductivity, and viscoelasticity (tan(δ)) of various tissues and conductive composites. CNT, carbon nanotube. Adapted from Reference 15.

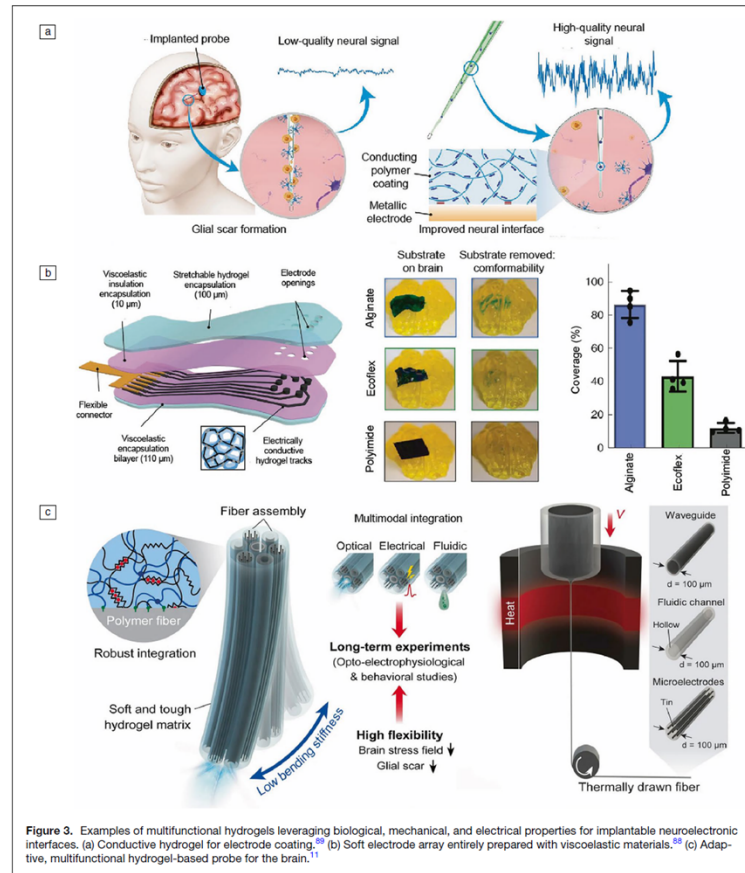


Figure 3. Examples of multifunctional hydrogels leveraging biological, mechanical, and electrical properties for implantable neuroelectronic interfaces. (a) Conductive hydrogel for electrode coating.²⁸ (b) Soft electrode array entirely prepared with viscoelastic materials.²⁹ (c) Adaptive, multifunctional hydrogel-based probe for the brain.¹¹

Conclusion

Implantable devices alleviate consequences of traumatic or disease-related conditions to a few million people worldwide. Although a handful of designs and associated technologies and materials are dominating the current clinical device portfolio, the last decade is propelling materials' innovation and manufacturing strategies toward the next generation of therapeutic implants that should be biomimetic, multifunctional, and lifelong standing. Hydrogels are already used in many clinical applications, mostly for scaffolding and drug delivery. Recent progress now aims at integrating these soft materials into bioelectronic implants and leveraging their customized structure, chemistry, and physical properties. Stealth implants that display tissue-like physical properties and miniaturized geometry promise minimal disruption of the glial and neural network and reliable and stable tissue-implant communication. In addition to mechanical biointegration, hydrogels in their conductive form also emerge as a promising class of transducing materials for bioelectronics; they offer a unique ionic-electronic transport and transfer network for recording and stimulation devices. Efforts in dispensing and patterning these soft conducting gels are now needed to reliably integrate them in neural implants with high spatial electrode distribution. Implant prototypes made entirely from hydrogels become possible; solutions to reliably pattern and electrically insulate conducting gel tracks without compromising the form factor of the implant have yet to be developed. Hydrogels offer a broad range of options in materials' design, structure, and properties that will translate in diverse implementation in implantable bioelectronics.

Biomaterials for Chips

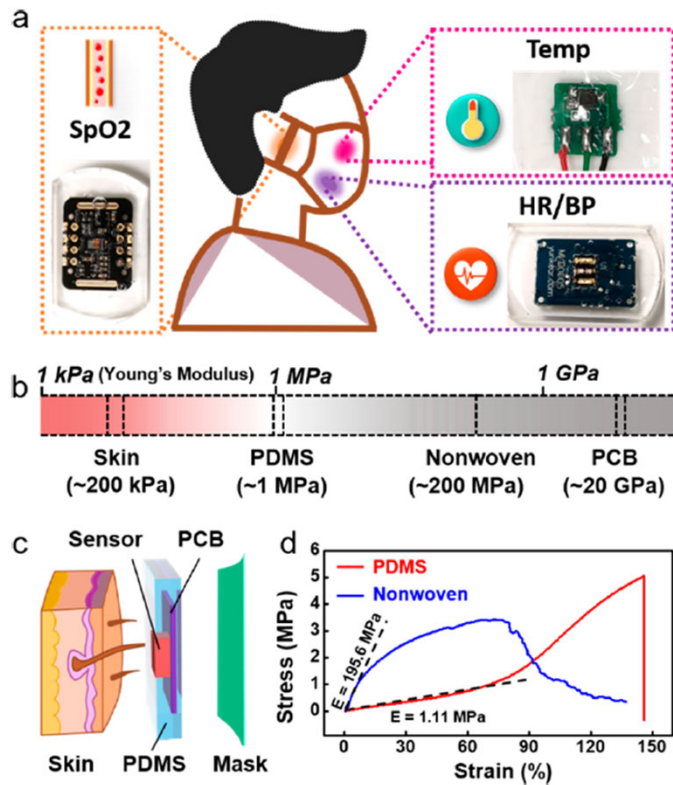


Figure 1. Schematic of the LOM. (a) Different sensors embedded in the PDMS. (b) Comparison of Young's modulus based on PCB, skin, and PDMS. (c) Scheme of the different parts of the LOM on skin. Embedded in PDMS, the Young's modulus of the system is more similar to that of our skin. (d) Strain–stress curve of and Young's modulus of PDMS and the nonwoven fabric of the mask.

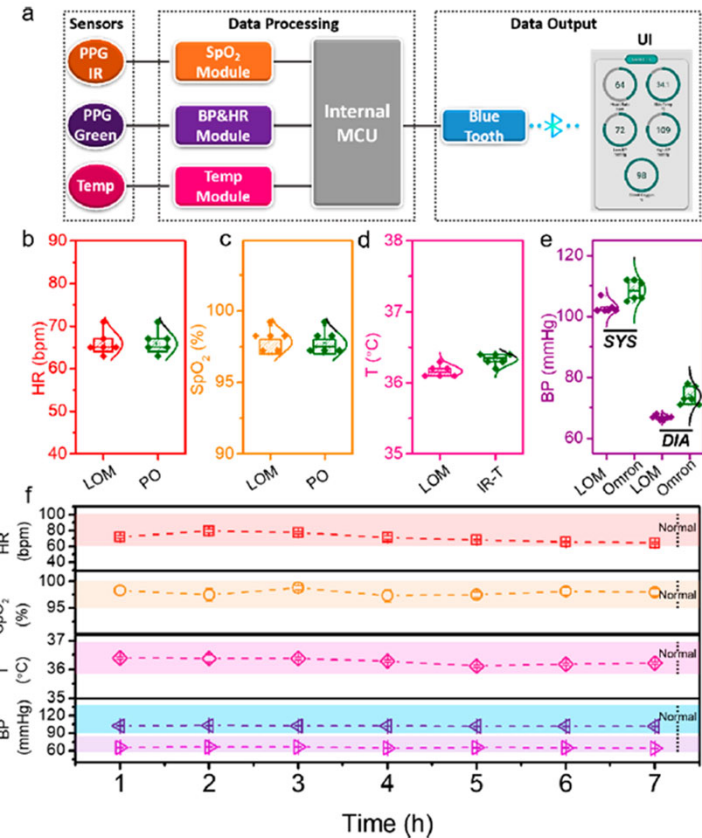


Figure 2. Recorded data from the LOM. (a) Scheme of the different parts of the system on the mask. (b–e) HR, SpO₂, T, and BP, compared with data collected from commercial products. (f) Remote real-time monitoring of a person using the mask for HR, SpO₂, T, and BP.

Nature-Inspired Biomaterials

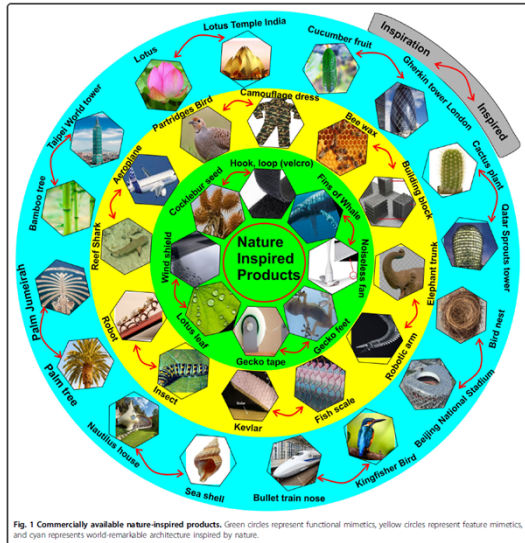


Fig. 1 Commercially available nature-inspired products. Green circles represent functional mimetics, yellow circles represent feature mimetics, and cyan represents world-remarkable architecture inspired by nature.

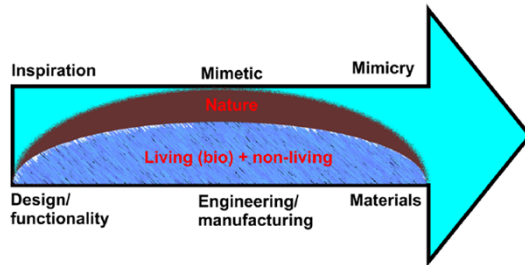


Fig. 2 Classification scheme. Arrow direction shows a generic classification of nature inspiration, mimetics and mimicry.

Katiyar 2021, Nature-inspired materials

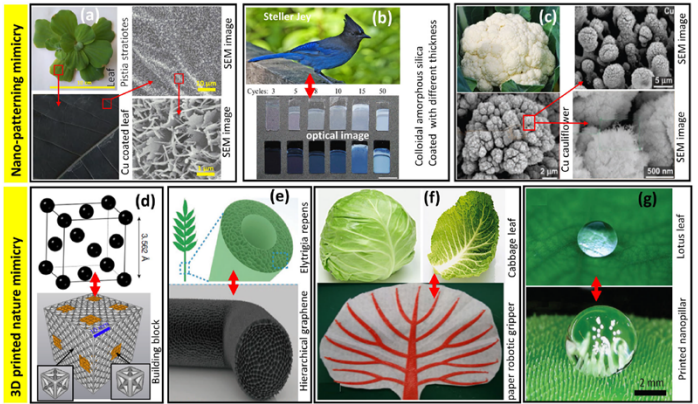


Fig. 4 Examples of nature-inspired bulk and surfaces. a Cu nanostructure for wide wavelength absorption generated through *Phanera pupurea*/*Pistia stratiotes* leaf as template¹²; b color alteration with different angles inspired by Steller's jay feather²³; c Cu nanostructure generated using laser, structure from cauliflower²⁴; d building block inspired by crystal structure²⁵; e hierarchical graphene ultralight inspired from Elytrigia repens²⁶; f soft robotic thermally driven paper gripper inspired by curling of cabbage leaf²⁷; g 3D printed nanopillar for superhydrophobic action inspired by a lotus leaf²⁸. Subfigure a adapted from ref. ¹² (© 2020 NPG); b from ref. ²³ (© 2017 Wiley-VCH); c from ref. ²⁴ (© 2020 Wiley-VCH); d from ref. ²⁵ (© 2019 NPG); e from ref. ²⁶ (© 2019 Wiley VCH); f from ref. ²⁷ (© 2019 Springer) and g from ref. ²⁸ (© 2019 Wiley VCH).

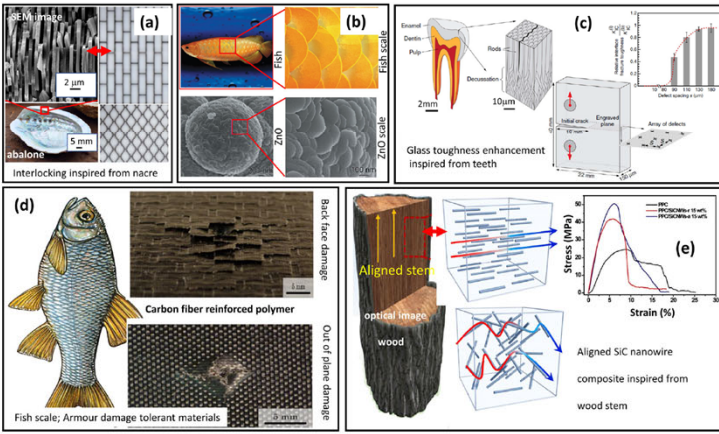


Fig. 5 Different nature-inspired examples. a Enhanced wall strength construction mimicry of interlocking aragonite plates in nacre²⁹; b fish scale generated using ZnO³⁰; c enhanced glass toughness inspired by tooth enamel³¹; d fiber-reinforced armor strength polymer inspired by fish scale³² and e the alignment of carbon nanotubes in nanocomposites inspired by wood stem³³. Subfigure a adapted from ref. ²⁹ (©2016 NPG); b from ref. ³⁰ (© 2015 NPG); c from ref. ³¹ (© 2014 NPG); d from ref. ³² (© 2020 Elsevier); e from ref. ³³ (© 2020 Elsevier).

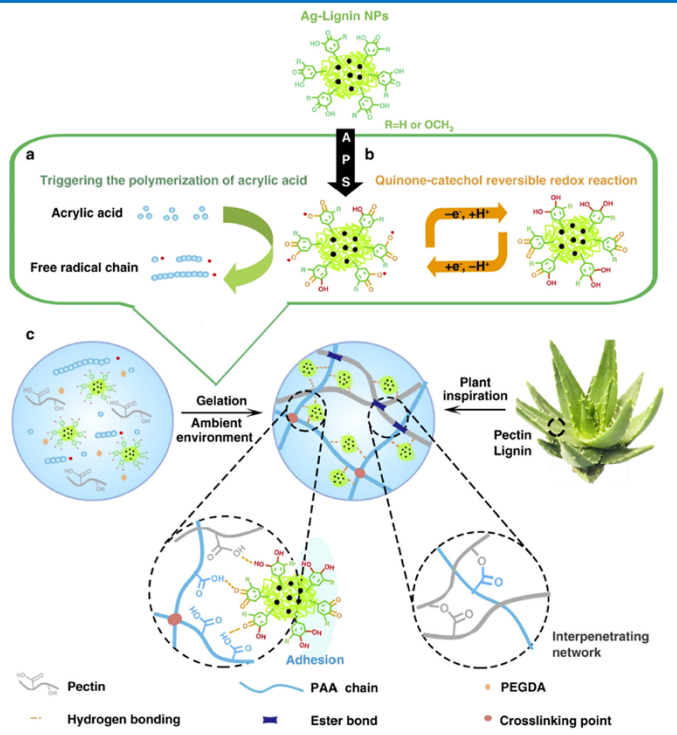


Fig. 8 Another example of an electrical gain inspiring the novel design of hydrogel. a-c The bioinspired strategy for the plant-inspired catechol chemistry-based self-adhesive, tough, and antibacterial NP-P-PAA hydrogel³⁴. Adapted from ref. ³⁴ (©2019 NPG).

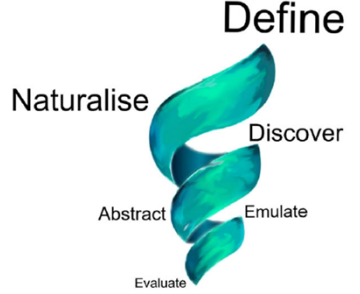


Fig. 12 The concept of design spiral. The figure shows the concept of a spiral adopted from the Biomimicry research institute.

Bio-Sommelier (Bimetallic Tongue)

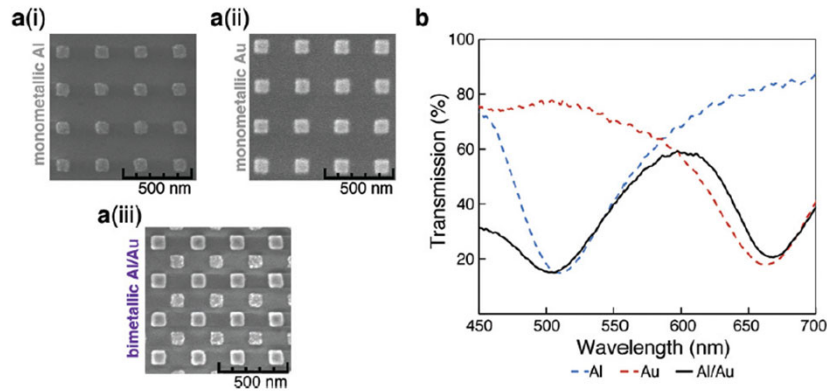
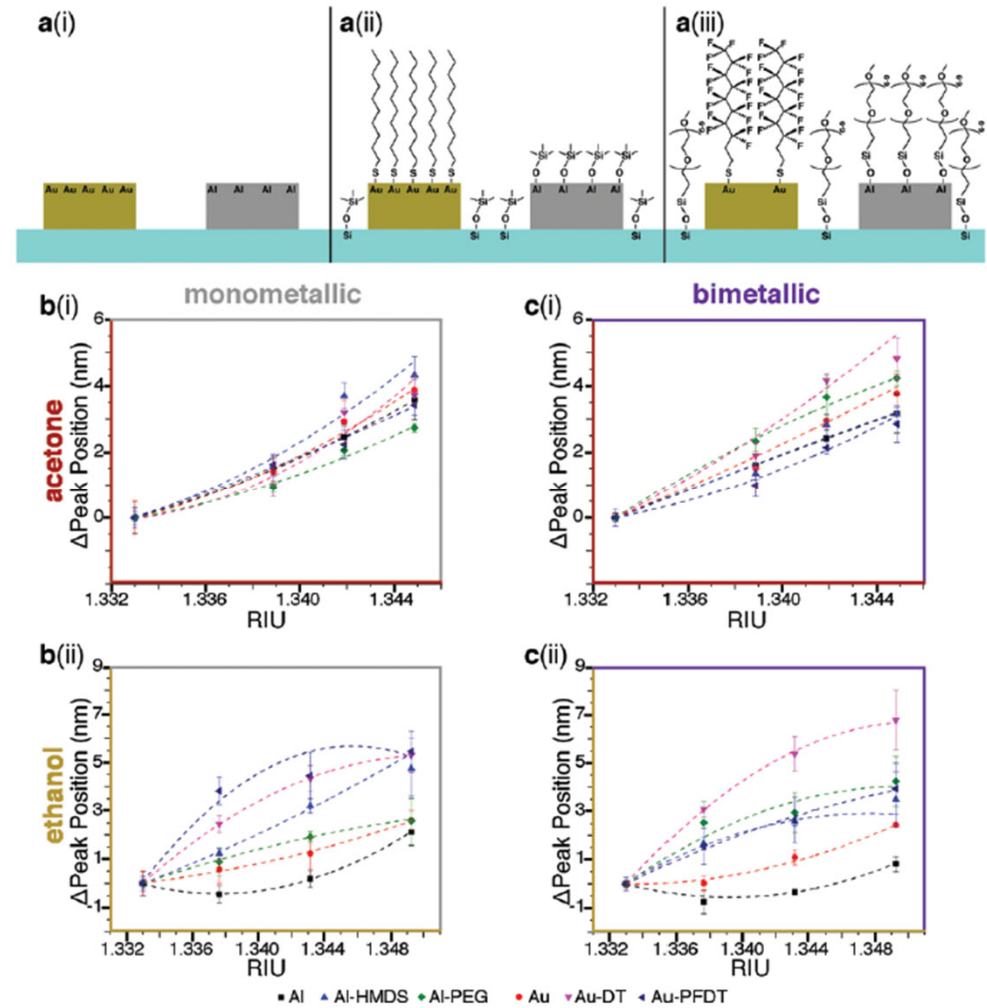


Fig. 1 Comparison of mono- and bimetallic LSPR sensors. (a) SEMs showing (i) monometallic Al, (ii) monometallic Au, and (iii) bimetallic Al/Au regions. (b) Transmission response of arrays of Al-only (dotted-blue), Au-only (dotted-red), and bimetallic Al/Au (black solid) in water.

Fig. 2 Effect of surface chemistry on the sensitivity of Au, Al, and Au/Al sensor arrays. (a) Surface chemistry combinations used: (i) native Al, Au (ii) Al-HMDS, Au-DT, and (iii) Al-PEG, Au-PFDT. (b) The shift in plasmonic response from water for monometallic arrays in 10%, 20%, and 30% solutions (v/v) of (i) acetone and (ii) ethanol. (c) The shift in plasmonic response from water for bimetallic arrays in 10%, 20%, and 30% solutions (v/v) of (i) acetone and (ii) ethanol. The different surface chemistries (native Al, Al-HMDS, Al-PEG, native Au, Au-DT, and Au-PFDT) alter the plasmonic peak of the nanostructures when exposed to the same organic solvent. This results in different peak-shifted curves. The RIU values for acetone and ethanol solutions were obtained from S. S. Kurtz, et al. (1965)¹ and T. A. Scott (1946),² respectively. For (b) and (c), the lines are present to guide the eye and the error bars are one standard deviation from the average.

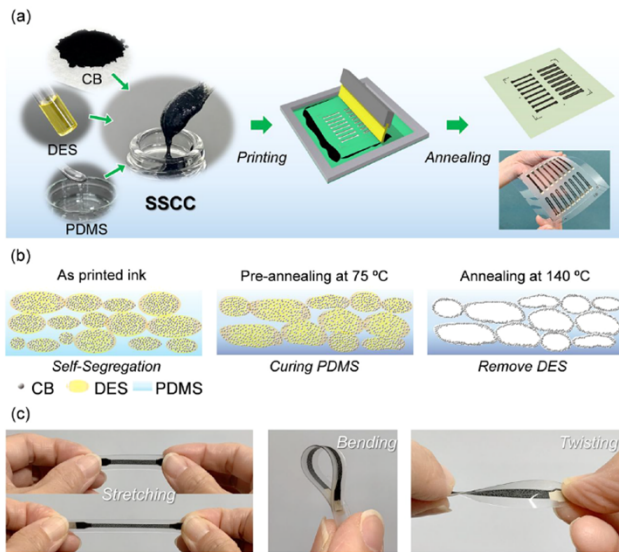
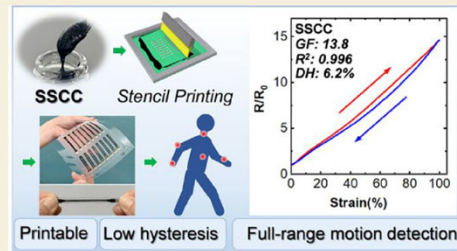


Macias 2019, Whisky tasting using a bimetallic nanoplasmonic tongue

Stretchable Strain Sensor

ABSTRACT: The hysteresis of stretchable composites raises significant challenges in the accuracy, reliability, and stability of stretchable strain sensors. Herein, we report a self-segregating conductive composite that overcomes these issues in printed stretchable strain sensors. This printable composite possesses self-segregation between polydimethylsiloxane and carbon black, which was induced by a deep eutectic solvent. Compared with that of the conventional composites with a random conductive network, our spontaneously formed conductive architecture exhibits superior electromechanical performance: (i) low hysteresis and high sensitivity, (ii) high conductivity and low elastic modulus, and (iii) excellent reliability and stability. Moreover, the composite can be applied directly to a simple stencil printing process without any complex ink synthesis and post-treatment of the fabricated device. This work provides a materials design strategy for achieving low mechanical and electrical hysteresis in a conductive composite. The fabricated sensors exhibit comprehensive performance capabilities appropriate for whole body human motion detection as a proof of concept.

KEYWORDS: stretchable strain sensor, conductive composite, self-segregation, low hysteresis, stencil printing



Yoshida 2022, Printed low-hysteresis stretchable strain sensor based on a self-segregating conductive composite

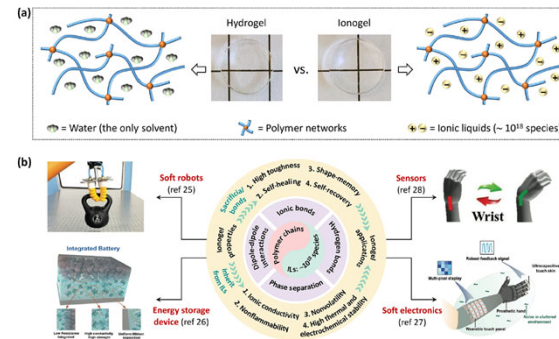


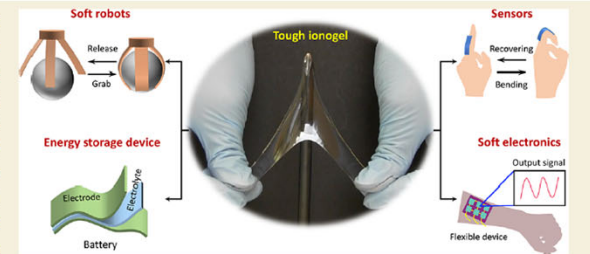
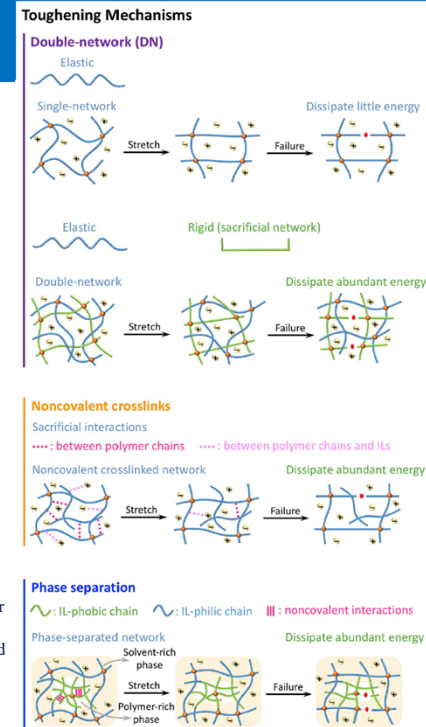
Figure 1. Properties and applications of ionogels. (a) Schematic depicting the structures of a hydrogel and ionogel. (b) Ionogels consist of polymers swollen with ionic liquids (ILs), of which there are an estimated $\sim 10^{18}$ ILs possible. The ILs can interact with the polymer in ways defined by the purple concentric band. The tan colored outer band shows properties that lead to applications, of which several are highlighted on the periphery.

Figure 3. Schematics illustrating toughening mechanisms in ionogels. For DN ionogels, rupturing the rigid polymer dissipates energy while the elastic portions maintain the network. For noncovalent crosslinked ionogels, breaking noncovalent interactions dissipates energy. The noncovalent interactions form both between the polymer chains and between the ILs and polymer chains. In phase-separated ionogels, IL-phobic chains form phase-separated domains that bond via noncovalent interactions, while IL-philic chains remain highly solvated. Disrupting the noncovalent interactions in the phase-separated domains dissipates energy, thereby toughening the ionogels.

ABSTRACT: Polymeric ionogels are polymer networks swollen with ionic liquids (*i.e.*, salts with low melting points). Ionogels are interesting due to their unique features such as nonvolatility, high thermal and electrochemical stability, excellent ionic conductivity, and nonflammability. These properties enable applications such as unconventional electronics, energy storage devices (*i.e.*, batteries and supercapacitors), sensors and actuators. However, the poor mechanical performance of ionogels (*e.g.*, fracture strength < 1 MPa, modulus < 0.1 MPa, and toughness < 1000 J m $^{-2}$) have limited their use, thus motivating the need for tough ionogels. This Perspective summarizes recent advances toward tough ionogels by highlighting synthetic methods and toughening mechanisms. Opportunities and promising applications of tough ionogels are also discussed.

KEYWORDS: ionogels, tough, phase separation, solvent exchange, double network, noncovalent cross-links

Wang 2022, Tough ionogels. synthesis, toughening mechanisms, and mechanical properties - a perspective



Rapid Testing

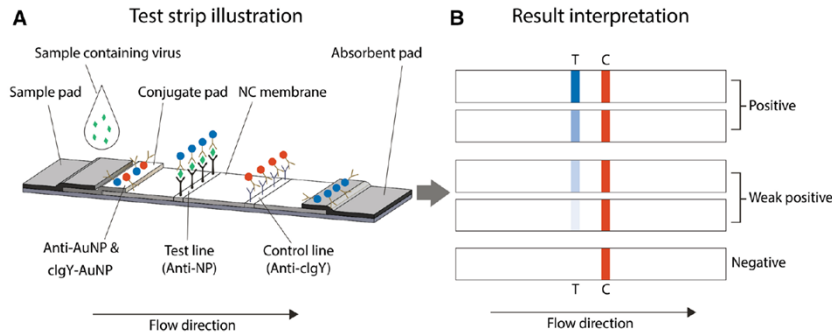


Figure 1. Lateral flow test strip design and assay principle (A). Mouse anti-nucleocapsid protein antibody conjugated to 150 nm gold particles (anti-AuNP) are for mouse anti-nucleocapsid protein (anti-NP) test line detection. Chicken IgY antibodies conjugated to 40 nm gold particles (cIgY-AuNP) are for goat anti-chicken IgY (anti-cIgY) control line detection. Visual result interpretation (B). The red colored control line (C) must be present for a test to be valid. The control line serves to monitor the proper liquid flow and that the bio-reagents of the test device are active. Presence of a visible blue test line (T) indicates the sample is positive for the SARS-CoV-2 virus. Absence of a blue test line indicates the sample is negative or below the detection limit of the test. The test cassette can also be read using a cassette reader for quantitative evaluation.

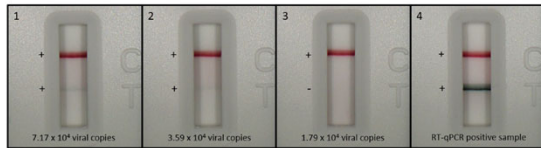


Figure 6. Representative RDT cassettes of each level of inactivated virus-spiked negative nasal swab samples at or around the LOD alongside an RT-qPCR positive swab sample. Weak positive blue test lines are visible in the "T" location of cassettes 1 and 2, both at and above 3.59×10^4 viral copies/RDT. No test line is visible on cassette 3, below 3.59×10^4 viral copies/RDT. For comparison, the RT-qPCR positive swab sample demonstrates a clearly visible test line on cassette 4 from a highly positive patient sample. Control lines are visible at location "C" for all cassettes 1-4.

Remove a sterile swab from the kit box, open the pouch, and slowly rotate the swab against the inside of the patient's nostril at least 10 times for a total of 10 seconds.

Gently remove the swab, and using the same swab, repeat for 10 seconds in the other nostril.

Open a single use flip top Sample Extraction Tube and place the nasal swab with specimen in the extraction tube reagent.

Rotate the swab 15 times while squeezing the tube for a minimum of 15 seconds.

Remove the swab by rotating against the extraction tube while squeezing the sides to release the liquid from the swab. Properly discard the swab.

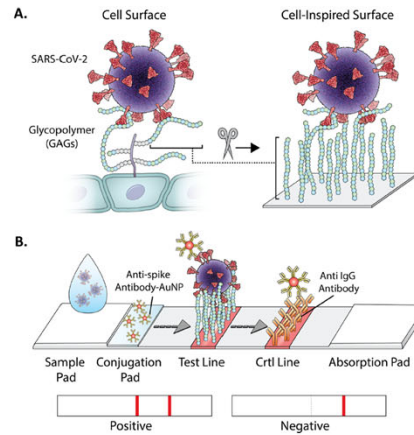
Close the extraction tube with the attached dropper lid.

Gently invert the tube and dispense 3 drops of the sample into the sample well.

Start timer. Interpret the test result at 15 minutes. The test result should not be interpreted after 60 minutes from starting of the test.

Figure 2. Pictorial description of SARS-CoV-2 antigen RDT intended sample testing procedure.

Frew 2021, A SARS-CoV-2 antigen rapid diagnostic test for resource limited settings



Kim 2022, GlycoGrip Cell surface-inspired universal sensor for beta corona viruses

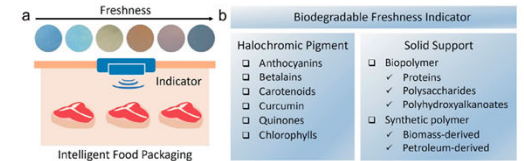
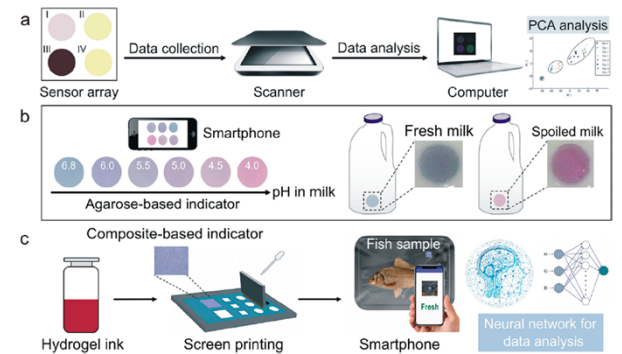


Figure 1. (a) Schematic illustration of intelligent food packaging installed with a freshness indicator. (b) Halochromic pigments and solid supports used for the development of biodegradable freshness indicators.

Table 1. Halochromic Pigments for Use in Biodegradable Freshness Indicators

Halochromic pigments		Typical colorimetric response to pH	References
Type	Major compounds		
Anthocyanins	Cyanidin	pH 2, 4, 5, 7, 9, 10, 12	26
	Delphinidin		
	Pelargonidin		
	Malvidin		
	Petunidin		
Betalains	Betacyanin	pH 2, 4, 5, 7, 9, 10, 12	31
	Betaxanthin		
Carotenoids	β -Carotene	pH <7, pH >7	38
	Lutein		
	Lycopene		
Curcumin	Curcumin	pH 2, 4, 5, 7, 9, 10, 12	42
Quinones	Alizarin	pH 2, 4, 5, 7, 9, 10, 12	48
	Shikonin	pH 2, 4, 5, 7, 9, 10, 12	
Chlorophylls	Chlorophyll a, b, c1, c2, and d	pH <7, pH 7, pH >7	22



Yu 2023, Boosting food system sustainability through intelligent packaging- application of biodegradable freshness indicators

DNA-based Electrochemical Biosensors

DNA-based electrochemical biosensors are popular because of their versatility, cost-efficiency, and compatibility with the signal amplification of DNA. One major challenge in commercializing these sensors is maintaining the stability of the immobilized DNA in suboptimal storage conditions. Thiol-gold bonds are susceptible to disruption due to high temperatures or drying, leading to degraded signals. Further damage to DNA can occur from reactive oxygen species (ROS) generated by the redox probe or from UV exposure to aqueous storage solutions. Thus, DNA monolayers are generally formed just prior to the use of the device, limiting their use outside of the laboratory.

As PVA is produced with a range of molecular weights, we evaluated multiple polymer molecular weight ranges: 9k–10k, 13k–23k, 30k–70k, and 89k–98k g/mol. Solutions of each PVA molecular weight were prepared as 1% weight by volume (w/v) aqueous solutions. The PVA solution was then drop casted onto the working electrode and allowed to air-dry to form a transparent thin-film coating (Figure 1).

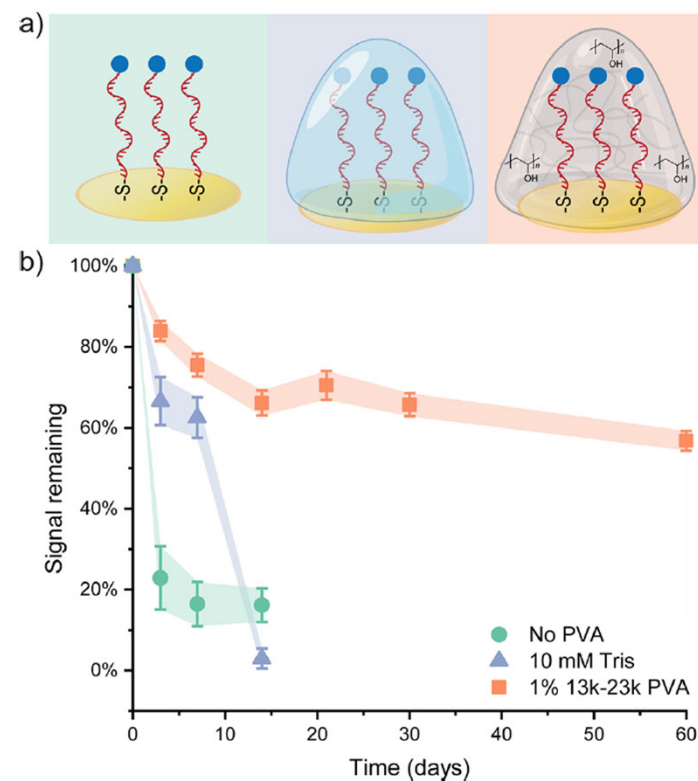
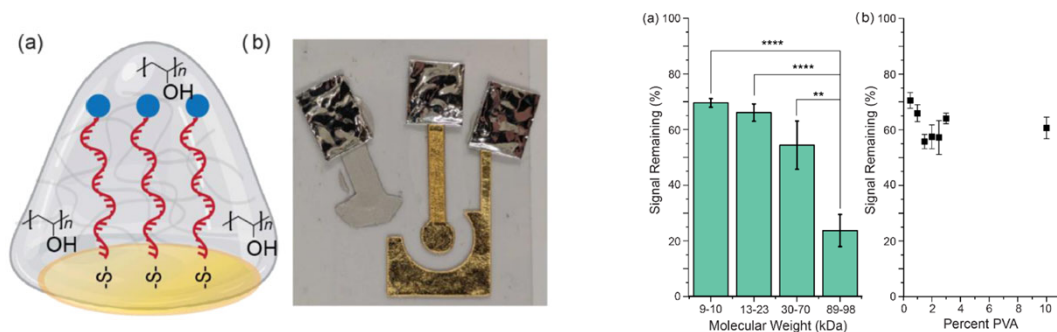
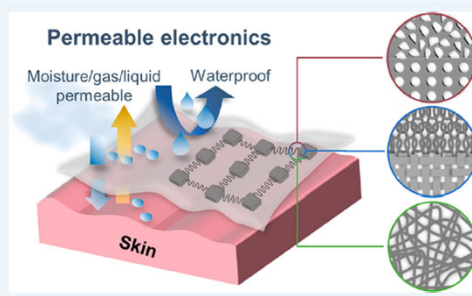


Figure 2. Comparison of the long-term storage of DNA-functionalized electrodes at room temperature. (a) DNA-functionalized electrodes were stored under, from left to right: coated with 1% PVA (13k–23k g/mol), stored in 10 mM Tris buffer (pH 8.5), or left dry. (b) MB signal remains for each of the three storage systems over the course of 60 days. Error bars represent standard error ($n = 12, 12, 11, 12, 10,$ and 15 for PVA; $n = 11, 11,$ and 12 for no PVA; $n = 12, 12,$ and 10 for 10 mM Tris, at each time point).

Permeable Electronics

ABSTRACT: Permeable electronics possess the capability of permeating gas and/or liquid while performing the device functionality when attached to human bodies. The permeability of wearable electronics can not only minimize the thermophysiological disturbance to the human body but also ensure a biocompatible human-device interface for long-term, continuous, and real-time health monitoring. To date, how to simultaneously acquire high permeability and multifunctionality is the major challenge of wearable electronics. Here, a critical discussion on the future development of wearable electronics toward permeability is presented. In this perspective, the critical metrics of permeable electronics are discussed, and the historical evolution of wearable technologies is reviewed with highlights of representative examples. The materials and structural strategies for developing high-performance permeable electronics are then analyzed.

KEYWORDS: permeability, wearable technologies, flexible and stretchable electronics, textile, thin-film technologies



Building blocks for permeable electronics

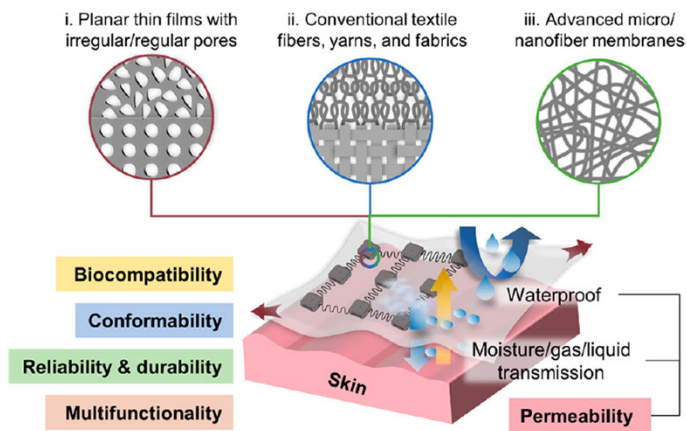


Figure 3. Schematic illustration showing the pathway to developing permeable electronics.

Huang 2022, Pathway to developing permeable electronics

